AN ABSTRACT OF THE THESIS OF

Sul Cho for the degree of Doctor of Philosophy in Mechanical Engineering presented on October 14, 1993.

Title: Nonlinear Adaptive Control of Highly Maneuverable High Performance Aircraft

Abstract approved:_____

R. R. Mohler

This thesis presents an effective control design methodology using a one-step-ahead prediction adaptive control law and an adaptive control law based on a Lyapunov function. These control law were applied to a highly maneuverable high performance aircraft, in particular, a modified F/A-18. An adaptive controller is developed to maneuver an aircraft at a high angle of attack even if the aircraft is required to fly over a highly nonlinear flight regime. The adaptive controller presented in this thesis is based on linear, bilinear, and nonlinear prediction models with input constraints. It is shown that the linear, bilinear, and nonlinear adaptive controllers can be constructed to minimize the given cost function or Lyapunov function with respect to the control input at each step. The control is calculated such that the system follows the reference trajectory, and such that control signal remains within its constraints. From several simulation results, the nonlinear controller is

controller is better than the linear controller. A nonlinear adaptive control law based on a Lyapunov function is designed such that control inputs are smoother than for the one-step-ahead prediction adaptive controller.

Nonlinear Adaptive Control of Highly Maneuverable High Performance Aircraft

by

Sul Cho

A THESIS

submitted to

Oregon State University

in partial fulfillment of

the requirements for the

degree of

Doctor of Philosophy

Completed October 14, 1993

Commencement June 1994

APPROVED:

Redacted for Privacy

Professor of Electrical and Computer Engineering in charge of major

Redacted for Privacy

Head of Department of Mechanical Engineering

Redacted for Privacy

Dean of Graduate School

Date thesis is presented October 14, 1993

Typed by Sul Cho for Sul Cho

ACKNOWLEDGEMENTS

It is with great pleasure that I acknowledge the inspirational guidance, continuing advice, and general support of my advisor, Dr. Ronald R. Mohler, during the completion of this thesis. I would also like to express my sincere appreciation to my committee members, Dr. W. Kolodziej, Dr. Timothy C. Kennedy, Dr. Robert E. Wilson, and Dr. Charles K. Sollitt.

I will never forget the creative members to the NASA project group, who were kind with their support and intellectual assistance. I am also grateful to NASA Langley Research Center for financial support of this research.

I am indebted also to the Department of Mechanical Engineering for continuous financial support and advice during my graduate studies at Oregon State University.

I must also acknowledge my church members for their encouragement and prayers, and my parents and brothers for their unending support and prayers during my period of work in the United States, and my wife Myungim and daughter Jungmin, for their understanding and patience during my long period of study.

Finally, I know not how to express my grateful thanks to my Lord Jesus Christ, through whom I have known the meaning of my life, for His constant love.

To my wife MyungIm and daughter Jungmin

TABLE OF CONTENTS

NOMENCLATURE

A.C. Aircraft aerodynamic center.

b Aerodynamic wing span.

BLPM Bilinear prediction model.

C_{D_o} Drag force coefficient.

C_L Lift force coefficient.

$C_{L_{\dot{\alpha}}}$ Lift coefficient per non-dimensional rate of change in angle of attack.

C_{L_o} Basic lift coefficient which depends on stabilator position, aircraft rigidity, altitude, and Mach number.

C_{L_q} Lift force coefficient per non-dimensional pitch rate.

C_l Roll moment coefficient with respect to body x-axis.

C_{l_β} Change in rolling moment coefficient due to sideslip.

C_{l_o} Basic roll coefficient which depends on sideslip angle, rudder, aileron, and Mach number.

C_{l_p} Roll coefficient per non-dimensional roll rate.

C_{l_r} Roll coefficient per non-dimensional yaw rate.

C_m Pitch moment coefficient with respect to body y- axis.

$C_{m_{\dot{\alpha}}}$ Pitch coefficient per non-dimensional rate of change in angle of attack.

C_{m_o} Basic pitch coefficient which depends on stabilator position, aircraft rigidity, altitude, and Mach number.

C_{m_q} Pitch coefficient per non-dimensional pitch rate.

C_n Yaw moment coefficient with respect to body z -axis.

C_{n_β} Change in yawing moment coefficient due to sideslip.

C_{n_o} Basic yaw coefficient which depends on sideslip angle, rudder, aileron, and Mach number.

C_{n_p} Yaw coefficient per non-dimensional roll rate.

C_{n_r} Yaw coefficient per non-dimensional yaw rate.

C_x Coefficient of aerodynamic forces along x- axis.

C_y Side force coefficient which depends on sideslip angle, rudder, aileron, and Mach number.

C_{y_β} Change in side force coefficient due to sideslip.

C_{y_o} Basic side force coefficient which depends on sideslip angle, rudder, aileron, and Mach number.

C_{y_p} Side force coefficient per non-dimensional roll rate.

C_{y_r} Side force coefficient per non-dimensional yaw rate.

C_z Coefficient of aerodynamic forces along z- axis.

C.G. Aircraft center of gravity.

$\bar{c}$ Aircraft mean aerodynamic chord.

D Drag force.

FL Aerodynamic angular acceleration with respect to x- axis.

FM Aerodynamic angular acceleration with respect to y- axis.

FN Aerodynamic angular acceleration with respect to z- axis.

F_x External forces along x-axis.

F_y External forces along y-axis.

F_z External forces along z-axis.

g Gravity constant.

h Altitude.

I_{xx} Moment of inertia with respect to body x-axis.

I_{yy} Moment of inertia with respect to body y-axis.

I_{zz} Moment of inertia with respect to body z-axis.

I_{xz} Product moment of inertia with respect to body x and z- axes.

J Performance Index.

K Gain in recursive least squares algorithm.

L Lift force.

LF Lyapunov function.

LPM Linear prediction model.

M Mach number.

m Aircraft mass.

M_x Roll moment.

M_y Pitch moment.

M_z Yaw moment.

NLPM Nonlinear prediction model.

n_z Normal acceleration with respect to stability axis.

p Aircraft x-body axis roll rate.

P Covariance Matrix.

p_x Position vector component along x-axis from C.G. to A.C.

p_y Position vector component along y-axis from C.G. to A.C.

p_z Position vector component along z-axis from C.G. to A.C.

p_{xe} x-axis vector component from C.G. to the engine thrust center.

p_{ye} y-axis vector component from C.G. to the engine thrust center.

p_{ze} z-axis vector component from C.G. to the engine thrust center.

q Aircraft y-body axis roll rate.

q Shift operator.

$\bar{q}$ Dynamic pressure at current altitude and Mach number.

r Aircraft z- body axis yaw rate.

S Wing area.

T_{cmd} Command signal of thrust magnitude.

T_x Thrust component along body x-axis.

T_y Thrust component along body y-axis.

T_z Thrust component along body z-axis.

u Aircraft speed along the x-body axis.

v Aircraft speed along the y-body axis.

w Aircraft speed along the z-body axis.

V Aircraft total speed.

W Aircraft weight.

X Body force along aircraft x-axis.

Y Body force along aircraft y-axis.

Z Body force along aircraft z-axis.

x_s Stability x-axis.

y_s Stability y-axis.

z_s Stability z-axis.

α Angle of attack.

$\hat{\alpha}$ Prediction of angle of attack.

α_{ref} Reference trajectory of angle of attack.

α_{cmd} Command signal of angle of attack.

β Sideslip angle.

δ_a Aileron deflection.

δ_f Trailing edge flap deflection.

δ_h Stabilator deflection.

$\delta_{h_{cmd}}$ Command of stabilator deflection.

δ_n Leading edge flap deflection.

δ_r Rudder deflection.

$\delta_{v_{cmd}}$ Command of thrust vector angle.

δ_v Thrust vector angle between T_x and T_z.

ς Engine cant angle.

λ Weighting factor in system identification.

ρ Standard air density at a given altitude.

ρ_i Weighting factor in cost function.

ϕ Aircraft body axes bank angle.

Φ Regression vector in system identification.

ψ Aircraft body axes yaw angle.

θ Aircraft body axes pitch angle.

$\hat{\theta}$ parameters to be estimated.

θ_T Thrust vectoring angle between T_x and T_z.

LIST OF FIGURES

LIST OF TABLES

NONLINEAR ADAPTIVE CONTROL OF HIGHLY MANEUVERABLE HIGH PERFORMANCE AIRCRAFT.

CHAPTER 1

INTRODUCTION

1.1 Objective.

A modern combat aircraft with high maneuverability and high performance beyond the stall region will have advantages in mission success over conventional fighters, will attain maximum climb performance, and will sustain turn capability even if there exist large changes in stability derivative coefficients. For such reasons, research in high angle of attack is presently at an advanced stage. The main objective of the thesis is to design a nonlinear adaptive controller that enables the aircraft to maneuver with superagility over domains which include high angles of attack.

1.2 Literature Review.

In design control laws, the usual first step is to describe the plant at a given operating point and then to develop a control law with a satisfactory performance for that plant model. Historically, the trend of flight control has been to use well-established single loop classical control system design techniques due to the excellent

performance of these methods for conventional maneuvers in traditional flight regimes for good aircraft models. The magnitude of the manual flight control problem is driven by the nonlinear and time-varying nature of aircraft dynamics. Linear models of these systems are only valid for small regions about trim conditions. The conventional solution to this problem is to perform point designs for a large set of trim conditions and construct a gain schedule by interpolating gains with respect to flight conditions [21]. Constant gain scheduling techniques have provided a method of designing variable gain control systems which can accommodate significant variations in the plant operating point parameters while continuing to make use of the accumulated knowledge and experience in the design of linear systems. The ability to use well-established theory and accumulated experience in the design of linear systems, while extending its use and applicability to control nonlinear systems, makes the concept of variable gain laws highly attractive. In particular, a constant gain control law may not meet high performance requirements in the presence of large changes in the operating point parameters. Thus, a variable gain control law approach has been developed to provide a class of controller which is highly maneuverable with high performance over a wide range of operating conditions[21], [50], [51]. Ostroff's approach [50], using the concept of variable gain, was introduced and applied to real systems. The objective of such an approach is to extend the operating range of the control law over the flight regime while continuing to use established linear control design and analysis techniques.

1.3 Motivation.

In Ostroff's approach [50], [51], the system equations were constructed as a linear model even if the system equations change according to flight conditions. Whenever flight conditions change, the variable gain output feedback is applied. The variable feedback gain is scheduled as a function of angle of attack. This means that we can get different variable gains for different scheduled parameters. Its design is quite complex and response up to the final high-alpha is somewhat sub-time optimal.

In the other approach proposed by Buffington, Sparks, and Banda [3], the control law is based on a linear H_∞ design in conjunction with trim-state linearized dynamics and an appropriate nonlinear gain scheduled according to dynamic pressure variation. The study in [3] considers a maximum change in angle of attack from 10° to 20° in about 3 second with a rise time of 1 second. While neither of the two approaches are nearly minimum time maneuvers as demonstrated here, they probably represent the best controllers based primarily on linear design methodology in conjunction with somewhat ad-hoc nonlinear corrections. This thesis shows that nonlinear control can be utilized effectively to control high performance aircraft such as F-18 Aircraft for rapid maneuvers with large changes in angle of attack even where classical linear feedback control without gain scheduling can yield poor performance or instability. Nonlinear feedback controllers that were generated in conjunction with a linear model reference without multiple regression terms failed for certain high-alpha maneuvers but with added nonlinear reference terms they lead to successful control. This thesis, however, indicates that the nonlinear feedback

controller generated in conjunction with a higher-order (more delay terms) linear model reference is quite effective. To improve performance of a nonlinear aircraft system, and to reduce the response time of states in maneuvering of aircraft at high angle of attack, another approach has been used.

1.4 Adaptive Control Law.

This thesis describes the design of an nonlinear adaptive controller for a high performance highly maneuverable aircraft. The main objective of the thesis is to find a nonlinear adaptive controller that enables the aircraft to maneuver with super agility at high angles of attack. The purpose for adaptive control is to provide a mechanism to account for changes in the system that is to be controlled. The traditional goal of adaptive aircraft control is to use concepts from linear theory to control a highly nonlinear system over a large flight regime. Adaptive control for a small class of nonlinear and time-varying systems is investigated in [1], [4], [17], [48], [54], [58]. The idea of adaptive model reference control is to identify the system. A model system generates a desired reference trajectory. Then, a controller uses this information to calculate a command signal so that the output of the system follows the reference trajectory. A block diagram of the model reference adaptive controller is shown in Figure 1.1. Two important elements have to be developed for an effective adaptation routine. First, a class of prediction models needs to be selected. A prediction model represents the dynamics of the system, and it has parameters that can be modified by an estimator. The estimator is the

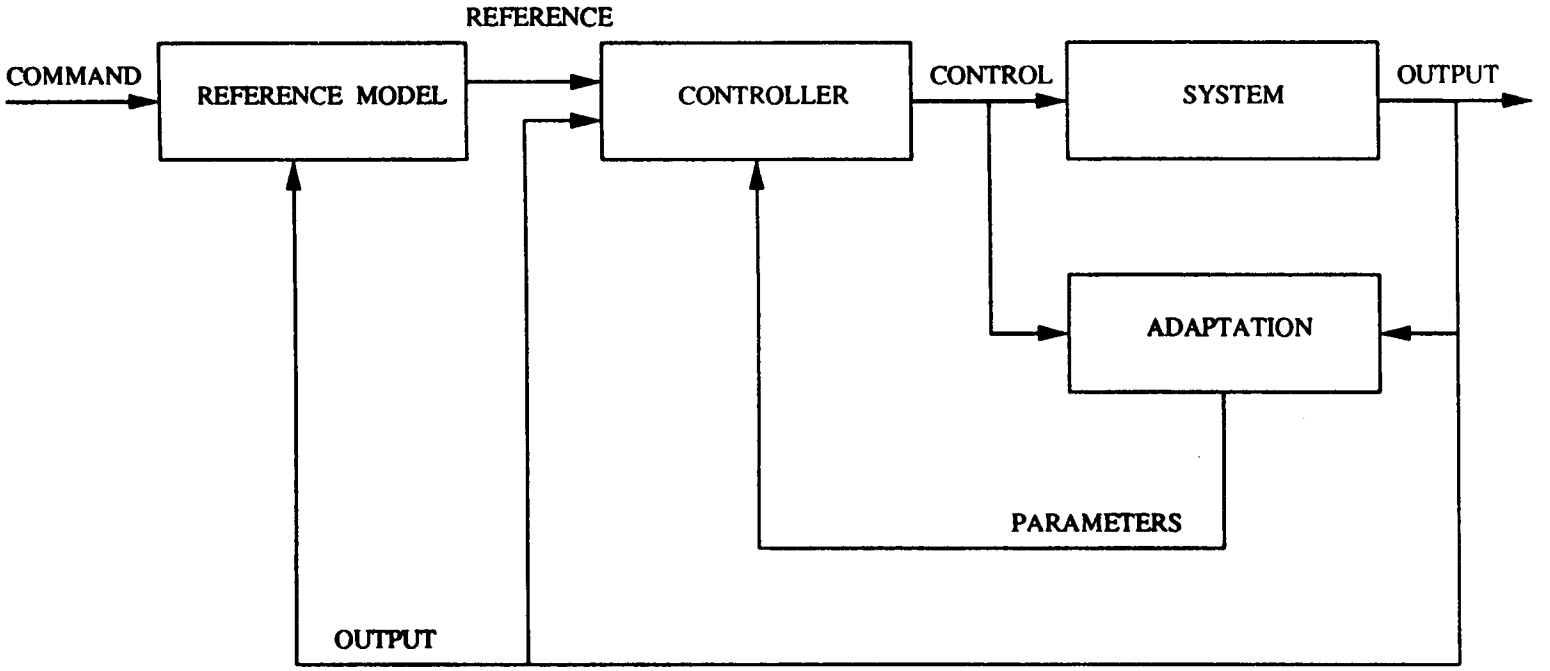

Figure 1.1 Block Diagram of Adaptive Control

second part of the adaptation. It estimates the values of the parameters to improve the prediction model. The simplest class of prediction models to consider include models with linear parameters. In this thesis, models of linear, bilinear, and nonlinear prediction were selected and performance validated.

The most common estimation algorithm for models as the recursive least squares algorithm. The idea is to choose parameters to be estimated such that the squared difference between the prediction model and actual system is minimized. The purpose of making the algorithm recursive is to allow for on-line identification of parameters.

The reference model [10] is an intermediate step that allows the system to follow the command signal while meeting a variety of design criteria (for instance : rise time, overshoot, settling time, etc.). The control is calculated such that the system follows the reference trajectory, and such that the control signal remains within its constraints. Each block of the adaptive controller will be described in detail in the chapters that follow.

An approach proposed in this thesis is based on the stability of bilinear control systems with nonlinear feedback. It can be assumed that while aircraft dynamic models are not bilinear with regard to natural controls, the closed loop system is equivalent to a bilinear system with nonlinear feedback. For example, the aerodynamic coefficients are nonlinear functions of aircraft angle of attack, mach number, altitude, and other variables. Consequently, control is composed of nonlinear states and / or output feedback.

The presentation is organized in the following way. Chapter 2 derives the nonlinear full dynamic equations of motion of aircraft and gives the actuator dynamics. Chapter 3 briefly discusses classes of model and system identification algorithms. In particular, several types of prediction model are introduced. The reference model is presented in the last section of Chapter 3. Chapter 4 describes the control calculation. Chapter 5 presents the performance of the complete controller and uses simulation results. Chapter 6 concludes this thesis and presents ideas for continued research.

CHAPTER 2

DYNAMIC EQUATION

2.1 Equations of Motion : Body axes.

The nonlinear equations of motion for an aircraft are derived using Newton's Second Law of motion. That is, the total sum of all external forces acting on a body must equal the time rate of change of linear momentum and the total sum of all external moments acting on a body must equal the time rate of change of angular momentum. But an aircraft in flight is a very complicated dynamic system. For example, the control surfaces move about their hinges. Bending and twisting of the various aerodynamic surfaces occur. The external forces that act on the aircraft are also complicated functions of its shape and motion. So the following critical assumptions are necessary to simplify the derivation of the aircraft equations of motion :

1) The airframe is regarded as a rigid body.
2) The earth is assumed to be fixed in space.
3) The mass and inertia remain constant for particular dynamic analysis.
4) The **x - z** plane is assumed to be a plane of symmetry.
5) Gravity is assumed to be aligned with **+z** axis of a local reference frame (Earth) fixed at sea level.
6) Gravity is assumed constant over the airplane volume.
7) The body frame (a reference frame fixed to the body of the airplane) is at the

center of mass and the frame is oriented so that +x is out the nose, +y is out the right wing, +z is out the belly, and they are orthogonal.

With the above assumptions, dynamic equations of motion are established by a nonlinear six-degree of freedom aerodynamic model. The nonlinear equations of motion are made up of three translational and three rotational equations. The translational equations of motion obtained by a force summation with respect to body axes are given by[14]

$$F_x = m(\dot{u} - rv + qw) \tag{2.1.1}$$

$$F_y = m(\dot{v} - pw + ru) \tag{2.1.2}$$

$$F_z = m(\dot{w} - qu + pv) \tag{2.1.3}$$

The rotational equations of motion obtained by a moment balance with respect to body axes are given by

$$M_x = \dot{p}I_{xx} - \dot{r}I_{xz} + (I_{zz} - I_{yy})qr - pqI_{xz} \tag{2.1.4}$$

$$M_y = \dot{q}I_{yy} + pr(I_{xx} - I_{zz}) + (p^2 - r^2)I_{xz} \tag{2.1.5}$$

$$M_z = \dot{r}I_{zz} - \dot{p}I_{xz} + (I_{yy} - I_{xx})pq + qrI_{xz} \tag{2.1.6}$$

where **u**, **v**, and **w** are the translational velocities; **p**, **q**, and **r** are the rotational rates; **m** is the aircraft mass; I_{xx}, I_{yy}, I_{zz}, and I_{xz} are the moments of inertia, and F_x, F_y, F_z, M_x, M_y, and M_z are the external forces and moments due to the aerodynamics

and propulsion. The orientation of the aircraft can be described by three consecutive rotations, whose order is important. The angular rotations are called the Euler angles. Euler angles, ϕ, θ, ψ, describe the orientation of the aircraft with respect to the earth (inertia axis) by [14]

$$\dot{\phi} = p + q\tan(\theta)\sin(\phi) + r\tan(\theta)\cos(\phi) \tag{2.1.7}$$

$$\dot{\theta} = q\cos(\phi) - r\sin(\phi) \tag{2.1.8}$$

$$\dot{\psi} = r\cos(\phi)\sec(\theta) + q\sin(\phi)\sec(\theta) \tag{2.1.9}$$

where ϕ is the roll angle, θ is the pitch angle, and ψ is the yaw angle.

The external forces are described by a summation of gravitational force,aerodynamic force, and thrust engine force as follows [45].

$$\begin{bmatrix} F_x \\ F_y \\ F_z \end{bmatrix} = \begin{bmatrix} F_x \\ F_y \\ F_z \end{bmatrix}_G + \begin{bmatrix} F_x \\ F_y \\ F_z \end{bmatrix}_A + \begin{bmatrix} F_x \\ F_y \\ F_z \end{bmatrix}_E \tag{2.1.10}$$

where the subscripts "G ", "A", and "E" denote gravitational,aerodynamic and thrust induced forces.

Each component of the gravitational force is given by

$$F_{x_G} = -mg\sin(\theta) \tag{2.1.11}$$

$$F_{y_G} = mg\cos(\theta)\sin(\phi) \tag{2.1.12}$$

$$F_{z_G} = mg\cos(\theta)\cos(\phi) \tag{2.1.13}$$

The aerodynamic forces are given by

$$F_{x_A} = \bar{q}SC_X \tag{2.1.14}$$

$$F_{y_A} = \bar{q}SC_Y \tag{2.1.15}$$

$$F_{z_A} = \bar{q}SC_Z \tag{2.1.16}$$

where C_X, C_Y, and C_Z are the coefficients of aerodynamic forces, $\bar{q}$, is aerodynamic pressure, g is gravity, and S is the wing surface.

The body frame rotational equations can be written in a form identical to (2.1.10), with the understanding that there are no moments due to gravity,

$$\begin{bmatrix} M_x \\ M_y \\ M_z \end{bmatrix} = \begin{bmatrix} M_x \\ M_y \\ M_z \end{bmatrix}_G + \begin{bmatrix} M_x \\ M_y \\ M_z \end{bmatrix}_A + \begin{bmatrix} F_x \\ F_y \\ F_z \end{bmatrix}_E \tag{2.1.17}$$

and the aerodynamic moments are given by

$$M_{x_A} = \bar{q}SbC_l \tag{2.1.18}$$

$$M_{y_A} = \bar{q}S\bar{c}C_m \tag{2.1.19}$$

$$M_{z_A} = \bar{q}SbC_n \tag{2.1.20}$$

where C_l, C_m, and C_n are the coefficients of aerodynamic moments, b is wingspan, $\bar{c}$ is the aircraft mean aerodynamic chord .

2.2 Model Description of A Modified F/A - 18 Aircraft.

The supermaneuverable aircraft model described in this section is based on a modification of F/A-18 aircraft. The controllers consist of stabilator, aileron, rudder, and thrusting vector. The aerodynamic inputs such as the stabilator, aileron, etc, are useful at normal flight conditions. Thrust vectoring is useful at high angle

of attack, low dynamic pressure operating conditions, where the aerodynamic control effectiveness is inadequate. The aircraft model is augmented with two dimensional thrust vectoring that provide pitch and yaw moments when deflected symmetrically and a roll moment when deflected asymmetrically. A model of the F/A-18 aircraft is shown in Figure 2.1[45].

From equation (2.1.1)-(2.1.3), it is seen that translational equations with respect to body axes are

$$\dot{u} = rv - qw - g\sin(\theta) + \frac{X}{m} + \frac{T_x}{m} \tag{2.2.1}$$

$$\dot{v} = pw - ru + g\cos(\theta)\sin(\phi) + \frac{Y}{m} + \frac{T_y}{m} \tag{2.2.2}$$

$$\dot{w} = qu - pv + g\cos(\theta)\cos(\phi) + \frac{Z}{m} + \frac{T_z}{m} \tag{2.2.3}$$

Similarly, rotational equations of motion with respect to body axis are

$$\dot{p} = C_{41}pq + C_{42}qr + C_{43}FN + C_{40}FL + \frac{C_{43}}{I_{zz}}(p_{ze}T_y - p_{ye}T_x) + \frac{C_{40}}{I_{xx}}(p_{ye}T_z - p_{ze}T_y) \tag{2.2.4}$$

$$\dot{q} = C_{51}pr + C_{52}(r^2 - p^2) + FM + \frac{p_{ze}T_x - p_{xe}T_z}{I_{yy}} \tag{2.2.5}$$

$$\dot{r} = C_{61}pq + C_{62}qr + C_{63}FL + C_{40}FN + \frac{C_{63}}{I_{xx}}(p_{ye}T_z - p_{ze}T_y) + \frac{C_{40}}{I_{zz}}(p_{xe}T_y - p_{ye}T_x) \tag{2.2.6}$$

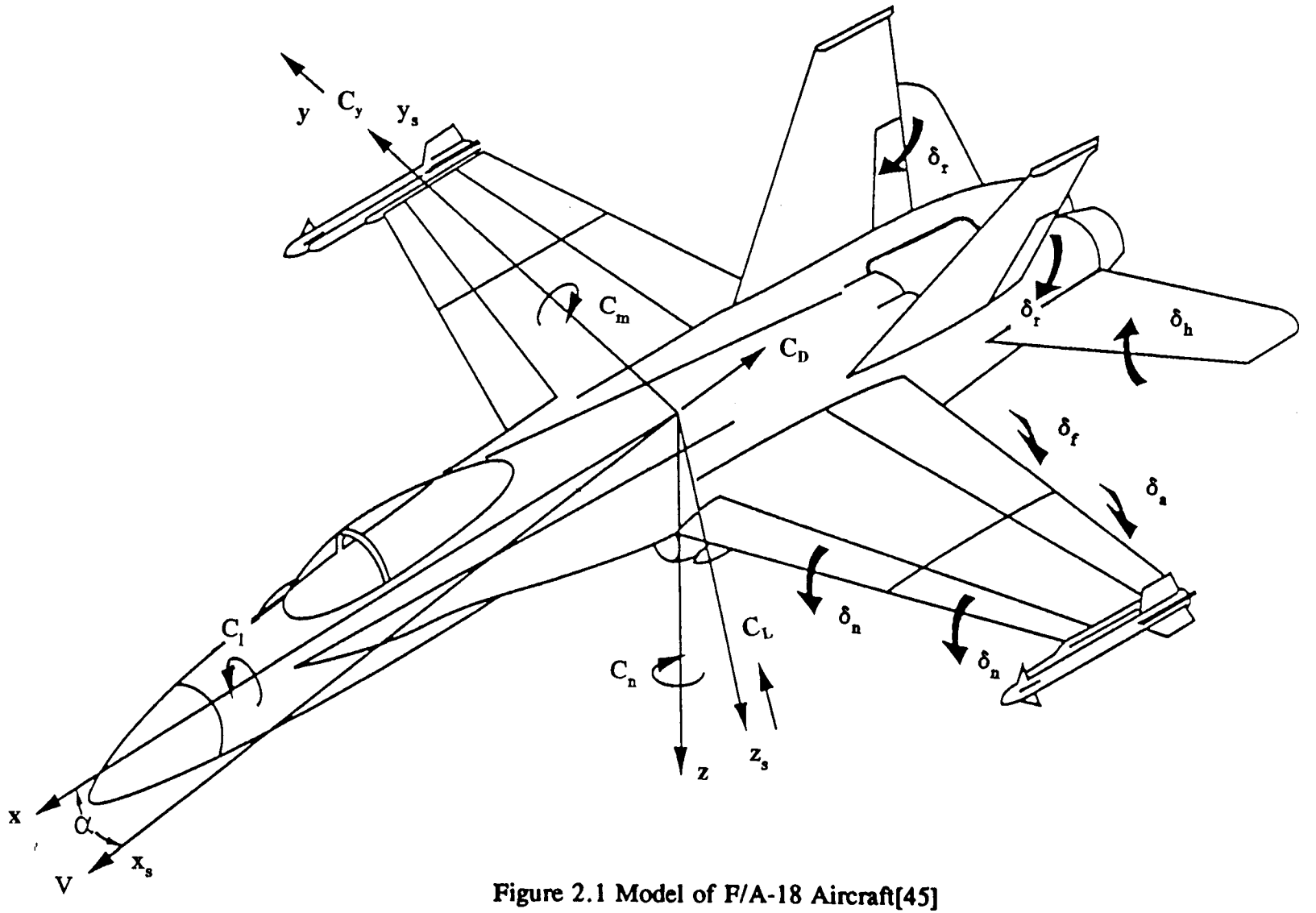

Figure 2.1 Model of F/A-18 Aircraft[45]

where the quantities **X**, **Y**, **Z**, **FL**, **FM**, and **FN** depend on the aerodynamic coefficients C_D, C_y, C_m, C_L, C_l, and C_n as follows.

$$D = \bar{q}SC_D \tag{2.2.7}$$

$$L = \bar{q}SC_L \tag{2.2.8}$$

$$X = -D\cos(\alpha) + L\sin(\alpha) \tag{2.2.9}$$

$$Y = \bar{q}SC_y \tag{2.2.10}$$

$$Z = -D\sin(\alpha) - L\cos(\alpha) \tag{2.2.11}$$

$$FL = \frac{\bar{q}SbC_l + p_yZ - p_zY}{I_{xx}} \tag{2.2.12}$$

$$FM = \frac{\bar{q}\bar{S}cC_m + p_zX - p_xZ}{I_{yy}} \tag{2.2.13}$$

$$FN = \frac{\bar{q}SbC_n + p_xY - p_yX}{I_{zz}} \tag{2.2.14}$$

The constants in the moment equations (2.2.4) - (2.2.6) are functions of the moment of inertia quantities I_{xx}, I_{yy}, I_{zz}, and I_{xz} as follows.

$$C_{40} = \frac{I_{xx}I_{zz}}{I_{xx}I_{zz} - I_{xz}^2} \tag{2.2.15}$$

$$C_{41} = \frac{C_{40}I_{xz}(I_{zz}+I_{xx}-I_{yy})}{I_{xx}I_{zz}} \tag{2.2.16}$$

$$C_{42} = \frac{C_{40}(I_{zz}I_{yy} - I_{zz}I_{zz} - I_{xz}I_{xz})}{I_{xx}I_{zz}} \tag{2.2.17}$$

$$C_{43} = \frac{C_{40}I_{xz}}{I_{xx}} \tag{2.2.18}$$

$$C_{51} = \frac{(I_{zz} - I_{xx})}{I_{yy}} \tag{2.2.19}$$

$$C_{52} = \frac{I_{xz}}{I_{yy}} \tag{2.2.20}$$

$$C_{61} = \frac{C_{40}(I_{xx}(I_{xx} - I_{yy}) + I_{xz}I_{xz})}{I_{xx}I_{zz}} \tag{2.2.21}$$

$$C_{62} = \frac{C_{40}I_{xz}(I_{yy} - I_{zz} - I_{xx})}{I_{xx}I_{zz}} \tag{2.2.22}$$

$$C_{63} = \frac{C_{40}I_{xz}}{I_{zz}} \tag{2.2.23}$$

The vector ($\mathbf{p_x}$, $\mathbf{p_y}$, $\mathbf{p_z}$) denotes the position vector from center of gravity to aerodynamic center and the vector ($\mathbf{p_{xe}}$, $\mathbf{p_{ye}}$, $\mathbf{p_{ze}}$) denotes the position vector from the center of gravity to the engine thrust center. The thrust components in each engine frame (where the engine **x**- axis is aligned with the engine centerline, and the **z**- axis is parallel to the body **z**-axis) are given below.

Left Engine :

$$T_x = T_L \cos(\delta_v)\cos(\varsigma) \tag{2.2.24}$$

$$T_y = T_L \sin(\delta_v)\cos(\theta_T) \tag{2.2.25}$$

$$T_z = T_L \cos(\delta_v)\sin(\theta_T) \tag{2.2.26}$$

Right Engine :

$$T_x = T_R \cos(\delta_v)\cos(\varsigma) \tag{2.2.27}$$

$$T_y = T_R \sin(\delta_v)\cos(\theta_T) \tag{2.2.28}$$

$$T_z = T_R \cos(\delta_v)\sin(\theta_T) \tag{2.2.29}$$

Accounting for the engine cant angle $\varsigma = 1.98°$, the right engine components transformed to body axes are

$$T_{XR} = T_R \cos(\delta_v)\cos(\varsigma) - T_R \sin(\delta_v)\cos(\theta_T)\sin(\varsigma) \tag{2.2.30}$$

$$T_{YR} = T_R \cos(\delta_v)\sin(\varsigma) + T_R \sin(\delta_v)\cos(\theta_T)\cos(\varsigma) \tag{2.2.31}$$

$$T_{ZR} = T_R \sin(\delta_v)\sin(\theta_T) \tag{2.2.32}$$

δ_v denotes thrust vectoring angle between T_x and T_z.

θ_T denotes thrust vectoring angle between T_y and T_z.

The left engine components are identified with ς replaced by $-\varsigma$. The engine cant angle has a negligible effect on the thrust forces, but it is more important in properly modeling the thrust moment. T_R and T_L represent the magnitude of thrust vectoring in each engine frame. Subscripts R and L stand for right and left engine, respectively. The magnitudes of T_R and T_L are determined as a function of altitude, Mach number, angle of attack,etc..

2.3 Mathematical Structure of Aerodynamic Coefficients.

The mathematical structure of the aerodynamic coefficients are based on the wind tunnel test of a high angle of attack vehicle model[5]. The aerodynamic coefficients are considered to be functions of the following control variables as well as angle of attack, sideslip, Mach number, altitude, roll, pitch and yaw rates: aileron deflection(δ_a), rudder deflection(δ_r) and stabilator deflection(δ_h). The effects of leading edge flap, trailing edge, speed brake, landing gear, etc, are not considered. In addition, lift and pitching moment coefficients have unsteady flow parts due to the time rate of change of angle of attack. The other coefficients have only steady flow parts; they are explicit functions of aircraft velocity states and control surface positions. The mathematical structure of the aerodynamic coefficients is described below.

Drag C_D :

$$C_D = C_{D_o}(\alpha, M, h, \delta h) \tag{2.3.1}$$

Lift C_L :

$$C_L = C_{L_o}(\alpha, M, h, \delta h) + \frac{\bar{c}}{2V}\left(C_{L_q}(\alpha, M, h)q + C_{L_{\dot\alpha}}(\alpha, M, h)\dot\alpha\right) \tag{2.3.2}$$

Pitching Moment C_m :

$$C_m = C_{m_o}(\alpha, M, h, \delta h) + \frac{\bar{c}}{2V}\left(C_{m_q}(\alpha, M, h)q + C_{m_{\dot\alpha}}(\alpha, M, h)\dot\alpha\right) \tag{2.3.3}$$

Side Force C_y :

$$C_y = C_{y_o}(\alpha,\beta,M,\delta a,\delta r) + C_{y_\beta}(\alpha,M,h)\beta + \frac{b}{2V}\left(C_{y_p}(\alpha,M,h)p + C_{y_r}(\alpha,M,h)r\right) \tag{2.3.4}$$

Rolling Moment C_l :

$$C_l = C_{l_o}(\alpha,\beta,M,\delta a,\delta r) + C_{l_\beta}(\alpha,M,h)\beta + \frac{b}{2V}\left(C_{l_p}(\alpha,M,h)p + C_{lr}(\alpha,M,h)r\right) \tag{2.3.5}$$

Yawing Moment C_n :

$$C_n = C_{n_o}(\alpha,\beta,M,\delta a,\delta r) + C_{n_\beta}(\alpha,M,h)\beta + \frac{b}{2V}\left(C_{n_p}(\alpha,M,h)p + C_{nr}(\alpha,M,h)r\right) \tag{2.3.6}$$

where aerodynamic variables, angle of attack, α, the sideslip angle, β , total speed, V, are defined as follows.

Angle of attack :

$$\alpha = \tan^{-1}\left(\frac{w}{u}\right) \tag{2.3.7}$$

Sideslip Angle :

$$\beta = \sin^{-1}\left(\frac{v}{V}\right) \tag{2.3.8}$$

Total Speed :

$$V^2 = u^2 + v^2 + w^2 \tag{2.3.9}$$

As aerodynamic coefficients are functions of angle of attack, sideslip angle, Mach number, altitude, and control variables such as stabilator, rudder, aileron, it is useful for state variables to be selected as angle of attack, sideslip angle, total speed, roll rate, pitch rate, and yaw rate.

Velocities in the x- , y-, and z- directions are given as follows:

$$u = V\cos(\alpha)\cos(\beta) \tag{2.3.10}$$

$$v = V\sin(\beta) \tag{2.3.11}$$

$$w = V\cos(\alpha)\sin(\beta) \tag{2.3.12}$$

By using aerodynamic variables defined above, the full nonlinear dynamic equations can be derived.

First, taking the derivative of angle of attack in equation (2.3.7),

$$\dot{\alpha} = \frac{u\dot{w} - \dot{u}w}{V^2} \tag{2.3.13}$$

$$= \frac{\dot{w}\cos(\alpha) - \dot{u}\sin(\alpha)}{V\cos(\beta)} \tag{2.3.14}$$

Using equation (2.2.1), (2.2.3), and (2.3.10)-(2.3.12), the differential equation of angle of attack including aerodynamic forces yields

$$\dot{\alpha} = q - \tan(\beta)(p\cos(\alpha) + r\sin(\alpha)) - \left(\frac{L}{mV\cos(\beta)}\right) + \alpha_{11} + \alpha_{12} \tag{2.3.15}$$

where

$$\alpha_{11} = g\left(\frac{\cos(\alpha)\cos(\theta)\cos(\phi) + \sin(\alpha)\sin(\theta)}{V\cos(\beta)}\right) \tag{2.3.16}$$

$$\alpha_{12} = \left(\frac{T_z \cos(\alpha) - T_x \sin(\alpha)}{mV\cos(\beta)} \right) \tag{2.3.17}$$

The differential equation of angle of attack with aerodynamic coefficients is given by

$$\dot{\alpha} = \alpha_{10} \left(\alpha_{13} q - \tan(\beta)(p\cos(\alpha) + r\sin(\alpha)) + \alpha_{11} - \frac{\rho S C_{L_o} V}{2m\cos(\beta)} + \alpha_{12} \right) \tag{2.3.18}$$

where

$$\alpha_{10} = \frac{1}{\left(1 + \frac{\rho \bar{c} S C_{L_{\dot{\alpha}}}}{4m\cos(\beta)} \right)} \tag{2.3.19}$$

$$\alpha_{13} = \left(1 - \frac{\rho \bar{c} S C_{L_q}}{4m\cos(\beta)} \right) \tag{2.3.20}$$

Second, taking the derivative of total speed in equation (2.3.9) with respect to time,

$$\dot{V} = \cos(\alpha)\cos(\beta)\dot{u} + \sin(\beta)\dot{v} + \sin(\alpha)\cos(\beta)\dot{w} \tag{2.3.21}$$

Using equation (2.2.1)-(2.2.3) and (2.3.10)-(2.3.11), differential equation of total speed yields

$$\dot{V} = V_{11} g + V_{12} - \left(\frac{D\cos(\beta) - Y\sin(\beta)}{m} \right) \tag{2.3.22}$$

where

$$V_{11} = \sin(\alpha)\cos(\beta)\cos(\theta)\cos(\phi) + \sin(\beta)\cos(\theta)\sin(\phi) - \cos(\alpha)\cos(\beta)\sin(\theta) \tag{2.3.23}$$

$$V_{12} = \left(\frac{T_x \cos(\alpha)\cos(\beta) + T_y \sin(\beta) + T_z \sin(\alpha)\cos(\beta)}{m} \right) \tag{2.3.24}$$

The differential equation of total speed with aerodynamic coefficients is given by

$$\dot{V} = V_{11} g + V_{12} + \left(\frac{\rho S b \sin(\beta) (C_{y_p} p + C_{y_r} r)}{2m} \right) V + V_{13} V^2 \tag{2.3.25}$$

where

$$V_{13} = \rho S \left(\frac{-C_{D_o} \cos(\beta) + C_{y_o} \sin(\beta) + C_{y_\beta} \sin(\beta) \beta}{2m} \right) \tag{2.3.26}$$

The differential equation of sideslip angle yields as follows

$$\dot{\beta} = \beta_{11} p + \beta_{12} r + \left(\frac{\beta_{13} g}{V \cos(\beta)} \right) + \beta_{15} V + \beta_{14} \tag{2.3.27}$$

where

$$\beta_{11} = \left(\sin(\alpha) + \frac{\rho S b \cos(\beta)}{4m} C_{y_p} \right) \tag{2.3.28}$$

$$\beta_{12} = \left(-\cos(\alpha) + \frac{\rho S b \cos(\beta)}{4m} C_{y_r} \right) \tag{2.3.29}$$

$$\begin{aligned} \beta_{13} = {} & \cos(\alpha)\sin(\beta)\cos(\beta)\sin(\theta) - \sin^2(\beta)\cos(\theta)\sin(\phi) + \\ & \cos(\theta)\sin(\phi) - \sin(\alpha)\cos(\beta)\sin(\beta)\cos(\theta)\cos(\phi) \end{aligned} \tag{2.3.30}$$

$$\beta_{14} = -\left(\frac{T_x \cos(\alpha)\sin(\beta) + T_y \cos(\beta) + T_z \sin(\alpha)\sin(\beta)}{mV} \right) \tag{2.3.31}$$

$$\beta_{15} = \rho S \left(\frac{\cos(\beta)(C_{y_o} + C_{y_\beta} \beta) - C_{D_o} \sin(\beta)}{2m} \right) \tag{2.3.32}$$

Similarly, the differential equations of rotational motion with aerodynamic coefficients are given as follows.

Roll rate :

$$\dot{p} = C_{41}pq + C_{42}qr + C_{43}\bar{q}S\left(\frac{bC_n + p_x C_y}{I_{zz}}\right) + C_{40}\bar{q}S\left(\frac{bC_l - p_z C_y}{I_{xx}}\right) + \left(\frac{C_{40}(p_{ye}T_y - p_{ye}T_x)}{I_{xx}}\right) \cdot \left(\frac{C_{43}p_y\cos(\alpha)}{I_{zz}} - \frac{C_{40}p_y\sin(\alpha)}{I_{xx}}\right)D - \left(\frac{C_{43}p_y\sin(\alpha)}{I_{zz}} + \frac{C_{40}p_y\cos(\alpha)}{I_{xx}}\right)L + \left(\frac{C_{40}(p_{ye}T_x - p_{ze}T_y)}{I_{xx}}\right)$$

$$= C_{41}pq + C_{42}qr + p_{15}\bar{c}\left(\frac{C_{L_q}q + C_{L_{\dot{\alpha}}}\dot{\alpha}}{2}\right)V + (p_{11}\beta + p_{16})V^2 + \left(\frac{p_{12}p + p_{13}r}{2}\right)bV + p_{17} \tag{2.3.33}$$

where

$$p_{11} = \frac{C_{43}\rho Sb}{2I_{zz}}C_{n_\beta} + \frac{C_{40}\rho Sb}{2I_{xx}}C_{l_\beta} + \rho\left(\frac{C_{43}Sp_x}{2I_{zz}} - \frac{C_{40}Sp_z}{2I_{xx}}\right)C_{y_\beta} \tag{2.3.34}$$

$$p_{12} = \frac{C_{43}\rho Sb}{2I_{zz}}C_{n_p} + \frac{C_{40}\rho Sb}{2I_{xx}}C_{l_p} + \rho\left(\frac{C_{43}Sp_x}{2I_{zz}} - \frac{C_{40}Sp_z}{2I_{xx}}\right)C_{y_p} \tag{2.3.35}$$

$$p_{13} = \frac{C_{43}\rho Sb}{2I_{zz}}C_{n_r} + \frac{C_{40}\rho Sb}{2I_{xx}}C_{l_r} + \rho\left(\frac{C_{43}Sp_x}{2I_{zz}} - \frac{C_{40}Sp_z}{2I_{xx}}\right)C_{y_r} \tag{2.3.36}$$

$$p_{14} = \rho\left(\frac{C_{43}Sp_y\cos(\alpha)}{2I_{zz}} - \frac{C_{40}Sp_y\sin(\alpha)}{2I_{xx}}\right) \tag{2.3.37}$$

$$p_{15} = -\rho\left(\frac{C_{43}Sp_y\sin(\alpha)}{2I_{zz}} + \frac{C_{40}Sp_z\cos(\alpha)}{2I_{xx}}\right) \tag{2.3.38}$$

$$p_{16} = \frac{C_{43}\rho Sb}{2I_{zz}}C_{n_o} + \frac{C_{40}\rho Sb}{2I_{xx}}C_{l_o} + \rho\left(\frac{C_{43}Sp_x}{2I_{zz}} - \frac{C_{40}Sp_z}{2I_{xx}}\right)C_{y_o} + p_{14}C_{D_o} + p_{15}C_{L_o} \tag{2.3.39}$$

$$p_{17} = -\frac{C_{43}p_{ye}}{I_{zz}}T_x + \left(\frac{C_{43}p_{ze}}{I_{zz}} - \frac{C_{40}p_{ze}}{I_{xx}}\right)T_y + \frac{C_{40}p_{ye}}{I_{xx}}T_z \tag{2.3.40}$$

Pitch rate :

$$\begin{aligned}\dot{q} &= C_{51}pr + C_{52}(r^2 - p^2) + \left(\frac{\bar{q}S\bar{c}C_m}{I_{yy}}\right) + \left(-\frac{p_z\cos(\alpha) - p_x\sin(\alpha)}{I_{yy}}\right)D + \\ &\left(\frac{\bar{q}S\bar{c}C_m}{I_{yy}}\right) + \left(\frac{p_z\sin(\alpha) + p_x\cos(\alpha)}{I_{yy}}\right)L + \left(\frac{p_{ze}T_x - p_{xe}T_x}{I_{yy}}\right) \\ &= C_{51}pr + C_{52}(r^2 - p^2) + q_{14}V^2 + q_{15}Vq + q_{16}V + q_{17}g + q_{18}\end{aligned} \tag{2.3.41}$$

where

$$q_{11} = p_x\sin(\alpha) - p_z\cos(\alpha) \tag{2.3.42}$$

$$q_{12} = p_x\cos(\alpha) + p_z\sin(\alpha) \tag{2.3.43}$$

$$q_{13} = \alpha_{10}(\bar{c}C_{m_{\dot{\alpha}}} + q_{12}C_{L_{\dot{\alpha}}}) \tag{2.3.44}$$

$$q_{14} = \frac{\rho S}{2I_{yy}}\left(\bar{c}C_{m_o} + q_{11}C_{D_o} + q_{12}C_{L_o} - \frac{\rho S\bar{c}C_{L_o}}{4m\cos(\beta)}q_{13}\right) \tag{2.3.45}$$

$$q_{15} = \rho S\bar{c}\left(\frac{\bar{c}C_{m_q} + q_{12}C_{L_q} + q_{13}\alpha_{13}}{4I_{yy}}\right) \tag{2.3.46}$$

$$q_{16} = -\rho S\bar{c}\left(\frac{\tan(\beta)(p\cos(\alpha)+r\sin(\alpha))q_{13}}{4I_{yy}}\right) \tag{2.3.47}$$

$$q_{17} = \rho S\bar{c}q_{13}\left(\frac{\cos(\alpha)\cos(\theta)\cos(\phi)+\sin(\alpha)\sin(\theta)}{4I_{yy}\cos(\beta)}\right) \tag{2.3.48}$$

$$q_{18} = \rho\bar{c}q_{13}\left(\frac{T_z\cos(\alpha)-T_x\sin(\alpha)}{4mI_{yy}\cos(\beta)}\right)+\left(\frac{p_{ze}T_x-p_{xe}T_z}{I_{yy}}\right) \tag{2.3.49}$$

Yaw rate :

$$\dot{r} = C_{61}pq+C_{62}qr+C_{43}\bar{q}S\left(\frac{bC_l-p_zC_y}{I_{xx}}\right)+C_{40}\bar{q}S\left(\frac{bC_n+p_xC_y}{I_{zz}}\right)+\left(\frac{C_{63}(p_{ye}T_z-p_{ze}T_y)}{I_{xx}}\right)-$$
$$\left(\frac{C_{40}p_y\cos(\alpha)}{I_{zz}}-\frac{C_{63}p_y\sin(\alpha)}{I_{xx}}\right)D-\left(\frac{C_{40}p_y\sin(\alpha)}{I_{zz}}+\frac{C_{63}p_y\cos(\alpha)}{I_{xx}}\right)L+$$
$$\left(\frac{C_{40}(p_{xe}T_y-p_{ye}T_x)}{I_{zz}}\right)$$

$$= C_{61}pq+C_{62}qr+r_{15}\bar{c}\left(\frac{C_{L_q}q+C_{L_{\dot{\alpha}}}\dot{\alpha}}{2}\right)V+(r_{11}\beta+r_{16})V^2+\left(\frac{r_{12}p+r_{13}r}{2}\right)bV+r_{17} \tag{2.3.50}$$

where

$$r_{11} = \frac{C_{63}\rho Sb}{2I_{XX}}C_{n_p}+\frac{C_{40}\rho Sb}{2I_{ZZ}}C_{l_p}+\rho\left(\frac{C_{40}Sp_x}{2I_{zz}}-\frac{C_{63}Sp_z}{2I_{xx}}\right)C_{y_p} \tag{2.3.51}$$

$$r_{12} = \frac{C_{63}\rho Sb}{2I_{zz}}C_{n_p}+\frac{C_{40}\rho Sb}{2I_{xx}}C_{l_p}+\rho\left(\frac{C_{40}Sp_x}{2I_{zz}}-\frac{C_{63}Sp_z}{2I_{xx}}\right)C_{y_p} \tag{2.3.52}$$

$$r_{13} = \frac{C_{63}\rho Sb}{2I_{zz}}C_{n_r}+\frac{C_{40}\rho Sb}{2I_{xx}}C_{l_r}+\rho\left(\frac{C_{40}Sp_x}{2I_{zz}}-\frac{C_{63}Sp_z}{2I_{xx}}\right)C_{y_r} \tag{2.3.53}$$

$$r_{14} = \rho\left(\frac{C_{40}Sp_y\cos(\alpha)}{2I_{zz}} - \frac{C_{63}Sp_y\sin(\alpha)}{2I_{xx}}\right) \tag{2.3.54}$$

$$r_{15} = -\rho\left(\frac{C_{40}Sp_y\sin(\alpha)}{2I_{zz}} + \frac{C_{63}Sp_y\cos(\alpha)}{2I_{xx}}\right) \tag{2.3.55}$$

$$r_{16} = \frac{C_{40}\rho Sb}{2I_{zz}}C_{n_o} + \frac{C_{63}\rho Sb}{2I_{xx}}C_{l_o} + \rho\left(\frac{C_{40}Sp_x}{2I_{zz}} - \frac{C_{63}Sp_z}{2I_{xx}}\right)C_{y_o} + r_{14}C_{D_o} + r_{15}C_{L_o} \tag{2.3.56}$$

$$r_{17} = -\frac{C_{40}p_{ye}}{I_{zz}}T_x + \left(\frac{C_{40}p_{ze}}{I_{zz}} - \frac{C_{63}p_{ze}}{I_{xx}}\right)T_y + \frac{C_{63}p_{ye}}{I_{xx}}T_z \tag{2.3.57}$$

2.4 Longitudinal Motion.

The dynamics of a rigid aircraft are described by the six simultaneous nonlinear equations as shown in equations (2.2.1) - (2.2.6). To develop the longitudinal equations of motion, it is assumed that the motion of the airplane can be analyzed by separating the equations into two groups. The X-forces, Z-forces,and pitching moment equations comprise the longitudinal equations. This means that disturbances to the equations of motion do not create any sideforce, Y, or any rolling moment, M_x, or yawing moment, M_z. Roll rate, yaw rate, and side velocity remain constant so three of the equations can be neglected. The remaining equations are simplified because $v = p = r = T_y = \phi = \psi = 0$, and the longitudinal motion can be derived as follows:

$$\dot{\alpha} = \alpha_{10}\left(\left(1-\frac{\rho S\bar{c}}{4m}C_{L_q}\right)q+\frac{g}{V}\cos(\theta-\alpha)-\frac{\rho SC_{L_o}}{2m}V-\frac{T_x\sin(\alpha)}{mV}+\frac{T_z\cos(\alpha)}{mV}\right) \quad (2.4.1)$$

$$\dot{V} = -g\sin(\theta-\alpha)-\frac{\rho SC_{D_o}V^2}{2m}+\frac{T_x\cos(\alpha)+T_z\sin(\alpha)}{m} \quad (2.4.2)$$

$$\dot{q} = \frac{\rho S}{2I_{yy}}(\bar{c}C_{m_o}+q11C_{D_o}+q12C_{L_o})V^2+\frac{\rho S\bar{c}}{4I_{yy}}(\bar{c}C_{m_q}+q12C_{L_q}+q13q10)Vq+ \frac{q13\rho S\bar{c}}{4I_{yy}}\left(\frac{g}{V}\cos(\theta-\alpha)-\frac{\rho S}{2m}C_{L_o}V-\frac{T_x\sin(\alpha)}{mV}+\frac{T_z\cos(\alpha)}{mV}\right)V+\frac{p_{ze}T_x-p_{xe}T_z}{I_{yy}} \quad (2.4.3)$$

$$\dot{\theta} = q \quad (2.4.4)$$

where

$$\alpha_{10} = \frac{1}{\left(1+\frac{\rho\bar{c}SC_{L_{\dot{\alpha}}}}{4m}\right)} \quad (2.4.5)$$

$$q_{10} = \left(1-\frac{\rho\bar{c}SC_{L_q}}{4m}\right) \quad (2.4.6)$$

$$q_{11} = p_x\sin(\alpha)-p_z\cos(\alpha) \quad (2.4.7)$$

$$q_{12} = p_x\cos(\alpha)+p_z\sin(\alpha) \quad (2.4.8)$$

$$q_{13} = \alpha_{10}(\bar{c}C_{m_{\dot{\alpha}}}+q_{12}C_{L_{\dot{\alpha}}}) \quad (2.4.9)$$

Normal acceleration with respect to stability axis, non-dimensionalized by gravity, is given as follows.

$$n_z = \frac{V(q - \dot{\alpha})}{g} \tag{2.4.10}$$

2.5 Actuator Dynamics

The input dynamics were described by three states--thrust magnitude (T), thrust vectoring angle (δ_v), and stabilator angle (δ_h). The stabilator and the thrust vectoring dynamics include a velocity limiter of 40 degrees per second for the stabilator angle, and 80 degrees per second for the thrust vectoring angle. Constraint for the stabilator angle rate of change is given by

$$-40°/\text{sec.} \leq \dot{\delta}_h \leq 40°/\text{sec.} \tag{2.5.1}$$

The range of the stabilator angle is limited according to the following[45]:

$$-24.0° \leq \delta_h \leq 10.5° \tag{2.5.2}$$

Constraint for the thrust vectoring angle rate of change is given by

$$-80°/\text{sec.} \leq \dot{\delta}_v \leq 80°/\text{sec.} \tag{2.5.3}$$

The range of the thrust vectoring angle is limited according to the following[45] :

$$-20° \leq \delta_v \leq 20° \tag{2.5.4}$$

Thrust magnitude dynamics are given by :

$$\dot{T} = (T_{cmd} - T) \tag{2.5.5}$$

where T_{cmd} represents the command signal of magnitude of thrust vector.

The magnitude of thrust is limited according to the following[45] :

$$0 \leq T \leq 18000 \text{ lbs} \tag{2.5.6}$$

CHAPTER 3

MODEL

Engineers and scientists are frequently confronted with the task of analyzing problems in the real world, synthesizing solutions to these problems, or developing theories to explain them. One of the first steps in any such task is the development of a mathematical model which describes the relationships among the system variables. In a sense, there is an impenetrable, but transparent screen between our world of mathematical descriptions and the real world [23]. We can look through this window and compare certain aspects of the physical system with its mathematical description, but we can never establish any exact connection between them. This model must not be oversimplified because conclusions drawn from it will not be valid in the real world. The model should not be so complex as to unnecessarily complicate the analysis. The question of nature's susceptibility to mathematical description has some deep philosophical aspects, and in practical terms we have to take a more pragmatic view of models. Our acceptance of models should be guided by usefulness rather than truth. Nevertheless, we shall occasionally use a concept of the true system, defined in terms of a mathematical description because such a fiction is helpful for devising identification methods and understanding their properties. Modeling is important since the choice of model is often the first step toward the prediction or control of a process. An appropriately chosen model structure can greatly simplify the parameter estimation procedure and facilitate the design of

prediction and control algorithms for the process.

3.1 Class of Models.

System models can be developed by two distinct methods. Analytical modeling consists of a systematic application of basic physical laws to system components and the interconnection of these components. Experimental modeling, or modeling by synthesis, is the selection of mathematical relationships which seem to fit observed input-output data. Experimental modeling is emphasized in this section.

Experimental models for linear deterministic finite dimensional systems can be described by state space, input-output, autoregressive moving average models,etc [18]. Generally, state space models can be seen to be a set of first order difference equation models. In this section, the input-output model among several modelings is discussed. The main reason to use input-output, rather than state space models, is that they employ only measured quantities subsequently used by the controller, and therefore are more natural in control system setting. Also, very often the model of the plant is not given prior to the controller synthesis, and has to be identified, either off-line, or on-line, using the available input-output data. In such a case the input-output modeling approach is more effective, since it has simpler model structure and results in fewer parameters to be identifed. Obviously, the input-output modeling approach also has its disadvantages. The main one is that it is basically a black-box-type technique, in which the phenomena "inside" the plant are of no interest, as long as its response to the input is modeled correctly. If the dynamics of the plant is

easily available from physical considerations the state space model usually can be constructed with no difficulties and its parameters have well understood interpretations. On the other hand, parameters of input-output models usually such as used here for adapting the control have no immediate physical interpretation [39].

In order to describe such input-output models in a succinct manner, we introduce the forward and backward shift operator q and q^{-1} . If y(t) denotes the value of the a sequence {y(t)} at time t, where $t \in \{0,1,\ldots\}$, then $qy(t)$ denotes the value of the sequence at time (t+1) and q^{-1} y(t) denotes the value of the sequence at time (t-1). That is,

$$qy(t) = y(t+1) \qquad \text{for } t \geq 0 \tag{3.1.1}$$

$$q^{-1}\, y(t) = y(t-1) \qquad \text{for } t \geq 1\ ; \quad q^{-1}\, y(0) = 0 \tag{3.1.2}$$

and consequently,

$$q^{i}\, y(t) = y(t+i) \qquad \text{for } t \geq 0 \tag{3.1.3}$$

$$q^{-i} y(t) = y(t-i) \qquad \text{for } t \geq i\ ; \quad q^{-1}\, y(0) = 0 \quad \text{for } 0 \leq t < i \tag{3.1.4}$$

The first approach is to simply assume that the model can be adequately described by a linear time-varying system. Such a linear time-varying system can be described by the equation.

$$A(q^{-1},t)y(t) = B(q^{-1},t)u(t) \tag{3.1.5}$$

where A and B are time varying polynomials of q^{-1}. A, without loss of generality, is assumed to be monic. Thus, $A(q^{-1},t)$ could be described by the equation below.

$$A(q^{-1},t) = 1 + a_1(t)\, q^{-1} + a_2(t)\, q^{-2} + a_3(t)\, q^{-3} + \ldots + a_n(t)\, q^{-n} \tag{3.1.6}$$

This leads to a simple traditional linear prediction model with the following form :

$$\hat{y}(t) = \Phi(t)^T \hat{\theta}(t) \tag{3.1.7}$$

$$\Phi(t)^T = [y(t-1), y(t-2), \ldots, y(t-n), u(t-1), u(t-2), \ldots, u(t-m)] \tag{3.1.8}$$

$$\hat{\theta}(t)^T = [-a_1(t), -a_2(t), \ldots, a_n(t), b_1(t), b_2(t), \ldots, b_m(t)] \tag{3.1.9}$$

The second approach is to simply add bilinear terms in u and y and thus to assume that the system can be adequately described by a bilinear time-varying discrete model even if aircraft dynamic models are not bilinear with regard to natural controls. Still the closed loop system would be equivalent to a bilinear system with nonlinear feedback.

A bilinear time-varying discrete system can be described by

$$y(t) = \sum_{i=1}^{my} a_i y(t-i) + \sum_{i=1}^{mz} b_i u(t-i) + \sum_{i=1}^{my} \sum_{j=1}^{mz} c_{ij} y(t-i) u(t-j) \tag{3.1.10}$$

where my, mz, are the orders of the output and input, respectively.

This leads to a simple prediction model with the following form :

$$\hat{y}(t) = \Phi(t)^T \hat{\theta}(t) \tag{3.1.11}$$

$$\Phi(t)^T = [y(t-1), y(t-2), \ldots, y(t-my), u(t-1), u(t-2), \ldots, u(t-mz), y(t-1)u(t-1), y(t-2)u(t-1), \ldots, y(t-my)u(t-mz)] \tag{3.1.12}$$

$$\hat{\theta}(t)^T = [-a_1(t), -a_2(t), \ldots, a_n(t), b_1(t), b_2(t), \ldots, b_m(t), c_{11}, c_{21}, \ldots, c_{my\,mz}] \tag{3.1.13}$$

The third approach for forming a prediction model is to use a more complex nonlinear representation. There are several standard input-output modeling

techniques for nonlinear systems in both discrete and continuous time settings. They include Volterra series, nonlinear time series, neural networks, etc. In this work, the time- series approach is used. This technique is a natural extension of discrete-time modeling of linear systems, known in the stochastic setting as auto-regressive moving average (ARMA) models. Therefore, an often used acronym is NARMA - for nonlinear ARMA [7]. The nonlinear time series expresses future values of outputs as a nonlinear function of a finite number of past values of output and of control. For the purpose of system identification this unknown nonlinear function is usually decomposed into a sum of nonlinear functions with parameters to be identified appearing linearly. This allows for easy application of parameter identification techniques from linear system theory, although their convergence in an on-line identification setting in a feedback loop is a far more complicated question than in the linear case. If the time series model is to be used for calculation of control action, it is also desirable that it should be easily solved for current value of control. In the aircraft problem, the physical model of the dynamics is well known and is easily expressible in state space form. Nevertheless, there are significant reasons to look at input-output black-box-type modeling as an alternative approach. The main problem arises from the aerodynamic stability derivatives. They are complex nonlinear functions of angle of attack, Mach number, and altitude [39]. If these relationships are entered into state space model, it appears so complicated that its usefulness for on-line control generation become quite doubtful. Furthermore, the exact form of the dependencies for stability derivatives on state variables is not known.

The model is given by

$$y(t) = F_G(y(t-1), y(t-2), \ldots, y(t-ny), u(t-1), u(t-2), \ldots, u(t-nz)) \tag{3.1.14}$$

where F_G (.) is some nonlinear function, ny and nz represent the order of output and input [24].

3.2 Prediction Model for A Modified F/A-18 Aircraft.

Typically, an open loop aircraft with a classical configuration operating in a trimmed condition at a conventional flight condition will exhibit two longitudinal modes of motion : the short period and phugoid. The short period mode is normally fast and oscillatory and can take place at nearly constant speed. It is dominated by angle of attack and pitch rate response. The phugoid mode is normally slow, oscillatory, and lightly damped and can take place at nearly constant angle of attack. As can be seen from section 3.1, several different approaches exist to formulate a prediction model for a nonlinear system. In this section, a prediction model of rapid angle of attack changes was considered. The first prediction model corresponds to the prediction in equation (3.1.7). The first approach is to simply assume that the model can be described by a linear time varying system. This is the simplest linear predictor, and it will be seen that it is also the least effective. The prediction model is described below [10].

$$\hat{\alpha}(t) = \Phi(t)^T \hat{\theta}(t-1) \tag{3.2.1}$$

$$\Phi^T(t) = [\,\alpha(t-1) \;\; q(t-1) \;\; \delta_h(t-1)\,] \tag{3.2.2}$$

Second, one more regressor was considered. This predictor model is similar to the first predictor model except that the order has been increased.

$$\hat{\alpha}(t) = \Phi(t)^T \hat{\theta}(t-1) \tag{3.2.3}$$

$$\Phi^T(t) = [\,\alpha(t-1)\; q(t-1)\; \alpha(t-2)\; q(t-2)\; \delta_h(t-1)\,] \tag{3.2.4}$$

The second prediction model is better than the first one because a higher-order linear model was able to identify some of the nonlinearities.

Third, thrust vectoring is added to the prediction models. The addition of the thrust vectoring into the prediction models is a relatively simple matter. It is described by the following equation.

$$\hat{\alpha}(t) = \Phi(t)^T \hat{\theta}(t-1) \tag{3.2.5}$$

$$\Phi^T(t) = [\,\alpha(t-1)\; q(t-1)\; \alpha(t-2)\; q(t-2)\; \delta_h(t-1)\; \delta_v(t-1)\,] \tag{3.2.6}$$

Another approach was made by Collins [10] as follows.

$$\hat{\alpha}(t) = \Phi(t)^T \hat{\theta}(t-1) \tag{3.2.7}$$

$$\Phi(t)^T = [\alpha(t-2),\, q(t-2),\, \alpha(t-3),\, q(t-3),\, \alpha(t-4),\, q(t-4),\, \delta_h(t-1),\; \delta_v(t-1),\, \delta_h(t-2),\, \delta_v(t-2),\, \delta_h(t-3),\, \delta_v(t-3)\,] \tag{3.2.8}$$

Some attempts are made to improve prediction models of nonlinear dynamic equations of aircraft. As aerodynamic coefficients are shown in equation (2.3.1) - (2.3.3), they are functions of angle of attack, Mach number, stabilator angle, and altitude. Specifically, coefficient values depend on angle of attack. For instance,

Figures 3.1- 3.7 show its values in case of Mach number M = 0.3 , stabilator angle (δh)= 0.0, and altitude = 15,000 ft [5]. In modeling, there exist some restrictions to be considered because of physical properties such as limitation of velocity and magnitude of inputs. Thrust vector must be considered for rapid high angle of attack maneuver. There are several prediction models of angle of attack as follows. Some attempts are made to improve prediction models of the nonlinear dynamic equation of aircraft.

A bilinear prediction model for the aircraft can be generated as in equation (3.1.10) so that

$$\hat{\alpha} = \Phi(t)^T \hat{\theta}(t-1) \tag{3.2.9}$$

$$\begin{aligned}\Phi(t)^T = [&\alpha(t-2), q(t-2), \alpha(t-3), q(t-3), \alpha(t-4), q(t-4), \delta_h(t-1),\\ &\delta_v(t-1), \delta_h(t-2), \delta_v(t-2), \delta_h(t-3), \delta_v(t-3), \alpha(t-2)\delta_h(t-1)\\ &\alpha(t-3)\delta_h(t-2), \alpha(t-4)\delta_h(t-3), \alpha(t-2)\delta_v(t-1)]\end{aligned} \tag{3.2.10}$$

This nonlinear prediction model for the aircraft was developed by Mohler et al [39]. A slightly more complex nonlinear prediction model for the aircraft is considered by adding quadratics and cubics in angle of attack which would naturally better fit the aerodynamic parameters

$$\hat{\alpha} = \Phi(t)^T \hat{\theta}(t-1) \tag{3.2.11}$$

$$\begin{aligned}\Phi(t)^T = [&\alpha(t-1), \alpha(t-1)^2, \alpha(t-1)^3, q(t-1), \alpha(t-1)q(t-1),\\ &\alpha(t-1)^2 q(t-1), \alpha(t-1)^3 q(t-1), \delta_h(t-1), \alpha(t-1)\delta_h(t-1),\\ &\alpha(t-1)^2 \delta_h(t-1), \alpha(t-1)^3 \delta_h(t-1), 1]\end{aligned} \tag{3.2.12}$$

A nonlinear prediction model proposed in this section, including the thrust vector, was developed as follows. The choice of elements of the regressors' vector, $\Phi(t)$, is motivated by the fact that nonlinearities in the short period dynamics are associated with angle of attack. Also it is recognized that due to the highly nonlinear nature of the aircraft dynamics it is probably impossible to fit a black-box-type model describing the plant's dynamics accurately in the whole ranged of flight condition. Instead, it is more practical to fit a simple approximate model including square and cubic terms of angle of attack, thrust vectoring, and coupling term between angle of attack and control inputs.

$$\hat{\alpha} = \Phi(t)^T \hat{\theta}(t-1) \tag{3.2.13}$$

$$\begin{aligned}\Phi(t)^T = [&\alpha(t-2),\ q(t-2),\ \alpha(t-3),\ q(t-3),\ \alpha(t-4),\ q(t-4),\ \delta_h(t-1),\\ &\delta_v(t-1),\ \delta_h(t-2),\ \delta_v(t-2),\ \delta_h(t-3),\ \delta_v(t-3),\ \alpha(t-2)\delta_h(t-1),\\ &\alpha(t-3)\delta_h(t-2),\ \alpha(t-2)q(t-2),\ \alpha(t-2)q(t-2),\ \delta_v(t-1)\alpha(t-2),\\ &\delta_v(t-2)\alpha(t-3),\ \alpha(t-2)^2,\ \alpha(t-3)^2,\ \alpha(t-2)^3,\ \alpha(t-2)^2 q(t-2),\\ &\alpha(t-2)^2\delta_h(t-1),\ \delta_v(t-1)\alpha(t-2)^2]\end{aligned} \tag{3.2.14}$$

As would be expected from Figures 3.1-3.7, it is difficult to control this modified F/A-18 aircraft during a large variation in angle of attack. In this section, several different simulations were performed to evaluate the model performance with two types of maneuver. The maneuver one corresponds to the maneuver presented by Ostroff in [49]. [50], [51]. The angle of attack is changed from 5 degrees, to 60

degrees, to 35 degrees, and back to 5degrees in 8 second interval. In maneuver two, the angle of attack is changed from 5 degrees, to 35 degrees, and to 85 degrees for an extended period of time. In particular, it is hard to control the angle of attack during maneuver one or maneuver two because stability derivative coefficients changes around 60 degrees and 85 degrees. Prediction error of angle of attack (difference between reference trajectory and angle of attack of actual system) is shown in Figures 3.8-3.17. The unit of prediction error is degree. The magnitude of prediction error has the range from -0.3 degrees to 0.2 degrees for all cases. The prediction errors of angle of attack depend on controller inputs as well as prediction models.

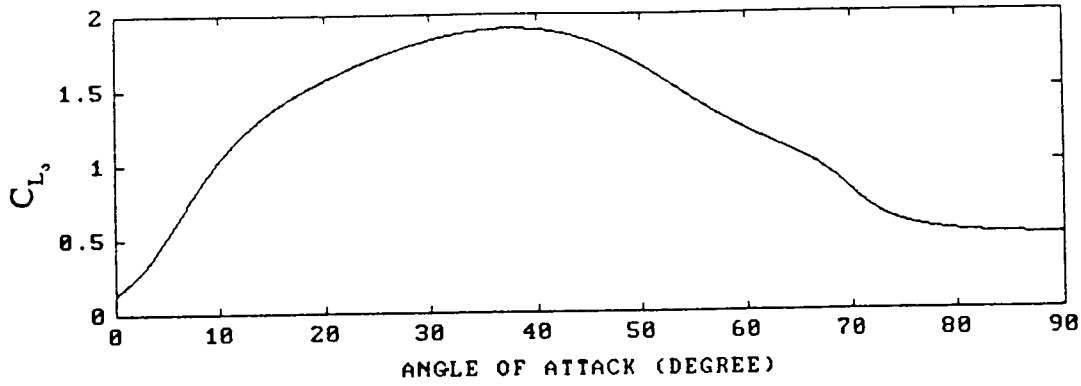

Figure 3.1 Stabilator Derivative C_{L_o} at M = 0.3, δ_h = 0.0, and h = 15,000 ft.

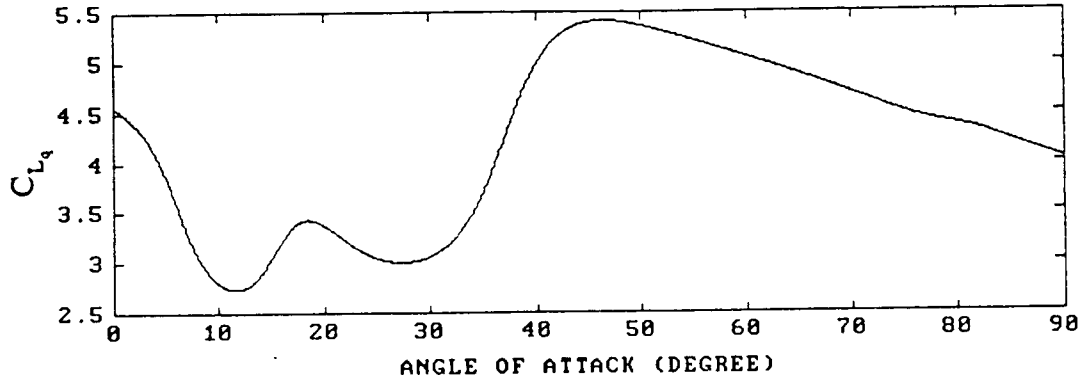

Figure 3.2 Stabilator Derivative C_{L_q} at M = 0.3, δ_h = 0.0, and h = 15,000 ft.

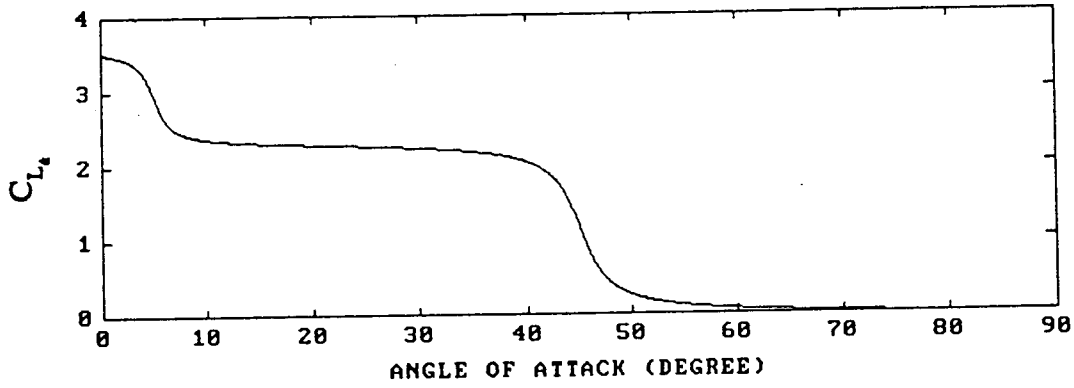

Figure 3.3 Stabilator Derivative C_{L_α} at M = 0.3, δ_h = 0.0, and h = 15,000 ft.

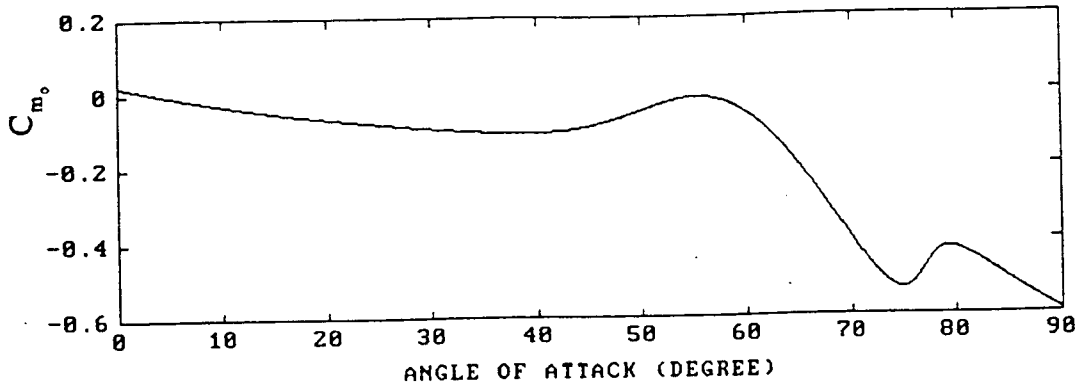

Figure 3.4 Stabilator Derivative C_{m_o} at M = 0.3, δ_h = 0.0, and h = 15,000 ft.

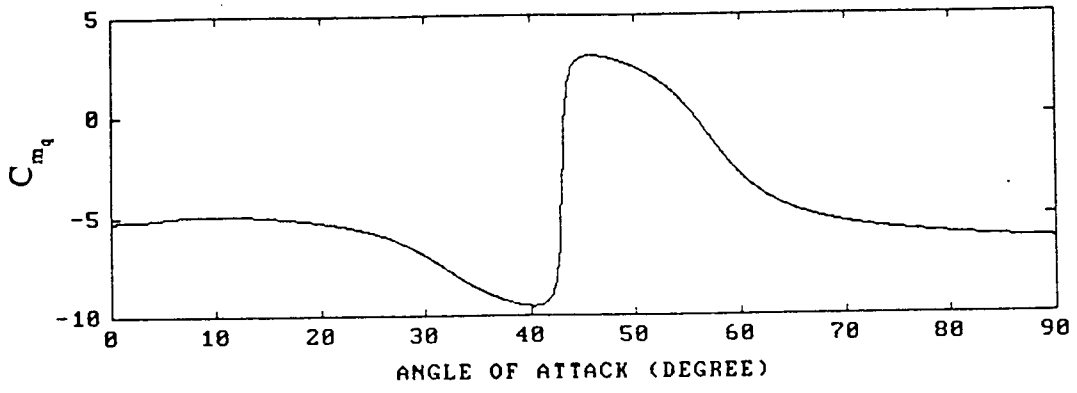

Figure 3.5 Stabilator Derivative C_{m_q} at M = 0.3, δ_h = 0.0, and h = 15,000 ft.

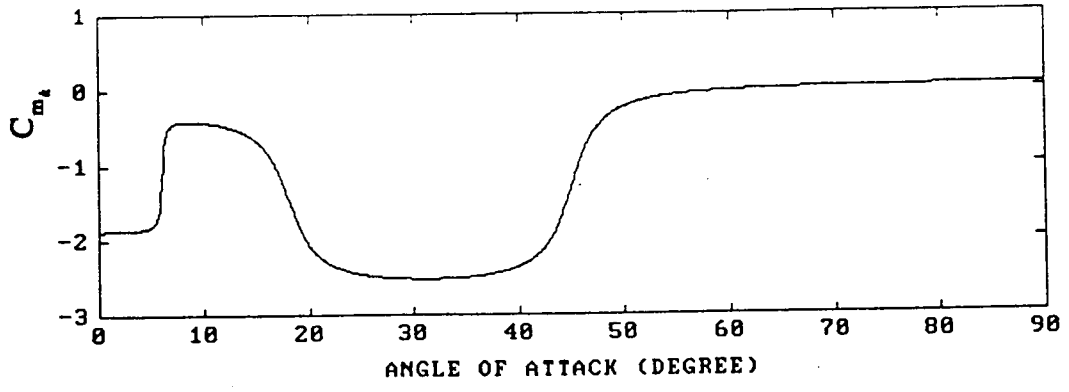

Figure 3.6 Stabilator Derivative C_{m_α} at M = 0.3, δ_h = 0.0, and h = 15,000 ft.

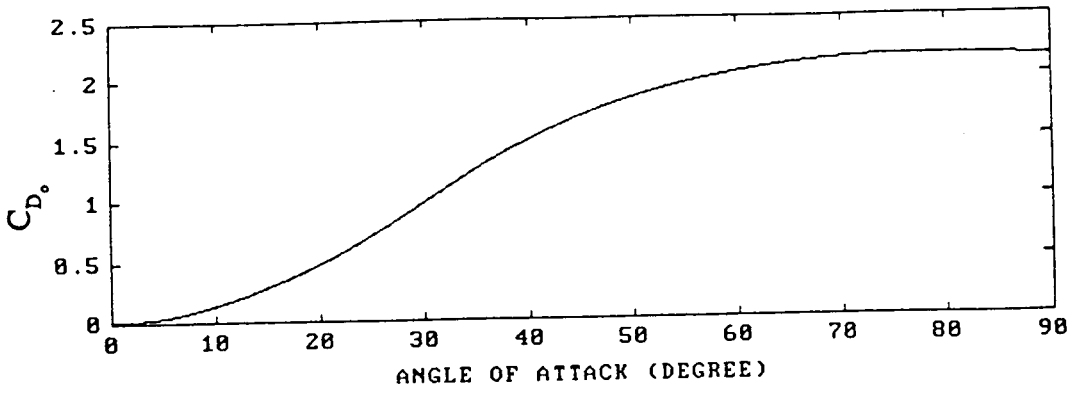

Figure 3.7 Stabilator Derivative C_{D_o} at M = 0.3, δ_h = 0.0, and h = 15,000 ft.

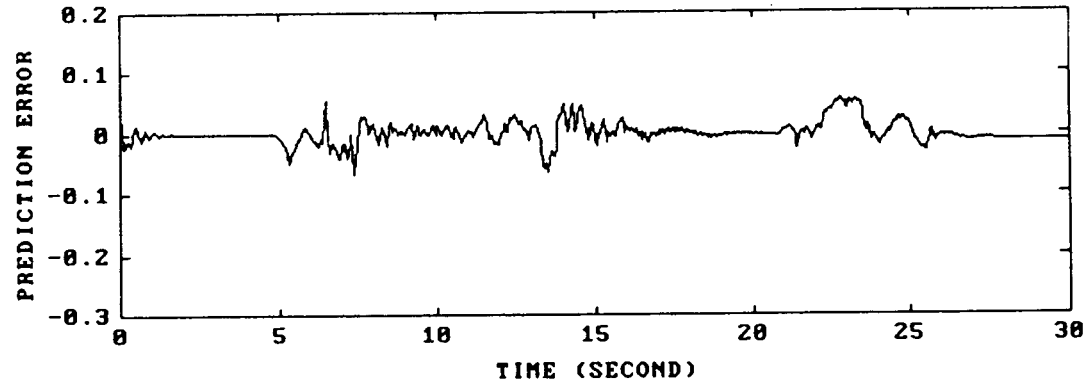

Figure 3.8 Prediction Error of Angle of Attack in case of Maneuver One, LPM, and Prediction Controller.

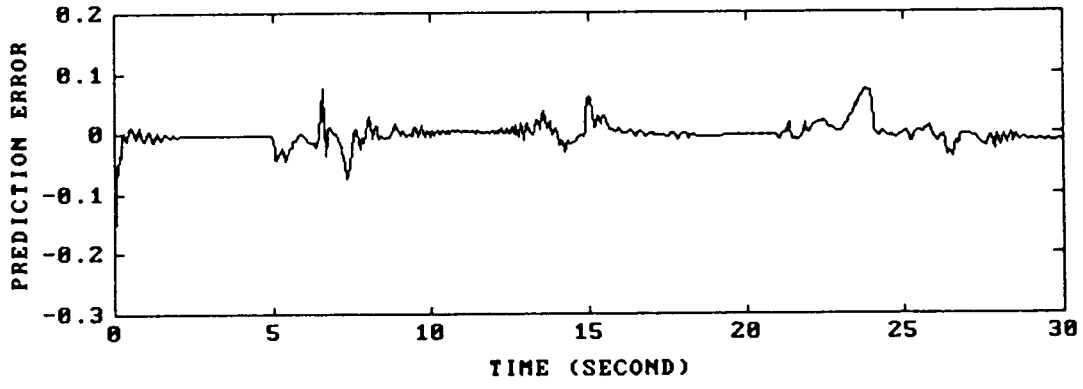

Figure 3.9 Prediction Error of Angle of Attack in case of Maneuver One, BLPM, and Prediction Controller.

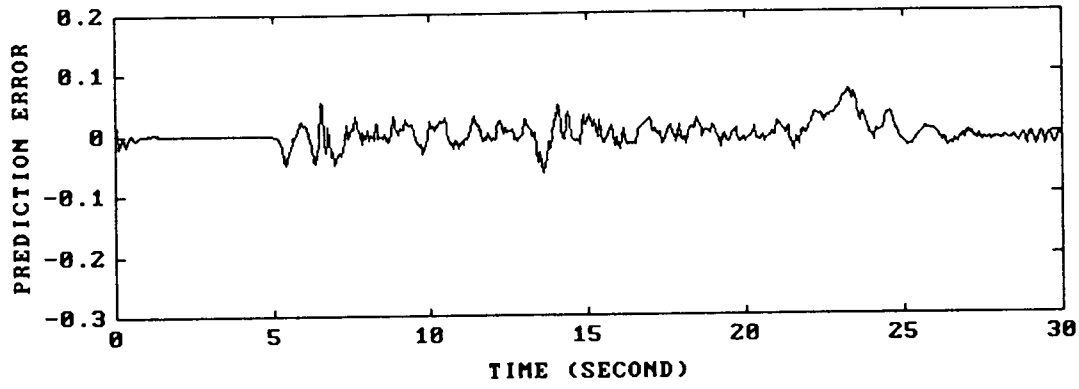

Figure 3.10 Prediction Error of Angle of Attack in case of Maneuver One, NLPM, and Prediction Controller.

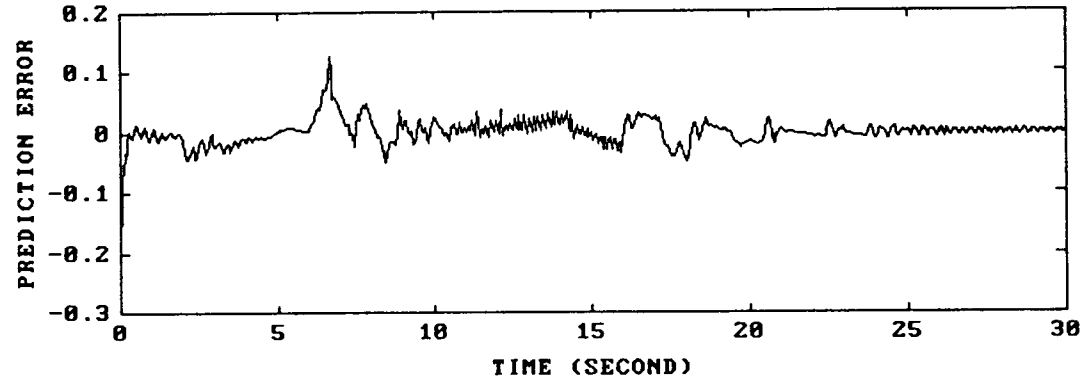

Figure 3.11 Prediction Error of Angle of Attack in case of Maneuver Two, LPM, and Prediction Controller.

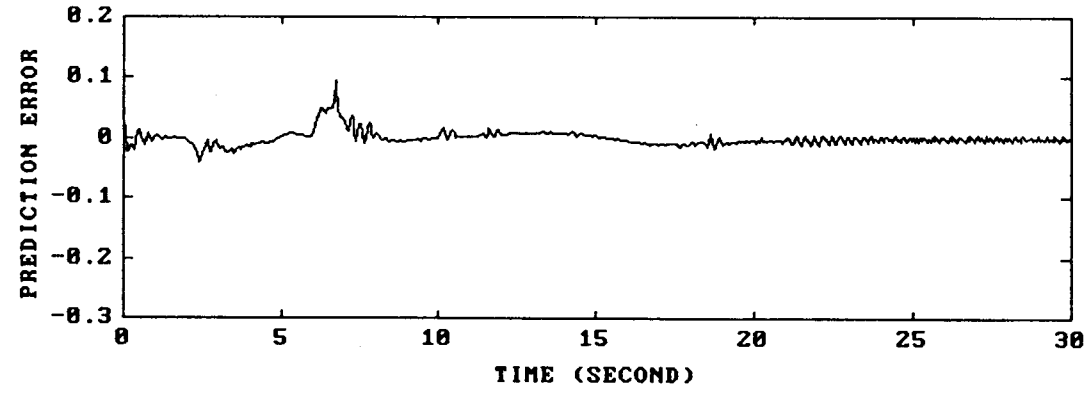

Figure 3.12 Prediction Error of Angle of Attack in case of Maneuver Two, BLPM, and Prediction Controller.

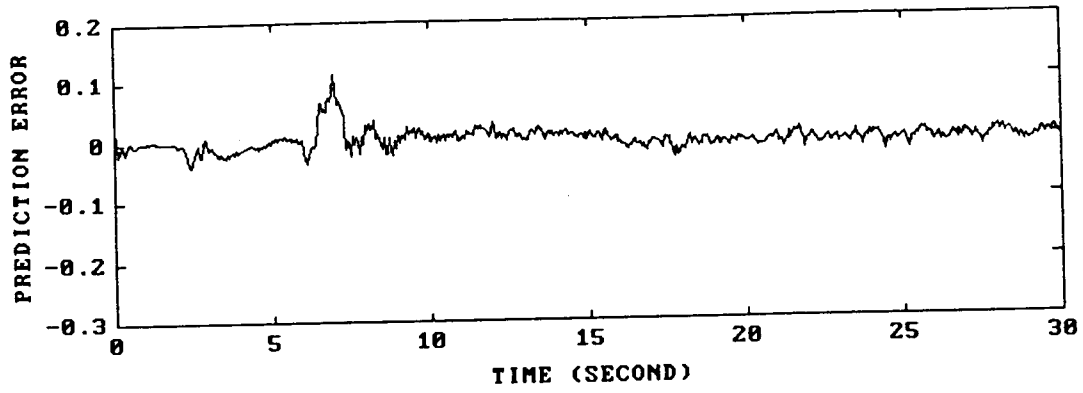

Figure 3.13 Prediction Error of Angle of Attack in case of Maneuver Two, NLPM, and Prediction Controller.

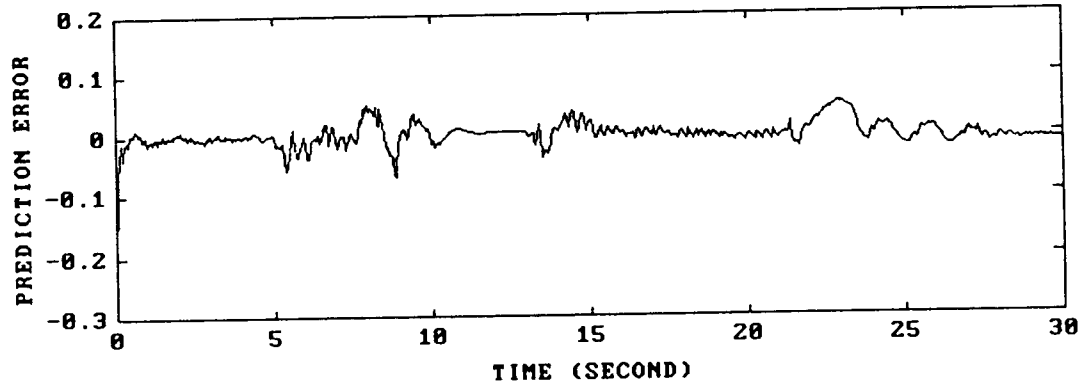

Figure 3.14 Prediction Error of Angle of Attack in case of Maneuver One, LPM, and LF Controller.

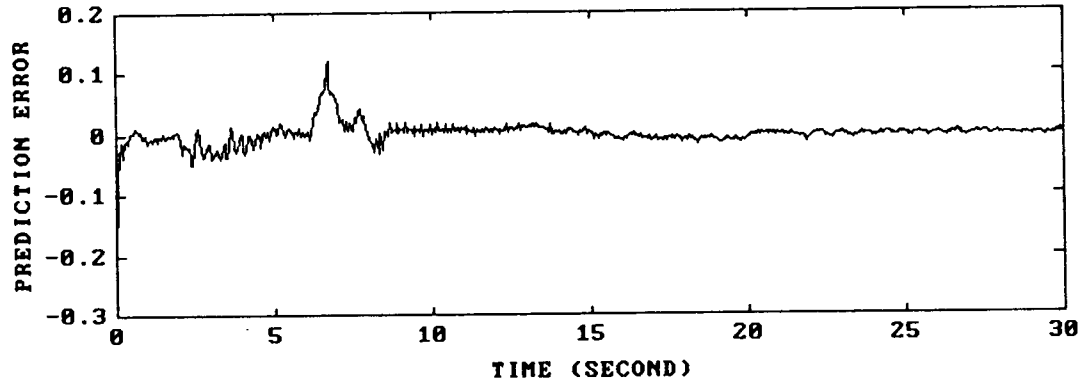

Figure 3.15 Prediction Error of Angle of Attack in case of Maneuver Two, LPM, and LF Controller.

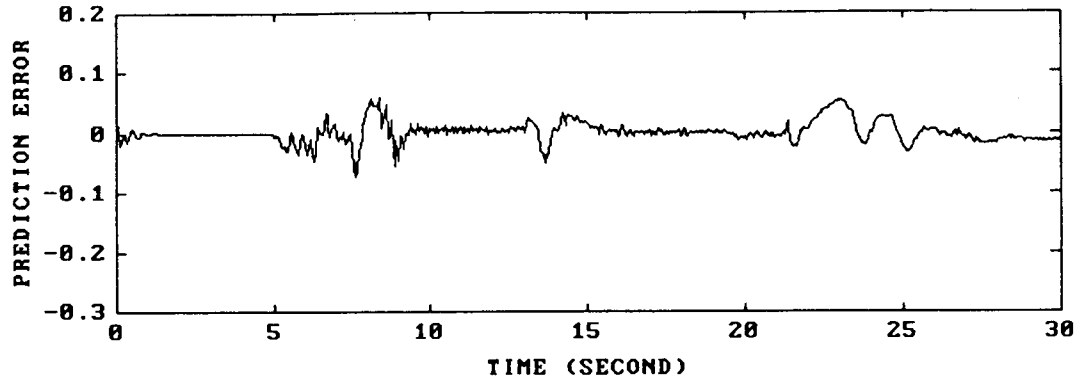

Figure 3.16 Prediction Error of Angle of Attack in case of Maneuver One, NLPM, and LF Controller.

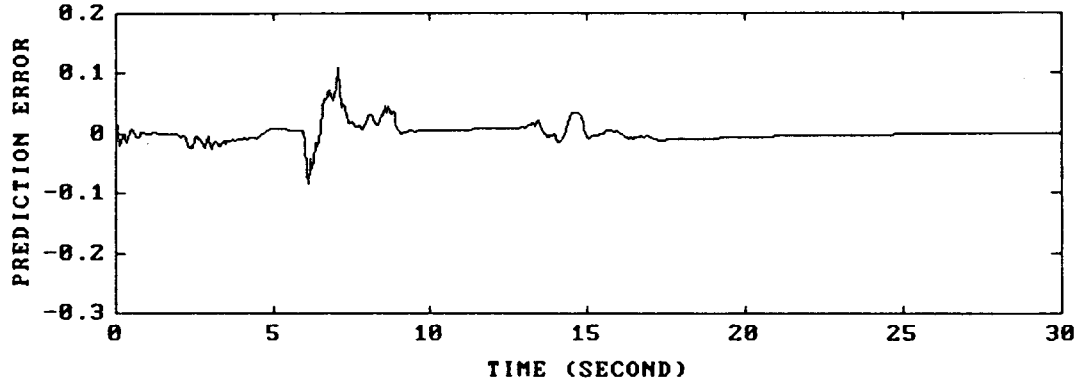

Figure 3.17 Prediction Error of Angle of Attack in case of Maneuver Two, NLPM, and LF Controller.

3.3 Parameter Estimation.

3.3.1 Overview of the Recursive Least Squares Algorithm.

The recursive-least-squares (RLS) algorithm is the most popular on-line parameter estimation algorithm. The basic least squares method produces a parameter estimate which is the result of minimization of the following quadratic cost function :

$$J_N = \frac{1}{N}\sum_{t=1}^{N} \lambda^{N-t}(y(t) - \hat{\theta}^T(t-1)\,\phi(t))^2 \qquad (3.3.1)$$

The problem is to obtain model parameter estimates which,in a least squares sense, minimize the difference between the actual output, y(t), and its value predicted by the model . The vector contains past input and output values and its dimension depends on the order of the model to be estimated.

This leads to the recursive least squares algorithm with a variable forgetting factor [18].

Parameter vector update law :

$$\hat{\theta}(t) = \hat{\theta}(t-1) + K(t)\,[y(t) - \hat{\theta}(t-1)^T\phi(t)] \qquad (3.3.2)$$

Gain update :

$$K(t) = \frac{P(t-1)\phi(t)}{\lambda + \phi(t)^T P(t-1)\phi(t)} \qquad (3.3.3)$$

Covariance matrix update :

$$P(t) = \frac{1}{\lambda}\left(P(t-1) - \frac{P(t-1)\phi(t)\phi(t)^T P(t-1)}{\lambda + \phi(t)^T P(t-1)\phi(t)}\right) \tag{3.3.4}$$

The basic RLS algorithm with $\lambda = 1$ has several important properties. First the least squares algorithm has a fast convergence rate (exponentially fast for a linear time invariant system with proper excitation). Also, the stability of the RLS algorithm combined with direct and indirect adaptive control is well understood and many proofs have been published in this area [4], [18], [23], [48]. The main disadvantage with the basic RLS is that the covariance matrix gradually decays to a small value and therefore the algorithm does not retain its adaptivity to adequately track time varying systems. The covariance matrix in the RLS algorithm tends towards zero which causes the adaptation to turn off. This is undesirable in the case where the parameters are time varying. Several modifications have been made to the RLS algorithm to correct this problem. A variety of modifications are proposed in the literature to keep the algorithm awake. The modifications in general are of two different types. The first idea is the inclusion of a forgetting factor. The second type of modifications that have been proposed is to manipulate the covariance matrix directly.

3.3.2 Forgetting Factor

(a) Least squares with exponential data weighting.

One method of ensuring that the algorithm retains its alertness is to make use of the parameter in equation (3.3.2) - (3.3.4). To use a value of $\lambda < 1$ means that the cost function in equation (3.3.4) is minimized with more recent errors receiving heavier weighting. The choice of λ also is important because too fast discounting of older data (small λ) will make the estimates uncertain and too slow discounting will make it difficult to track fast parameter variations. It has been shown in Soderstrom, Ljung, and Gustavsson [18] that a good choice in such cases is

$$\lambda(t) = \lambda_o \lambda(t-1) + (1-\lambda_o) \tag{3.3.5}$$

with typical values $\lambda(t_o) = 0.95$, $\lambda_o = 0.99$. The effect of this is to impose exponential data weighting for a transient period during algorithm startup. This algorithm works well only if the process has excitation. Otherwise, exponential forgetting leads to covariance windup.

(b) RLS with constant trace and scaling

Sripada and Fisher [57] have proposed the following four modifications to the basic least squares algorithm :

(1) Normalization.

(2) Scaling.

(3) Constant trace through a variable forgetting factor.

(4) An information content based on criterion for turning adaptation on or off.

The importance of normalization and forgetting factor has already been discussed earlier. The modification with respect to scaling is concerned with improving the numerical properties of the algorithm but has no effect on the convergence properties of the algorithm. Property(3) concerns updating of the covariance matrix. The forgetting factor $\lambda(t)$ is selected so that the trace of the covariance matrix is constant. The following choice of $\lambda(t)$ ensure that $0 < \lambda(t) \leq 1$ and that trace P(.) is constant :

$$\lambda(t)=1-\frac{1}{2}\left(1+r-\left[(1+r)^2-4\frac{\|P_s(t-1)\phi(t)_{ns}\|^2}{tr\ P_s(t-1)}\right]^{\frac{1}{2}}\right) \tag{3.3.6}$$

where

$$r=\phi(t)_{ns}^T P(t-1)_s \phi(t)_{ns} \tag{3.3.7}$$

$P_s(.)$ corresponds to the scaled covariance matrix and $\phi(t)_{ns}$ corresponds to the normalized and scaled regressor. The constant trace of $P_s(.)$ ensures an upper bound on the maximum eigenvalue. The modification of Equation(3.3.4) determines the extent of discounting of old information in the current update of $P_s(.)$.

3.3.3 Covariance Modification.

(a) Covariance Resetting

The simplest way to modify the covariance matrix is to reset it periodically. This method was suggested and the convergence for the linear time invariant case was shown by Goodwin and Teoh [18]. The proofs presented in [18] covered most

of the covariance modifications presented here. Thus, the covariance matrix in equation (3.3.4) is replaced by the following:

If t/N = integer

$$P(t) = kI \qquad 0 < k_{min} < k < k_{max} < \infty \tag{3.3.8}$$

Otherwise

$$P(t)=[I-K(t)\phi(t)^T]\frac{P(t-1)}{\lambda(t)} \tag{3.3.9}$$

where k is a positive integer.

(b) Constant Covariance.

Another method proposed by Shar and Cluett in [55], is to maintain a constant covariance by the addition of a properly scaled identity matrix. This leads to the following algorithm.

$$P'(t) = [I-K(t)\phi(t)^T]\frac{P(t-1)}{\lambda(t)} \tag{3.3.10}$$

Let τ = trace($P'(t)$) and C_0, C_1 denote two positive constants such that $C_1 > C_0$.

If $\tau > C_0$

$$P(t) = P'(t) + \frac{C_1-\tau}{n} I \tag{3.3.11}$$

If $\tau \leq C_0$

$$P(t) = \frac{C_0}{\tau} P'(t) + \frac{C_1-C_0}{n} I \tag{3.3.12}$$

The algorithm ensures a constant trace of C_1, and the following bounds are placed of

the eigenvalues of P(t).

$$\frac{C_1 - C_0}{n} \leq \lambda[P(t)] \leq C_1 \tag{3.3.13}$$

n represents the size of covariance matrix.

(c) Covariance Regularization.

This mechanism for updating the covariance matrix was first proposed by Praly and modified by Ortega et al.[46] for use in their work on robust adaptive control. The basic idea is a combination of a covariance resetting feature and a guarantee of lower and upper bounds on the covariance matrix. This algorithm replaces equation (3.3.4) as follows.

where C_0, C_1 denote two strictly positive constants such that $C_1 > C_0$:

$$P'(t) = [I - K(t)\phi(t)^T]\frac{P(t-1)}{\lambda(t)} \tag{3.3.14}$$

$$P(t) = \left(1 - \frac{C_0}{C_1}\right)P'(t) + C_0 I \tag{3.3.15}$$

This modification maintains the following bound on the eigenvalues of the covariance.

$$C_0 \leq \lambda[P(t)] \leq C_1 \tag{3.3.16}$$

Its performance was reasonable, but the best results were obtained by combining the matrix regularization with the constant covariance. This resulted in the following algorithm.

Let τ = trace $(P'(t))$, C_0, C_1 denote two positive constants such that $C_1 > C_0$, and

$0 < C_2 < 1.$

If $\tau > C_0$

$$P(t) = C_2 P'(t) + \frac{C_1 - C_2 \tau}{n} I \tag{3.3.17}$$

If $\tau \leq C_0$

$$P(t) = \frac{C_0}{\tau} P'(t) + \frac{C_1 - C_0}{n} I \tag{3.3.18}$$

One way to interpret this algorithm is that it is a combination of the constant covariance and the covariance resetting.

3.4 Reference Model

The reference model is an important part of the adaptive control system. The desired performance is expressed in terms of a reference model, which gives the desired response to a command signal. For model reference adaptive control, a command signal is fed through a model system, and then the actual system is made to track the output of the model system. In general, the model reference signal is a feed forward signal and it has no feedback from the real plant. This proved to be ineffective for nonlinear time varying systems when there are some input limitations.

The approach proposed in the section uses feedback from the real plant to improve the reference trajectory. The class of models for the reference trajectory that were investigated are simply filters that use the past values of the states. Thus,

the reference model has no internal states of its own. A simple first order filter can be formed as follows :

$$\alpha_{ref}(t) = \zeta\,\alpha(t-1) + (1-\zeta)\,\alpha_{cmd} \qquad 0 \le \zeta \le 1 \qquad (3.4.1)$$

If the system being controlled was a deterministic linear time invariant system with unlimited control, the two approaches would be identical because the output of the system at (t - 1) would be equal to the reference trajectory at time (t - 1). Thus the reference model would not need any feedback from the system.

With the first order model reference, an excellent performance was achieved when the input dynamics and velocity constraints were ignored [8]. For the complete system, a second order filter was found to be sufficient to get excellent performance. A general second order filter is described in equation (3.4.2).

$$\alpha_{ref}(t) = (\zeta_1 + \zeta_2)\,\alpha(t-1) - \zeta_1\zeta_2\,\alpha(t-2) + (1 + \zeta_1\zeta_2 - \zeta_1 - \zeta_2)\,\alpha_{cmd}(t) \qquad (3.4.2)$$

The results for this reference trajectory when used on the complete system are displayed in section 5.5.

CHAPTER 4

CONTROL CALCULATION

The controller was designed to perform or meet several goals. First and most importantly, the control values are calculated such that the angle of attack of the aircraft follows the reference model. The control values are also calculated such that the thrust vectoring returns to zero if it is no longer needed, and a certain amount of smoothness is desired for the control signals.

4.1 One-step-ahead prediction contro

The following cost function is defined for control law calculation.

$$J = \frac{1}{2}\rho_1[\alpha_{ref}(t+1)-\hat{\alpha}(t+1)]^2+\frac{1}{2}\rho_2[\delta_{h_{cmd}}(t)-\delta_{h_{cmd}}(t-1)]^2 + \frac{1}{2}\rho_3[\delta_{v_{cmd}}(t)-\delta_{v_{cmd}}(t-1)]^2+\frac{1}{2}\rho_4[\delta_{v_{cmd}}(t)]^2 \tag{4.1.1}$$

where $\alpha_{ref}(.)$ represents reference trajectory of angle of attack.

Let the prediction model in equation (3.2.5) be described by,

$$\hat{\alpha}(t+1) = a(t-1)\,\delta_{h_{cmd}}(t) + b(t-1)\,\delta_{v_{cmd}}(t) + \bar{\phi}(t)^T\,\bar{\theta}(t-1) \tag{4.1.2}$$

where

$$\phi(t) = [\delta_{h_{cmd}}(t),\quad \delta_{v_{cmd}}(t),\quad \bar{\phi}(t)] \tag{4.1.3}$$

$$\theta(t-1)^T = [\, a(t-1),\ b(t-1),\ \bar{\theta}(t-1)^T \,] \tag{4.1.4}$$

$$\bar{\phi}(t) = [\, \alpha(t-1),\ q(t-1),\ \alpha(t-2),\ q(t-2) \,] \tag{4.1.5}$$

Taking the derivative of **J** with respect to the control yields

$$\begin{aligned} \frac{dJ}{d\delta_{h_{cmd}}} &= \rho_1[\alpha_{ref}(t+1)-\hat{\alpha}(t+1)](-a)+\rho_2[\delta_{h_{cmd}}(t)-\delta_{h_{cmd}}(t-1)] \\ \frac{dJ}{d\delta_{v_{cmd}}} &= \rho_1[\alpha_{ref}(t+1)-\hat{\alpha}(t+1)](-b)+\rho_3[\delta_{v_{cmd}}(t)-\delta_{v_{cmd}}(t-1)] \\ &\quad +\rho_4[\delta_{v_{cmd}}(t)] \end{aligned} \tag{4.1.6}$$

Consequently, the external control command yields

$$\begin{bmatrix} \delta_{h_{cmd}}(t) \\ \delta_{v_{cmd}}(t) \end{bmatrix} = \begin{bmatrix} \rho_1 a^2+\rho_2 & \rho_1 ab \\ \rho_1 ab & \rho_1 b^2+\rho_3+\rho_4 \end{bmatrix}^{-1} \begin{bmatrix} \rho_1 a\eta+\rho_2\delta_{h_{cmd}}(t-1) \\ \rho_1 b\eta+\rho_3\delta_{v_{cmd}}(t-1) \end{bmatrix} \tag{4.1.7}$$

where

$$\eta = \alpha_{ref} - \bar{\phi}(t)^T\bar{\theta}(t-1) \tag{4.1.8}$$

To include the velocity and magnitude limits in the control calculation, two extra conditions are added. The first condition requires that $\delta_{v_{cmd}}(t)$ be recalculated if $\delta_{h_{cmd}}(t)$ has reached the magnitude limit. The second condition requires that $\delta_{v_{cmd}}(t)$ be recalculated if $\delta_{h_{cmd}}(t)$ is a value requiring 80 degrees per second. $\delta_{v_{cmd}}(t)$ is recalculated as follows:

$$\delta_{v_{cmd}}(t) = \frac{\eta - a\delta_{h_{cmd}}(t)}{b} \tag{4.1.9}$$

After the control values have been calculated, they are limited by 40 degrees per second for $\delta_{h_{cmd}}(t)$ and by 80 degrees per second for $\delta_{v_{cmd}}(t)$.

4.2 Control Law Based on A Lyapunov Function.

Consider a type of bilinear system as follows.

$$x_{k+1} = A_k x_k + B u_k + \sum_{i=1}^{2} N_i x_k u_{il} \tag{4.2.1}$$

where $x_k \in R^2$ are state variables, $u_k = [\ \delta_{h_{cmd}}(t),\ \delta_{v_{cmd}}(t)]^T \in R^2$ are input variables, and u_{il} , is each component of input variable. A_k, B_k, and N_i are appropriate matrices.

A Lyapunov function candidate is defined as follows.

$$V_k = (x_{ref} - x_k)^T P (x_{ref} - x_k) + u_k{}^T R u_k \tag{4.2.2}$$

where T represents transpose of vector or matrix. P and R are positive definite and symmetric, respectively. $x_{ref} = [\ x_{ref,1}\ ,\ \ x_{ref,2}\ ]^T$ represents reference trajectories. The difference of a Lyapunov function candidate is given by

$$\Delta V_k = V_k - V_{k-1} \tag{4.2.3}$$

In this section, main objective is to find a controller which minimizes the derivative of a Lyapunov function candidate in condition under $\Delta V_k < 0$. Equation (4.2.1) can

be rewritten as follows.

$$x_{k+1} = A_k x_k + \bar{B} u_k \tag{4.2.4}$$

where

$$\bar{B} = [\,(B_1 + N_1 x_k) \quad (B_2 + N_2 x_k)\,] \tag{4.2.5}$$

Also define

$$B = [\,B_1 \,|\, B_2\,] \tag{4.2.6}$$

Taking the derivative of equation (4.2.3) with respect to the controls , and setting to 0

$$\frac{\partial \Delta V_k}{\partial u_k} = 0 \tag{4.2.7}$$

The controls give as follows.

$$u_k = (\bar{B}^T P \bar{B} + R)^{-1} (\bar{B}^T P (x_{ref} - A_k x_k)) \tag{4.2.8}$$

To include the velocity and magnitude limits in control calculation, two extra conditions are added. The first condition requires that $\delta_{v_{cmd}}(t)$ be recalculated if $\delta_{h_{cmd}}(t)$ has reached the magnitude limit. The second condition requires that $\delta_{v_{cmd}}(t)$ be recalculated if $\delta_{h_{cmd}}(t)$ is a value requiring 80 degrees per second. $\delta_{v_{cmd}}(t)$ is recalculated as follows.

$$\delta_{v_{cmd}}(t) = \frac{\eta_{11}P(1,1)b_1 + \eta_{11}P(1,2)b_2 + \eta_{22}P(1,2)b_1 + \eta_{22}P(2,2)b_2}{b_1^2P(1,1) + 2b_1b_2P(1,2) + b_2^2P(2,2)} \tag{4.2.9}$$

where

$$aa_1 = x_{ref,1} - A_k(1,1)x_{1,k-1} - A_k(1,2)x_{2,k-1} \tag{4.2.10}$$

$$a_1 = -(B_k(1,1) + N_{1,k}(1,1)x_{1,k-1}N_{1,k}(1,2)x_{2,k-1}) \tag{4.2.11}$$

$$b_1 = -(B_k(1,2) + N_{2,k}(1,1)x_{1,k-1}N_{2,k}(1,2)x_{2,k-1}) \tag{4.2.12}$$

$$aa_2 = x_{ref,2} - A_k(2,1)x_{1,k-1} - A_k(2,2)x_{2,k-1} \tag{4.2.13}$$

$$a_2 = -(B_k(2,1) + N_{1,k}(2,1)x_{1,k-1}N_{1,k}(2,2)x_{2,k-1}) \tag{4.2.14}$$

$$b_2 = -(B_k(2,2) + N_{2,k}(2,1)x_{1,k-1}N_{2,k}(2,2)x_{2,k-1}) \tag{4.2.15}$$

$$\eta_{11} = aa_1 - a_1 \tag{4.2.16}$$

$$\eta_{22} = aa_2 - a_2 \tag{4.2.17}$$

$A_k(i,j)$ represents i th row and j th column of A_k.

If the value of equation (4.2.3) with recalulated inputs is over 0, that is to say,

$$\Delta V_k = (V_k - V_{k-1}) > 0 \tag{4.2.18}$$

inputs are recalculated as follows.

The control law calculation is based on minimization of equation (4.2.1) with respect to control inputs. As this case also requires the velocity and magnitude limits in the control calculation, two extra conditions are added. The first condition requires that $\delta_{v_{cmd}}(t)$ be recalculated if $\delta_{h_{cmd}}(t)$ has reached the magnitude limit. The second condition requires that $\delta_{v_{cmd}}(t)$ be recalculated if $\delta_{h_{cmd}}(t)$ is a value requiring 80 degrees per second. $\delta_{v_{cmd}}(t)$ is recalculated as follows:

$$\delta_{v_{cmd}}(t) = -\frac{(aa_1 + a_1\delta_{h_{cmd}}(t-1))b_1 + (aa_2 + a_2\delta_{h_{cmd}}(t-1))b_2}{b_1^2 + b_2^2} \qquad (4.2.18)$$

After the control values have been calculated they are limited by 40 degrees per second for $\delta_{h_{cmd}}(t)$ and by 80 degrees per second for $\delta_{v_{cmd}}(t)$

CHAPTER 5

APPLICATION TO A MODIFIED F/A-18 AIRCRAFT

In the design of real systems, some restrictions exist due to system physical limits. For example, the input dynamics are described by three states : thrust magnitude, thrust vectoring angle, and stabilator angle. Each state has the limitation as follows.

The range of the stabilator angle is given in equation (2.5.2)

$$-24.0° \leq \delta_h \leq 10.5°$$

The range of the thrust vectoring angle is given in equation (2.5.4)

$$-20° \leq \delta_v \leq 20°$$

The range of thrust is limited according to the following equation.

$$0 \leq T \leq 18000 \text{ lbs}$$

The stabilator and the thrust vectoring dynamics include a velocity limit of 40 degrees per second for the stabilator angle, and 80 degrees per second for the thrust vectoring angle. Considering the limitations of input properties, the linear and bilinear prediction models are used to design the controller.

5.1 Linear prediction model.

The linear prediction model shown in equations (3.2.7)-(3.2.8) is rewritten as follows.

$$\hat{\alpha}(t+1) = b_0(t-1)\delta_{h_{cmd}}(t) + b_1(t-1)\delta_{v_{cmd}}(t) + \bar{\Phi}(t)^T\bar{\theta}(t-1) \quad (5.1.1)$$

$$\bar{\Phi}(t)^T = [\alpha(t-1), q(t-1), \alpha(t-2), q(t-2), \alpha(t-3), q(t-3), \delta_{h_{cmd}}(t-1), \delta_{v_{cmd}}(t-1), \delta_{h_{cmd}}(t-2), \delta_{v_{cmd}}(t-2)] \quad (5.1.2)$$

$$\theta(t-1)^T = [\, b_0(t-1), b_1(t-1), \bar{\theta}(t-1)^T\,] \quad (5.1.3)$$

$$\phi(t)^T = [\, \delta_{h_{cmd}}(t), \delta_{v_{cmd}}(t), \bar{\Phi}(t)^T\,] \quad (5.1.4)$$

5.2 Bilinear Prediction model.

The bilinear prediction model for the aircraft described in equations (3.2.9)-(3.2.10) can be rewritten as follows.

$$\hat{\alpha}(t+1) = b_{11}(t-1)\delta_{h_{cmd}}(t) + b_{12}(t-1)\delta_{h_{cmd}}(t)\alpha(t-1) + b_{13}(t-1)\delta_{v_{cmd}}(t) + b_{14}(t-1)\delta_{v_{cmd}}(t)\alpha(t-1) + \bar{\Phi}(t)^T\bar{\theta}(t-1) \quad (5.2.1)$$

$$\bar{\Phi}(t)^T = [\alpha(t-1), q(t-1), \alpha(t-2), q(t-2), \alpha(t-3), q(t-3), \delta_{h_{cmd}}(t-1), \delta_{v_{cmd}}(t-1), \delta_{h_{cmd}}(t-2), \delta_{v_{cmd}}(t-2), \alpha(t-2)\delta_{h_{cmd}}(t-1), \alpha(t-3)\delta_{h_{cmd}}(t-2)] \quad (5.2.2)$$

$$\hat{\theta}(t-1)^T = [\, b_{11}(t-1), b_{12}(t-1), b_{13}(t-1), b_14(t-1), \bar{\theta}(t-1)^T\,] \quad (5.2.3)$$

$$\phi(t)^T = [\, \delta_{h_{cmd}}(t), \delta_{h_{cmd}}(t)\alpha(t-1), \delta_{v_{cmd}}(t), \delta_{v_{cmd}}(t)\alpha(t-1), \bar{\Phi}(t)^T\,] \quad (5.2.4)$$

5.3 Nonlinear Prediction model.

The noilinear prediction model for the aircraft described in equations (3.2.13) - (3.2.14) can be rewritten as follows.

$$\hat{\alpha}(t+1) = c_{11}(t-1)\delta_{h_{cmd}}(t) + c_{12}(t-1)\delta_{h_{cmd}}(t)\alpha(t-1) + c_{13}(t-1)\delta_{h_{cmd}}(t)\alpha(t-1)$$
$$+ c_{14}(t-1)\delta_{v_{cmd}}(t) + c_{15}(t-1)\delta_{v_{cmd}}(t)\alpha(t-1)$$
$$+ c_{16}(t-1)\delta_{v_{cmd}}(t)\alpha(t-1) + \bar{\Phi}(t)^T\bar{\theta}(t-1)$$

$$\bar{\Phi}(t)^T = [\alpha(t-1),\ q(t-1),\ \alpha(t-2),\ q(t-2),\ \alpha(t-3),\ q(t-3),\ \delta_h(t-1), \tag{5.3.1}$$
$$\delta_v(t-1),\ \delta_h(t-2),\ \delta_v(t-2),\ \alpha(t-1)\delta_h(t-1),\ \alpha(t-2)\delta_h(t-1),$$
$$\alpha(t-1)q(t-1), \alpha(t-2)q(t-2),\ \delta_v(t-1)\alpha(t-2), \tag{5.3.2}$$
$$\delta_v(t-2)\alpha(t-3),\ \alpha(t-2)^2,\ \alpha(t-3)^2,\ \alpha(t-2)^3,\ \alpha(t-2)^2q(t-2)]$$

$$\hat{\theta}(t-1)^T = [\ c_{11}(t-1),\ c_{12}(t-1),\ c_{13}(t-1),\ c_14(t-1),\ c_{15}(t-1),\ c_{16}(t-1),\ \bar{\theta}(t-1)^T\ ] \tag{5.3.3}$$

$$\phi(t)^T = [\delta_{h_{cmd}}(t),\ \delta_{h_{cmd}}(t)\alpha(t-1),\ \delta_{h_{cmd}}(t)\alpha(t-1)^2,\ \delta_{v_{cmd}}(t),\ \delta_{v_{cmd}}(t)\alpha(t-1), \tag{5.3.4}$$
$$\delta_{v_{cmd}}(t)\alpha(t-1)^2,\ \bar{\Phi}(t)^T]$$

5.4 System Identification.

Adaptation was performed using the modified RLS described in section (3.3.3).

Parameter vector update law :

$$\hat{\theta}(t) = \hat{\theta}(t-1) + K(t)(y(t) - \hat{\theta}(t-1)^T\phi(t)) \tag{5.4.1}$$

Gain update :

$$K(t) = \frac{P(t-1)\phi(t)}{\lambda + \phi(t)^T P(t-1)\phi(t)} \tag{5.4.2}$$

Covariance matrix update :

$$P'(t) = \frac{1}{\lambda}\left(P(t-1) - \frac{P(t-1)\phi(t)\phi(t)^T P(t-1)}{\lambda + \phi(t)^T P(t-1)\phi(t)}\right) \tag{5.4.3}$$

Let τ = trace($P'(t)$), C_0, C_1 denote two positive constants such that $C_1 > C_0$, and $0 < C_2 < 1$.

IF $\tau > C_0$

$$P(t) = C_2 P'(t) + \frac{C_1 - C_2\tau}{n} I \tag{5.4.4}$$

IF $\tau \leq C_0$

$$P(t) = \frac{C_0}{\tau} P'(t) + \frac{C_1 - C_0}{n} I \tag{5.4.5}$$

C_0, C_1, and C_2 are defined in Table 1.

Table 1 Weighting Factors in the Covariance Matrix

	C_0	C_1	C_2
LPM	0.98	1200	600
BLPM	0.98	1600	800
NLPM	0.98	2400	1200

Initial estimates of parameters are set to zero, and the simulation is initiated at trim conditions corresponding to alpha=5°. Then the adaptive controller is simulated with $\alpha_{cmd} = 5°$ for 5 seconds.

Initial parameters to be estimated are calculated by using the control law which minimize the performance index of equation (4.1.1) starting with $P(t) = 100*I_{dent}$, and $\lambda = 1$. I_{dent} and θ_o are given matrix and vector, respectively.

Initial θ_o in the linear prediction model of equation (3.2.7)-(3.2.8) is given as follows.

θ_o = [-0.001012 0.001357 1.036904 0.090038 0.361469 0.017329
-0.0071329 0.004686 -0.013450 0.004761 -0.352008 -0.039106]

Initial θ_o in the bilinear prediction model of equation (3.2.9)-(3.2.10) is given as follows.

θ_o = [-0.00421 0.003162 1.01936 0.091322 0.34389 0.01817
-0.01149 0.003054 -0.01350 0.002314 -0.36961 -0.038011
0.00008 -0.000512 -0.00036 -0.000642]

Initial θ_o in the nonlinear prediction model of equation (3.2.13)-(3.2.14) is given as follows.

θ_o = [- 0.00651 0.001212 1.01984 0.09006 0.34449 0.016663
- 0.01561 0.000224 - 0.01298 - 0.00023 - 0.36889 - 0.0383118
- 0.00009 - 0.001628 - 0.00055 - 0.00085 - 0.001721 0.0007598
0.00001 0.000015 0.00000 0.00000 0.000002 -0.000007]

Units of angle of attack, pitch rate, pitch angle, stability angle, and thrust vector angle are degrees, and unit of magnitude of thrust is pounds.

5.5 Reference Model.

The second-order reference trajectory is used. The parameters of the (5.5.2)
reference trajectory were not fixed but varied according to the gain schedule listed in the Table 2. The second reference trajectory is

$$\alpha_{ref}(t) = C_1(\zeta)\alpha(t-1) - C_2(\zeta)\alpha(t-2) + (1 - C_1(\zeta) + C_2(\zeta))\alpha_{cmd}(t) \quad (5.5.1)$$

where

$$\zeta = |\alpha_{cmd}(t-1) - \alpha(t-1)|$$

The values were chosen such that all but the first filter correspond to a constant percent overshoot with different rise times. The first filter simply put two discrete poles on the real axis, one at 0.87 and the other at 0.89. This is not an optimal gain schedule, and undoubtedly it can be improved.

Table 2 Constants for the Equation (5.5.1)

	$C_1(\zeta)$	$C_2(\zeta)$		$C_1(\zeta)$	$C_2(\zeta)$
$0 \le \zeta < 1$	1.7600	0.7743	$6 \le \zeta < 8$	1.8073	0.8221
$1 \le \zeta < 2$	1.7215	0.7517	$8 \le \zeta < 10$	1.8241	0.8365
$2 \le \zeta < 3$	1.7563	0.7796	$10 \le \zeta < 15$	1.8407	0.8509
$3 \le \zeta < 4$	1.7734	0.7937	$15 \le \zeta < 25$	1.8572	0.8655
$4 \le \zeta < 6$	1.7904	0.8079	$25 \le \zeta$	1.8736	0.8801

5.6 Control Law Calculation.

5.6.1 One-Step-Ahead Prediction Controller.

This controller was calculated to minimize the cost function in equation (4.1.1)

$$\begin{bmatrix} \delta_{h_{cmd}}(t) \\ \delta_{v_{cmd}}(t) \end{bmatrix} = \begin{bmatrix} \rho_1 a^2+\rho_2 & \rho_1 ab \\ \rho_1 ab & \rho_1 b^2+\rho_3+\rho_4 \end{bmatrix}^{-1} \begin{bmatrix} \rho_1 a\eta+\rho_2 \delta_{h_{cmd}}(t-1) \\ \rho_1 b\eta+\rho_3 \delta_{v_{cmd}}(t-1) \end{bmatrix} \tag{5.6.1}$$

The variables a and b are given as follows.

Linear prediction model :

$$a = b_o(t-1) \tag{5.6.2}$$

$$b = b_1(t-1) \tag{5.6.3}$$

Bilinear prediction model :

$$a = b_{11}(t-1) + b_{12}(t-1)\alpha(t-1) \tag{5.6.4}$$

$$b = b_{13}(t-1) + b_{14}(t-1)\alpha(t-1) \tag{5.6.5}$$

Nonlinear prediction model :

$$a = c_{11}(t-1) + c_{12}(t-1)\alpha(t-1) + c_{13}(t-1)\alpha(t-1)^2 \tag{5.6.6}$$

$$b = c_{14}(t-1) + c_{15}(t-1)\alpha(t-1) + c_{16}(t-1)\alpha(t-1)^2 \tag{5.6.7}$$

This leads to the following control law calculation :

$$\delta_{h_{cmd}}(t) = \frac{\delta_{h_{cmd}}(t-1)(b^2\rho_1\rho_2+\rho_2\rho_3+\rho_2\rho_4)+(a\eta-ab\delta_{v_{cmd}}(t-1)\rho_1\rho_3+a\eta\rho_1\rho_4}{b^2\rho_1\rho_2+a^2\rho_1(\rho_3+\rho_4)+\rho_2(\rho_3+\rho_4)} \tag{5.6.8}$$

$$\delta_{v_{cmd}}(t) = \frac{\delta_{v_{cmd}}(t-1)(b^2\rho_1\rho_3+\rho_2\rho_3)+(b\eta - ab\delta_{h_{cmd}}(t-1)\rho_1\rho_2}{b^2\rho_1\rho_2+a^2\rho_1(\rho_3+\rho_4)+\rho_2(\rho_3+\rho_4)} \tag{5.6.9}$$

where

$$\eta = \alpha_{ref} - \bar{\phi}(t)^T\bar{\theta}(t-1) \tag{5.6.10}$$

5.6.2 Control Law based on A Lyapunov Function.

The control law is given as follows.

$$u_k = (\bar{B}^T P\bar{B}+R)^{-1}(\bar{B}^T P(x_{ref}-A_k x_k)) \tag{5.6.11}$$

Linear prediction model :

$$\bar{B} = [b_0(t-1),\ b_1(t-1)] \tag{5.6.12}$$

Nonlinear prediction model :

$$\begin{aligned}\bar{B} = [&c_{11}(t-1), c_{12}(t-1)\alpha(t-1), c_{13}(t-1)\alpha(t-1)^2,\\ &c_{14}(t-1), c_{15}(t-1)\alpha(t-1), c_{16}(t-1)\alpha(t-1)^2]\end{aligned} \tag{5.6.13}$$

$$x_{ref} - A_k x_k = \alpha_{ref} - \bar{\phi}(t)^T\bar{\theta}(t-1) \tag{5.6.14}$$

Matrix R has components R_{ij} , for i, j = 1, 2 .

5.7 Simulation.

In this section, longitudinal motions shown in equation (2.4.1) - (2.4.4) were analyzed and simulated with the adaptive control algorithm described in section 5.6. Two control signals, stabilator angle and thrust vectoring angle, are used with

scheduled thrust magnitude. Several different simulations were used to evaluate the model performance. The two cases of maneuver were defined in section 3.2 The maneuver presented here were simulated at 15,000ft and 0.3 Mach. A dotted line in figure 5.1 displays the command signal from 5 degrees, to 60 degrees, 35 degrees, and to 5 degrees in case of maneuver one while adotted line of figure 5.9 displays the command signal from 5 degrees,to 35 degrees,and to 85 degree.

5.7.1 Simulation Data.

The longitudinal equation was simulated using a fixed step fourth-order Runge Kutta method with an integration time step of 0.01 second. A comparison was made between an integration time of 0.01 and 0.001, and no noticeable difference was detected. Trim conditions of nonlinear longitudinal motion in equations (2.4.1) - (2.4.4) are given as follows.

Table3 Trim Conditions

Angle of Attack	5 degree	Stabilator Angle	0 degree
Pitch Rate	0 degree	Thrust Vector Angle	0 degree
Pitch Angle	6.3 degree	Magnitude of Thrust	3000 lbs
Total Speed	450 ft/sec		

The aircraft constant values for the simulation are shown in Table 4.

Table 4 Aircraft Constant Values

m	1035.308 slugs	p_y	0.0 ft
w	33310 lbs	p_z	0.233 ft
I_{yy}	169,945 slugs ft^2	p_{xe}	-19.37 ft
I_{xz}	- 2,971 slugs ft^2	p_{ye}	0.0 ft
S	400 ft^2	p_{ze}	0.233 ft
$\bar{c}$	11.52 ft	g	32.174 ft/sec^2
p_x	- 0.297 ft	ρ	0.001496slugs/ft^3

The weighting factor in the cost function are given with Table 5. In case of the linear prediction model, gain schedules of weighting factor are not applied in maneuver one and two. In case of the bilinear and the nonlinear prediction model, gain schedules of weighting factor are applied at 35 degrees of angle of attack. The weighting factors in a Lyapunov function are given with Table 6. In case of maneuver one, the gain schedules of weighting factor are applied at 5, 52, and 60 degrees in the linear prediction model while gain schedules of weighting factor are applied at 5, 49, and 60 degrees in nonlinear prediction model. In case of maneuver two, the gain schedule are applied at 35 degrees in the nonlinear prediction model.

5.7.2 Simulation Results.

In Figures 5.1-5.80, the longitudinal motion of a modified F/A-18 aircraft is demonstrated successfully by accurate computer simulations. The prediction model used in the design example is discussed in section 3.2. The plant has fourth-order longitudinal dynamics for short period and phugoid modes, two adaptive controllers with stabilator and thrust vectoring.

Table 5 Weighting Factors in the Cost Function

	ρ_1	ρ_2	ρ_3	ρ_4
Maneuver Both in case of LPM	100	0.001	0.001	0.001
Maneuver One in case of BLPM	94.84	0.001	0.001	0.097
α = 35.45°	95	0.0001	0.01	0.0001
Maneuver Two in case of BLPM	94.836	0.001	0.001	0.0966
α = 35.22°	89	0.07	0.00001	0.0004
Maneuver One in case of NLPM	94.209	0.001	0.001	0.0975
α = 35.84°	95	0.0001	0.01	0.0001
Maneuver Two in case of NLPM	95	0.001	0.001	0.1
α = 35.24°	97	0.0001	0.1	0.0002

The command trajectory of angle of attack is generated by a second-order filter described in equation (3.4.2). Another command trajectory, magnitude of thrust, is given as the dotted line in Figure 5.7.

Table 6 Weighting Factors in a Lyapunov Function

	P	R_{11}	R_{12}	R_{22}
Maneuver One in case of LPM	9984	2.689	2.019	1.516
α = 5.19°	9984	2.689	2.019	1.516
α = 52.28°	9984	2.689	1.967	1.4956
α = 60.38°	9984	2.689	1.969	1.4956
Maneuver Two in case of LPM	9984	2.689	2.0219	1.5184
Maneuver One in case of NLPM	4999	0.68225	0.4013	0.3861
α = 5.01°	5000	0.688	0.49	0.38
α = 49.64°	7000	0.68225	0.43	0.28
α = 60.36°	7000	0.688	0.49	0.38
Maneuver Two in case of NLPM	4999	0.68225	0.4013	0.3861
α = 35.37°	7000	0.658	0.44	0.38

The command trajectory of angle of attack is generated by a second-order filter described in equation (3.4.2). Another command trajectory, magnitude of thrust, is given as the dotted line in Figure 5.7. The main purpose of these adaptive controllers is to control the angle of attack as fast as possible to follow the command trajectory of angle of attack. Similarly, Ostroff investigated the maneuver by using numerous trim-state linearization studies accompanied by scheduled variable gain in a PIF controller [51] for the case of maneuver one. The angle of attack trajectories obtained by one-step-ahead prediction controller in case of the linear prediction, the bilinear prediction, and the nonlinear prediction model are shown in Figure 5.1, 5.17, and 5.33, respectively. The character of the response for maneuver one in the linear prediction model, the bilinear prediction model, and the nonlinear prediction model, is similar to the response reported by Ostroff in [51]. In the linear prediction model, the angle of attack reaches 55 degrees in approximately 2.0 seconds and settling time to 60 degrees of angle of attack takes about 3 seconds with maximum pitch rate of about 48 degrees per second and normal acceleration of about 2.3g. In the case of maneuver one, it is shown that, in the bilinear and the nonlinear prediction model, the angle of attack is slightly faster to achieve the command trajectory of angle of attack than that in the linear prediction model, and has a smaller value of oscillation near the command trajectory. The angle of attack trajectories obtained by the controller based on a Lyapunov function in case of the linear prediction, and the nonlinear prediction model, are shown Figure 5.49 and 5.65. The command trajectory of angle of attack is scheduled like the dotted line in Figure 5.49. The angle of attack reaches 55 degrees in approximately 3.5 seconds

and settling time to 60 degrees of angle of attack takes about 5 seconds in the case of the linear prediction model while in approximately 3.5 seconds and 4 seconds in the case of the nonlinear prediction model. The value of the maximum pitch rate is 30 degrees per seconds with normal acceleration of about 2.2g in case of both. The magnitude of thrust is scheduled due to equation (2.5.5). These are shown in Figures 5.7, 5.15, 5.23, 5.31, 5.39, and 5.47.

In case of maneuver two, the angle of attack trajectories obtained by one-step-ahead prediction controller for linear prediction and nonlinear prediction models are shown in Figures 5.9 and 5.41. The angle of attack reaches from 35 degrees to 80 degrees in approximately 2.5 seconds. Settling time to 85 degrees of angle of attack takes about 3.5 seconds with a maximum pitch rate of 50 degrees per second and normal acceleration of about 2.1g. The magnitude of thrust is scheduled due to equation (2.5.5). These are shown in Figures 5.55, 5.63, 5.70, and 5.79. The angle of attack trajectories by the controller based on a Lyapunov function is similar to that of a one-step-ahead prediction controller. In case of maneuver two, the nonlinear controllers are smoother than the linear controller. Also, the controller based on a Lyapunov function is smoother than the one-step-ahead prediction controller. The nonlinear controller is more effective than the linear controller as angle of attack is increased. The controller trajectories have small chattering in order to smooth the angle of attack while the angle of attack takes some time to attain the command trajectory in order to smooth the controller trajectory. It is requred that there is a tradeoff between prediction controller and angle of attack trajectory.

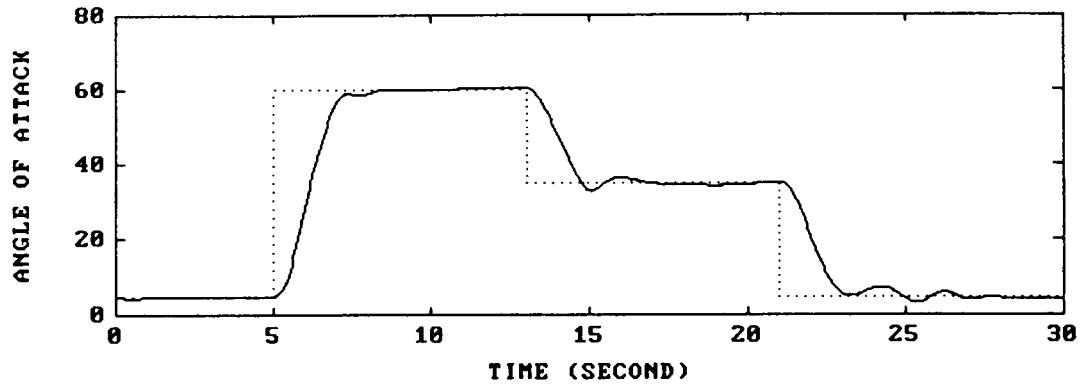

Figure 5.1 Angle of Attack in case of Maneuver One, LPM, and Prediction Controller

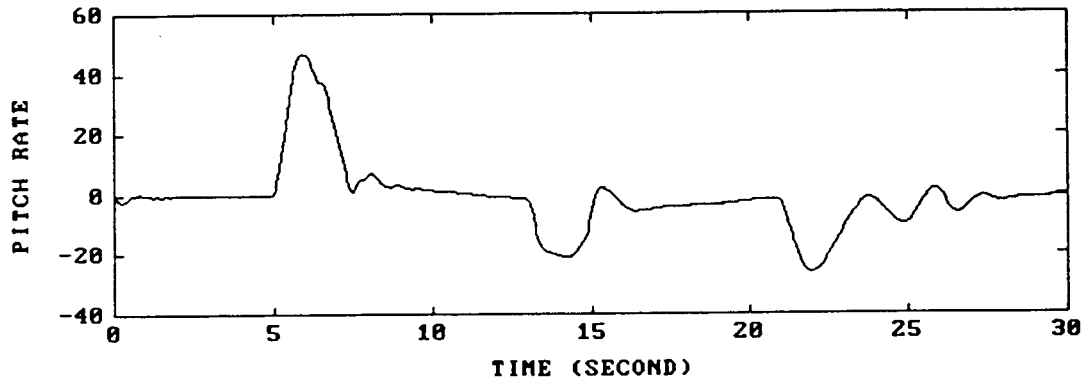

Figure 5.2 Pitch Rate in case of Maneuver One, LPM, and Prediction Controller

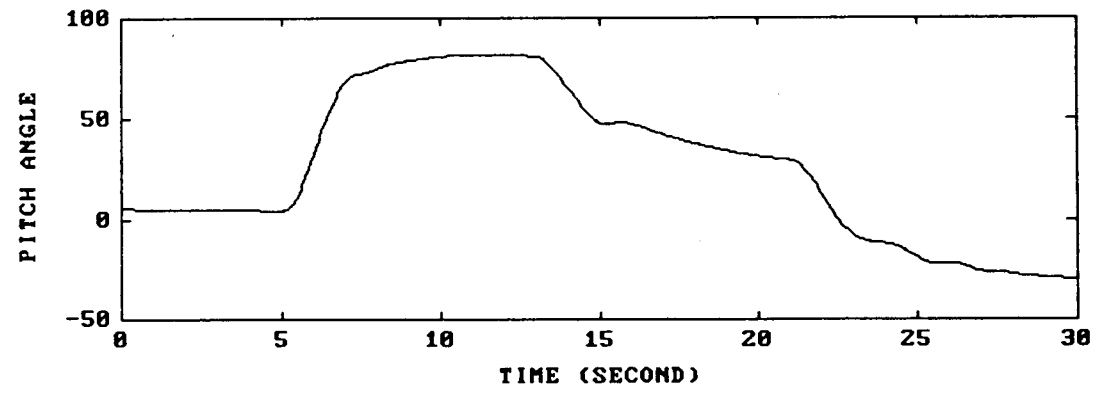

Figure 5.3 Pitch Angle in case of Maneuver One, LPM, and Prediction Controller

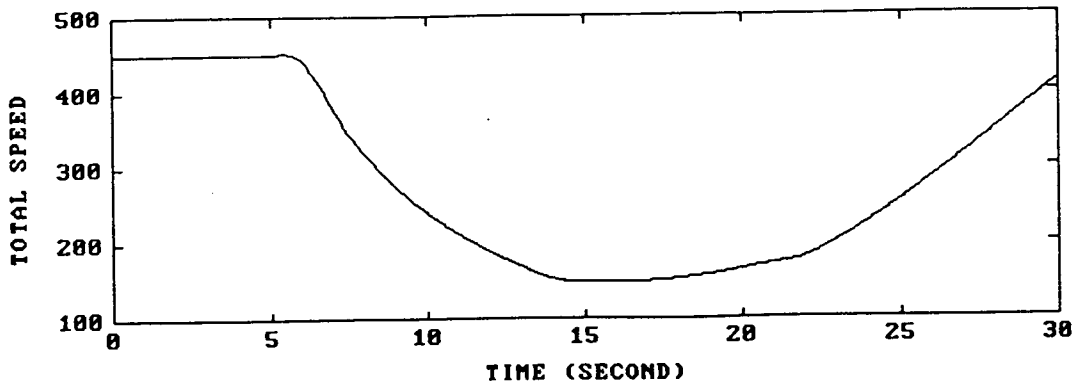

Figure 5.4 Total Speed in case of Maneuver One, LPM, and Prediction Controller

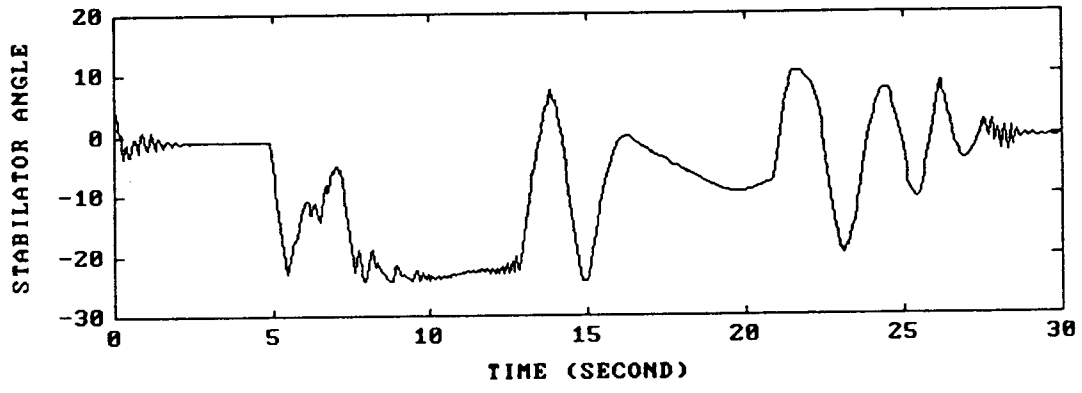

Figure 5.5 Stabilator Angle in case of Maneuver One, LPM, and Prediction Controller

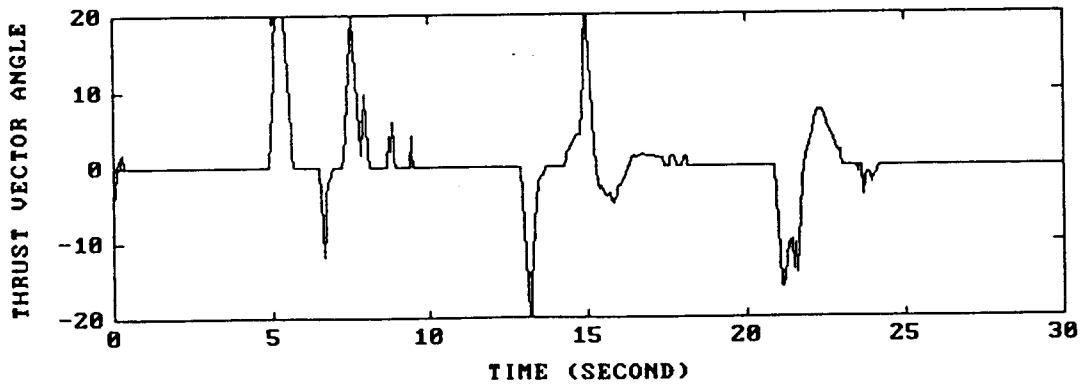

Figure 5.6 Thrust Vector Angle in case of Maneuver One, LPM, and Prediction Controller.

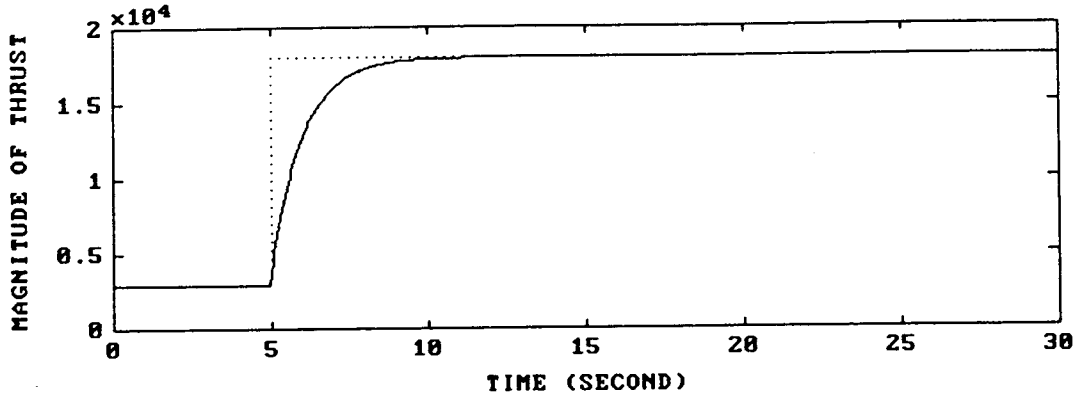

Figure 5.7 Magnitude of Thrust in case of Maneuver One, LPM, and Prediction Controller

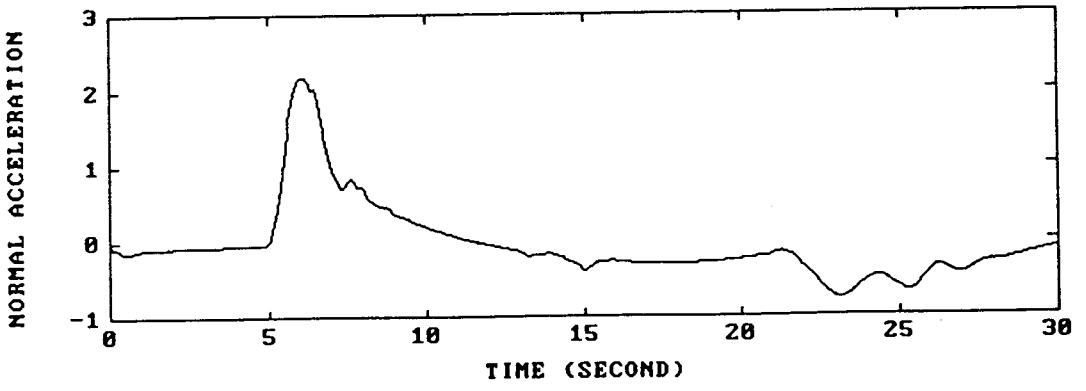

Figure 5.8 Normal Acceleration in case of Maneuver One, LPM, and Prediction Controller

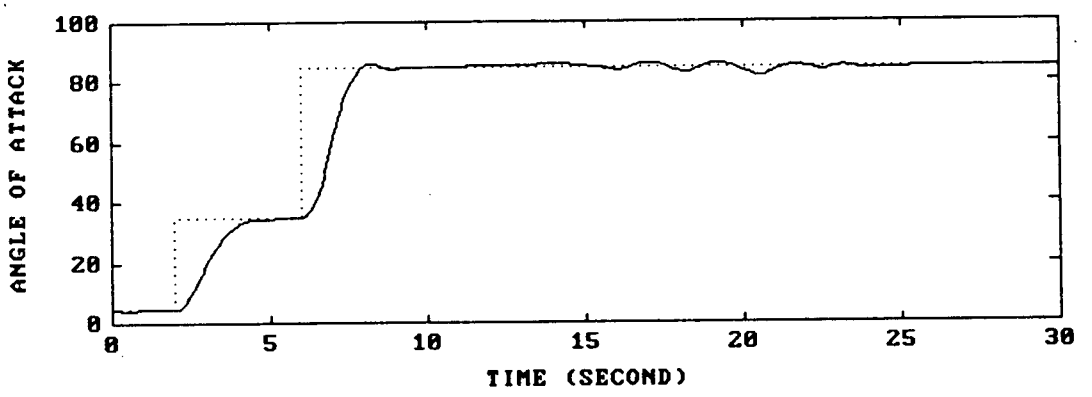

Figure 5.9 Angle of Attack in case of Maneuver Two, LPM, and Prediction Controller

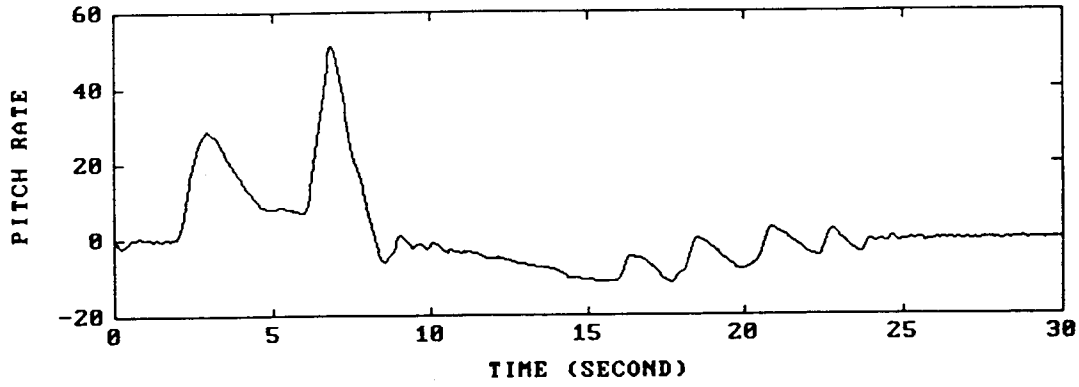

Figure 5.10 Pitch Rate in case of Maneuver Two, LPM, and Prediction Controller

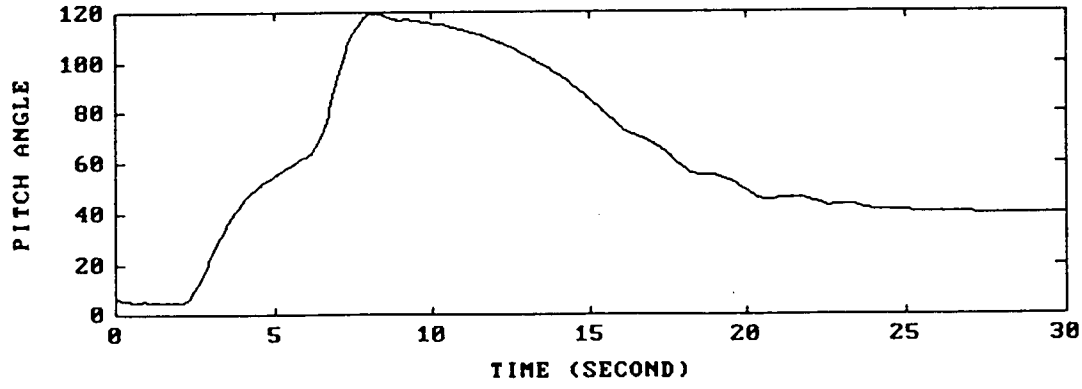

Figure 5.11 Pitch Angle in case of Maneuver Two, LPM, and Prediction Controller

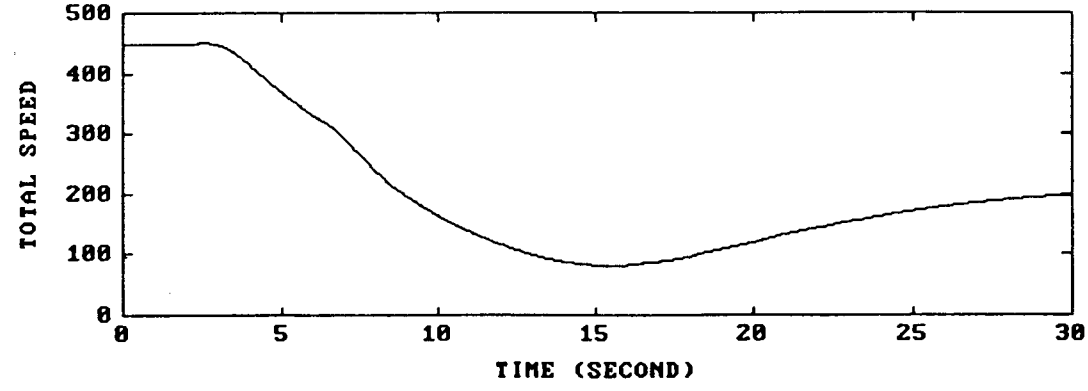

Figure 5.12 Total Speed in case of Maneuver Two, LPM, and Prediction Controller

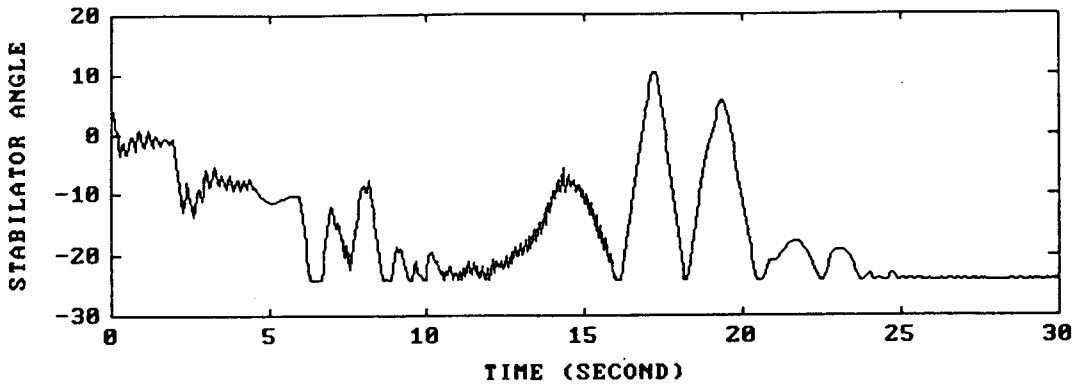

Figure 5.13 Stabilator Angle in case of Maneuver Two, LPM, and Prediction Controller

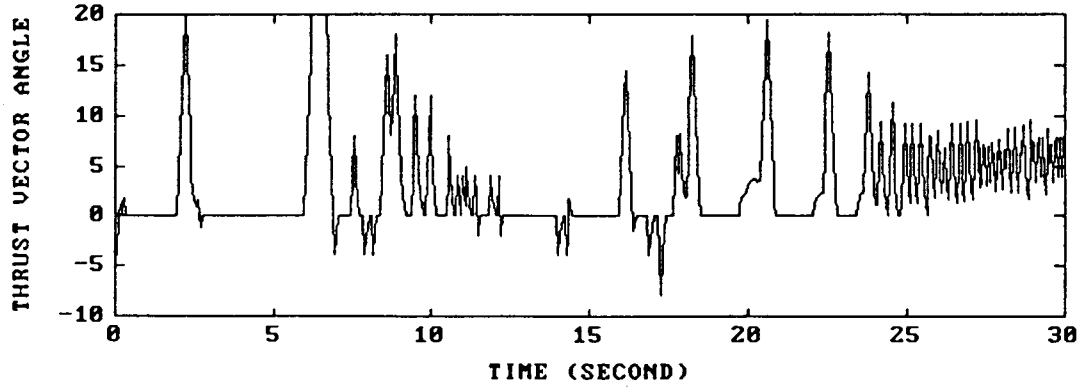

Figure 5.14 Thrust Vector Angle in case of Maneuver Two, LPM, and Prediction Controller

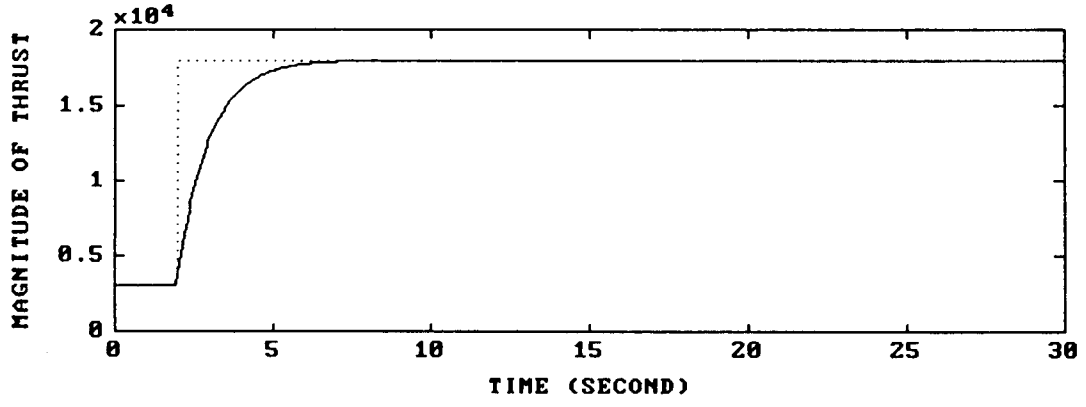

Figure 5.15 Magnitude of Thrust in case of Maneuver Two, LPM, and Prediction Controller

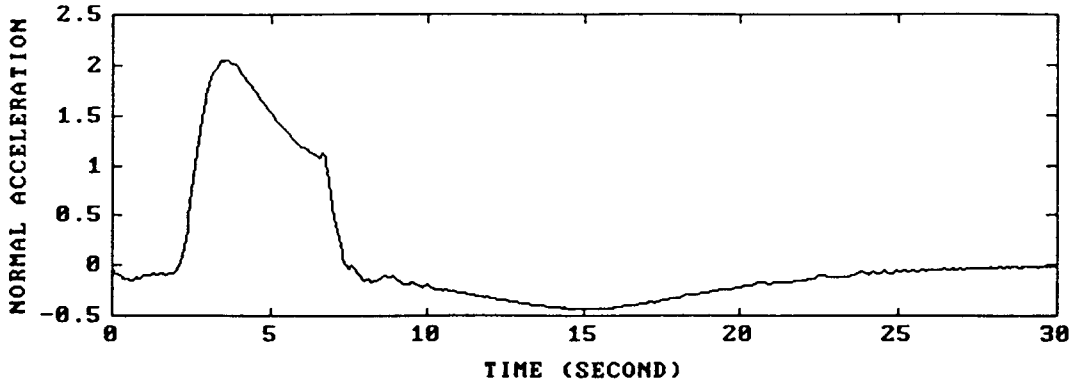

Figure 5.16 Normal Acceleration in case of Maneuver Two, LPM, and Prediction Controller

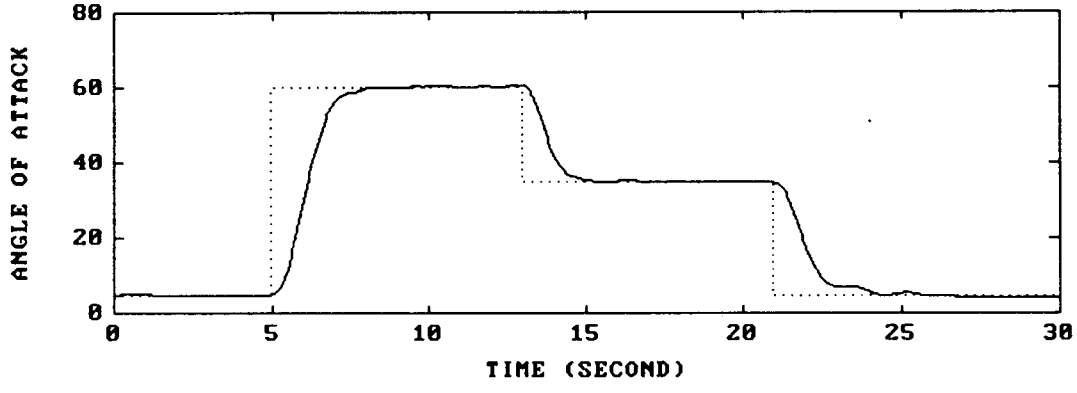

Figure 5.17 Angle of Attack in case of Maneuver One, BLPM, and Prediction Controller.

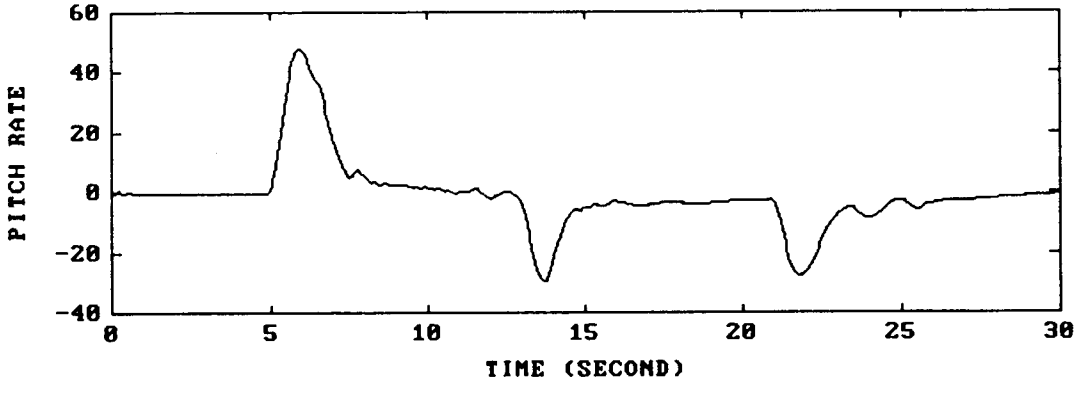

Figure 5.18 Pitch Rate in case of Maneuver One, BLPM, and Prediction Controller

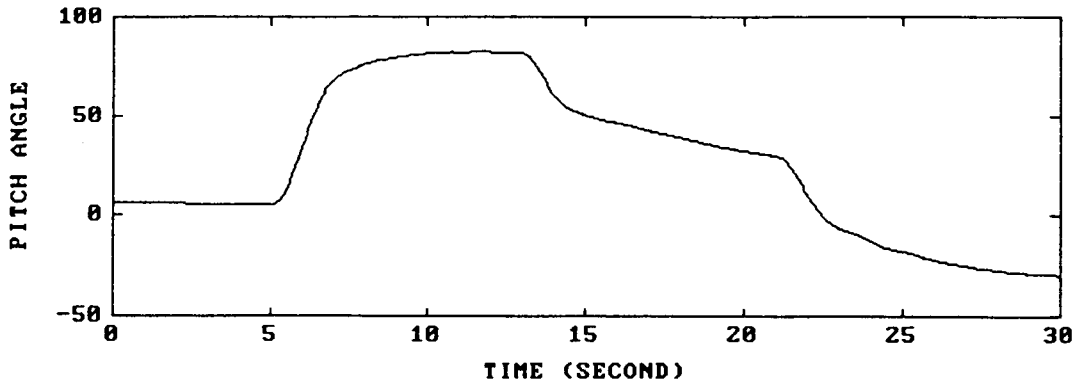

Figure 5.19 Pitch Angle in case of Maneuver One, BLPM, and Prediction Controller

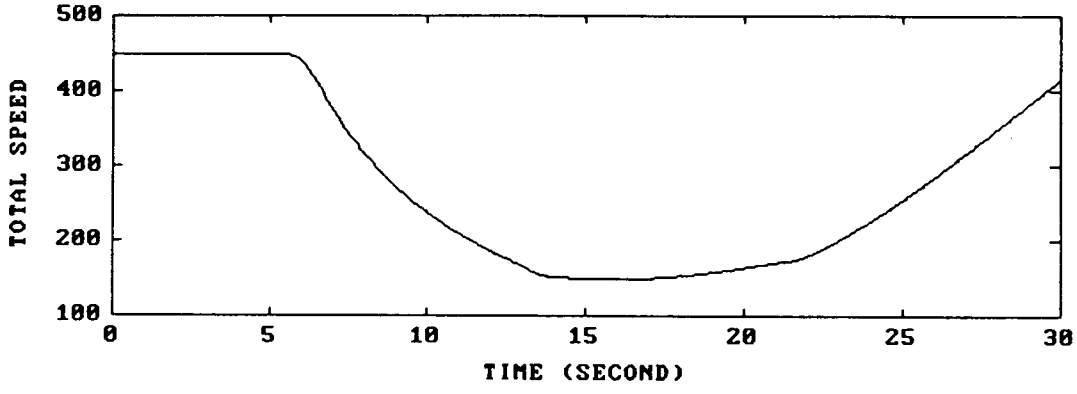

Figure 5.20 Total Speed in case of Maneuver One, BLPM, and Prediction Controller

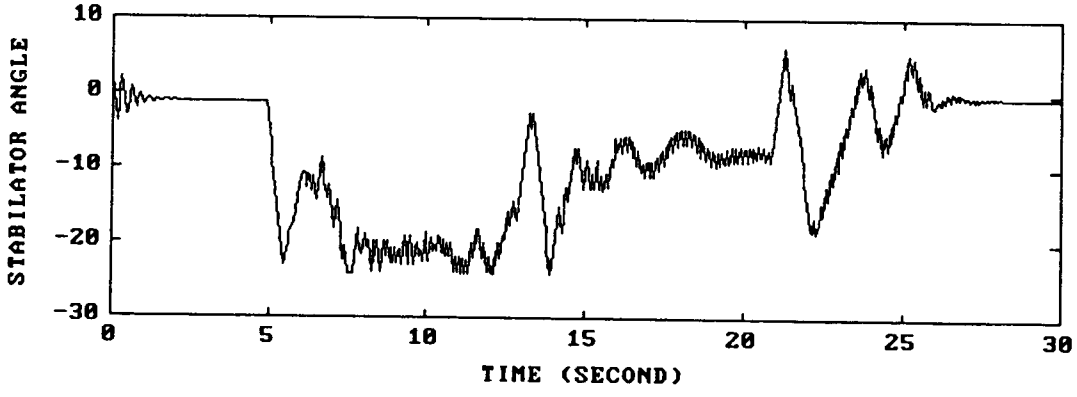

Figure 5.21 Stabilator Angle in case of Maneuver One, BLPM, and Prediction Controller

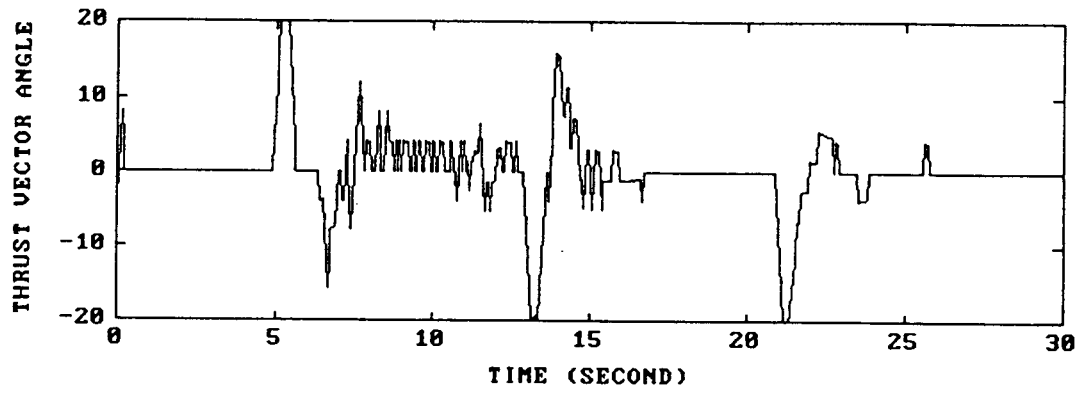

Figure 5.22 Thrust Vector Angle in case of Maneuver One, BLPM, and Prediction Controller.

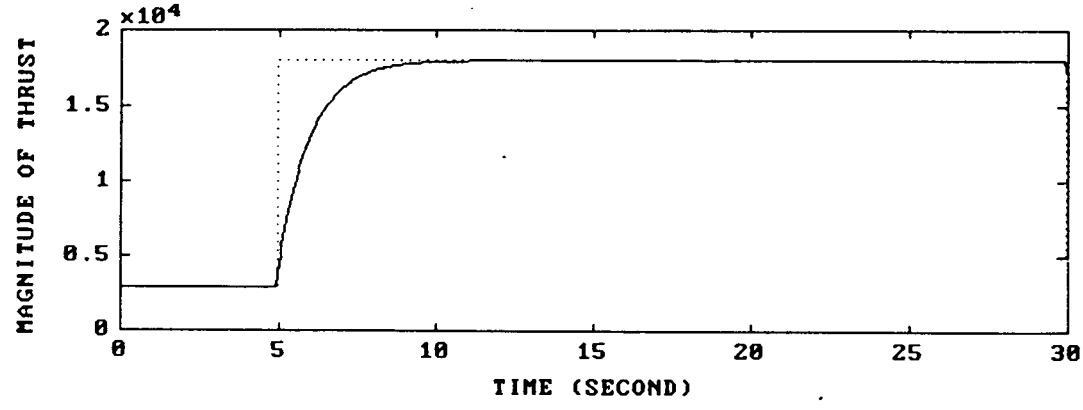

Figure 5.23 Magnitude of Thrust in case of Maneuver One, BLPM, and Prediction Controller

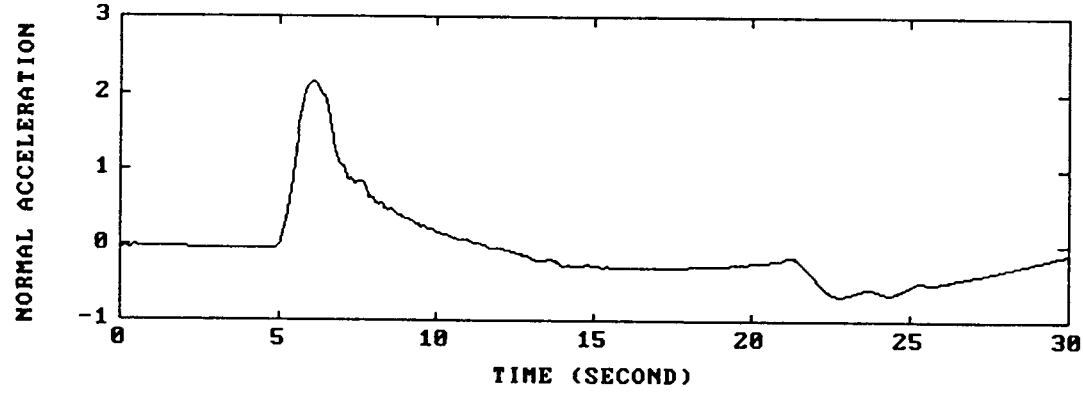

Figure 5.24 Normal Acceleration in case of Maneuver One, BLPM, and Prediction Controller

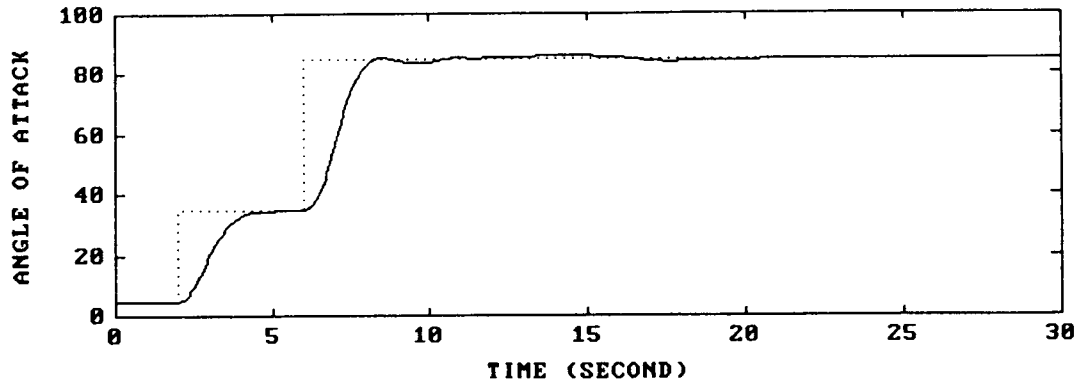

Figure 5.25 Angle of Attack in case of Maneuver Two, BLPM, and Prediction Controller

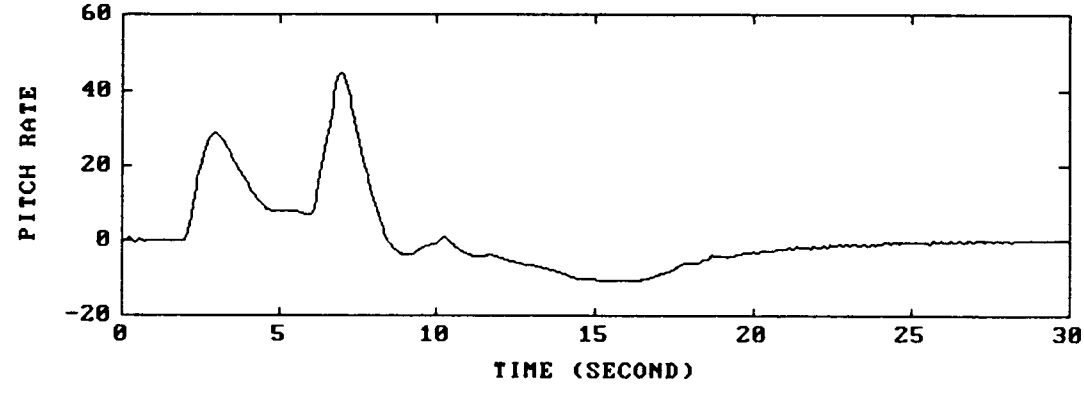

Figure 5.26 Pitch Rate in case of Maneuver Two, BLPM, and Prediction Controller

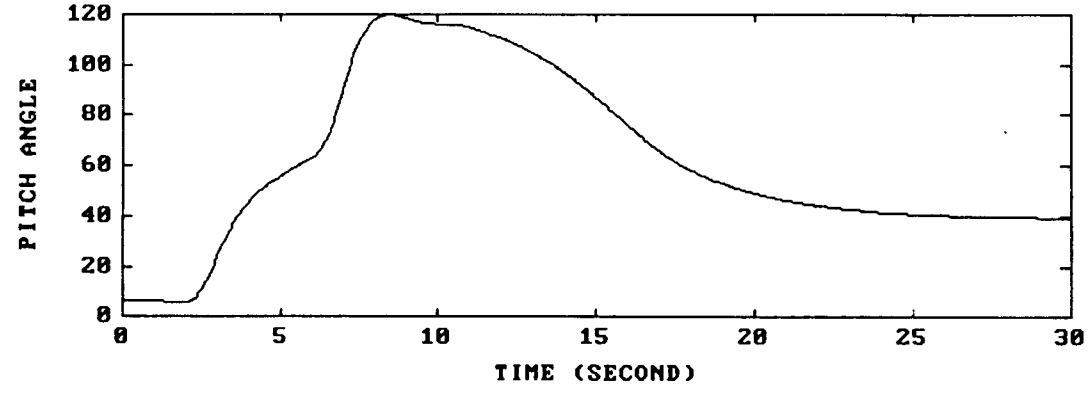

Figure 5.27 Pitch Angle in case of Maneuver Two, BLPM, and Prediction Controller

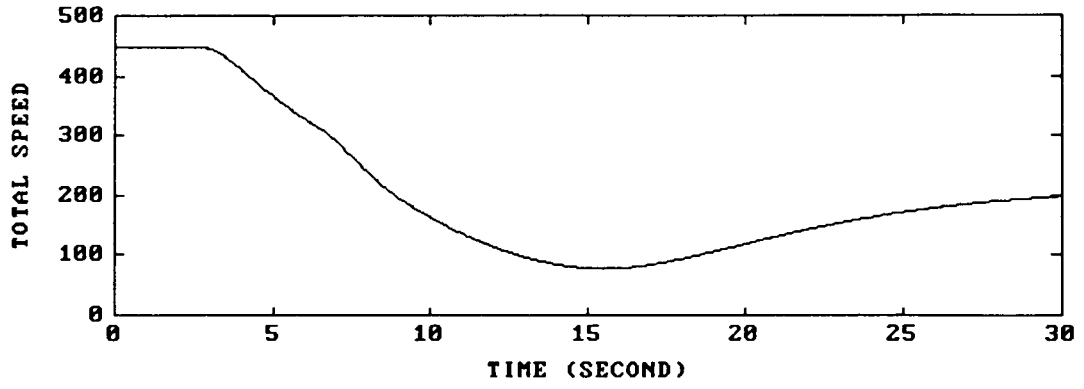

Figure 5.28 Total Speed in case of Maneuver Two, BLPM, and Prediction Controller

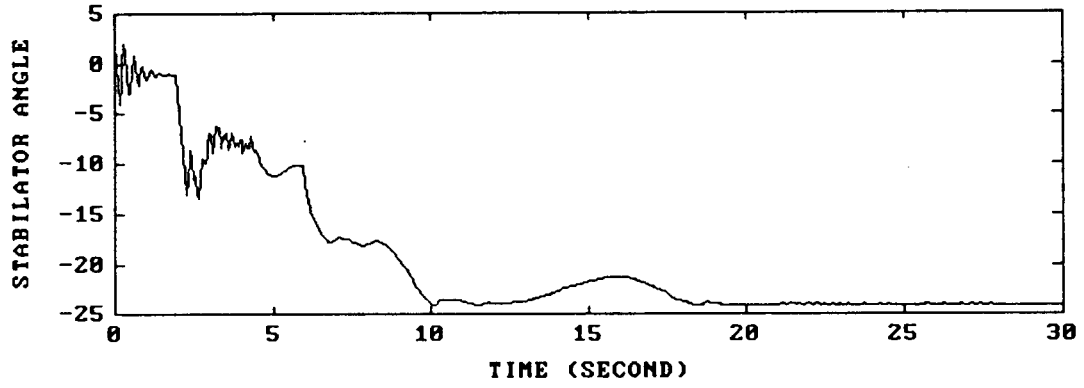

Figure 5.29 Stabilator Angle in case of Maneuver Two, BLPM, and Prediction Controller

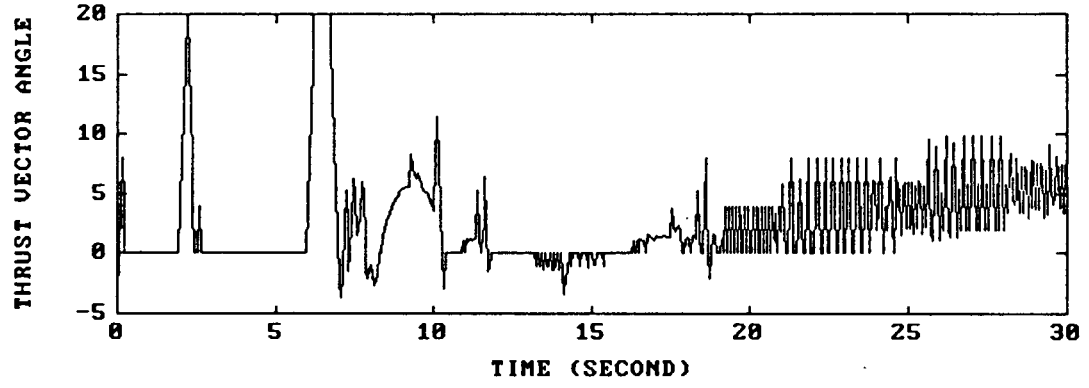

Figure 5.30 Thrust Vector Angle in case of Maneuver Two, BLPM, and Prediction Controller

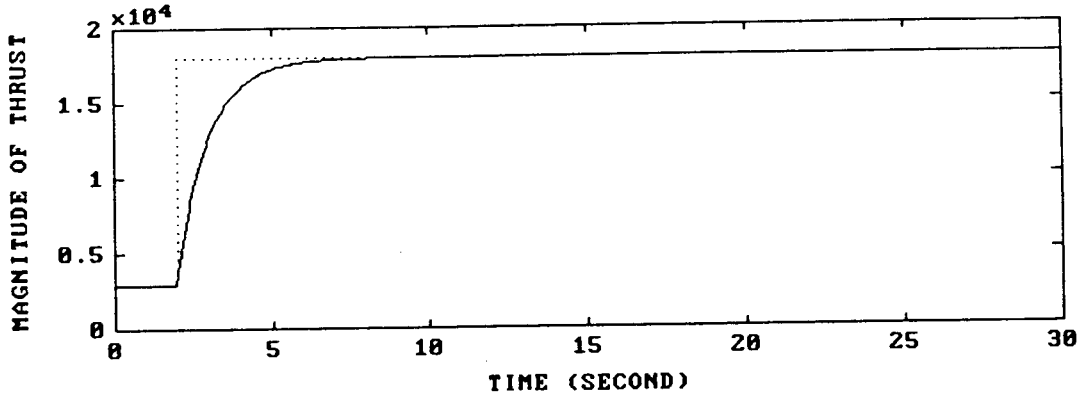

Figure 5.31 Magnitude of Thrust in case of Maneuver Two, BLPM, and Prediction Controller

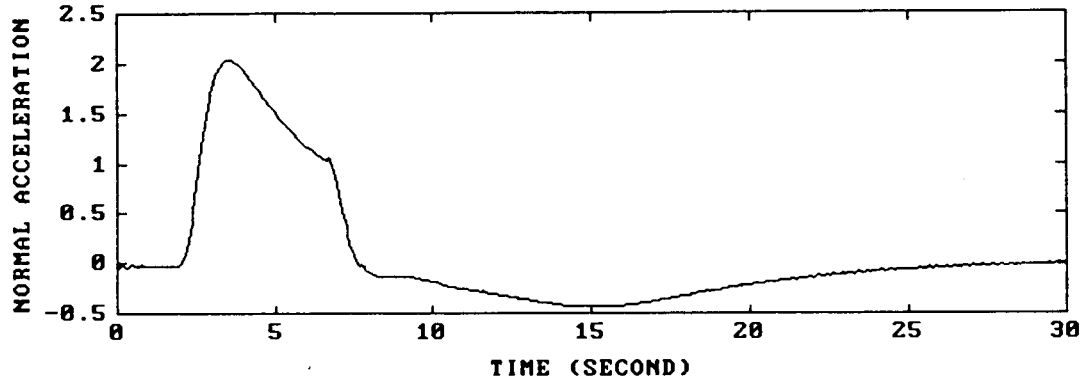

Figure 5.32 Normal Acceleration in case of Maneuver Two, BLPM, and Prediction Controller

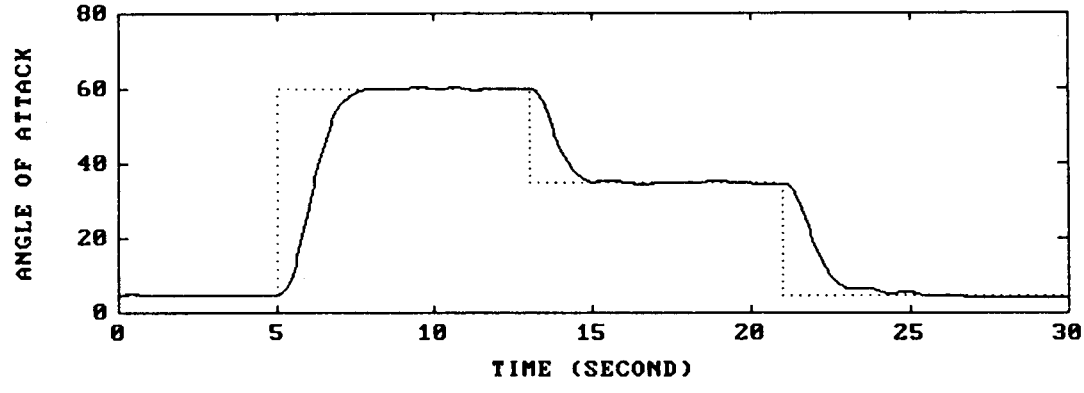

Figure 5.33 Angle of Attack in case of Maneuver One, NLPM, and Prediction Controller.

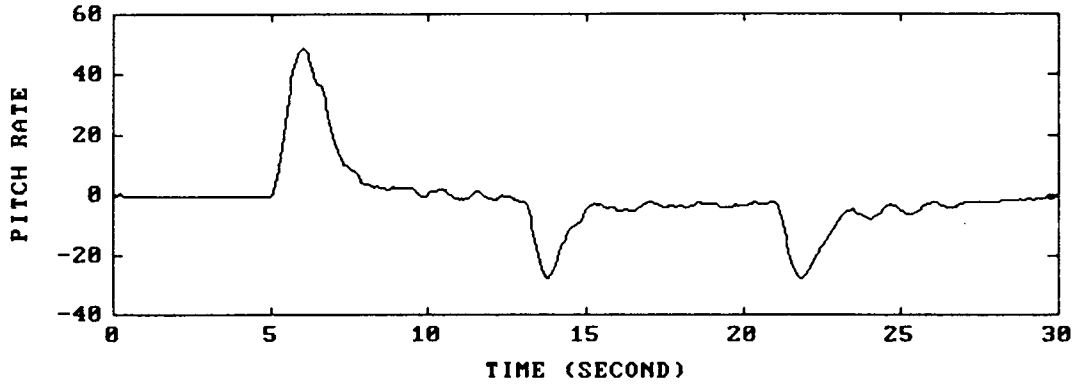

Figure 5.34 Pitch Rate in case of Maneuver One, NLPM, and Prediction Controller

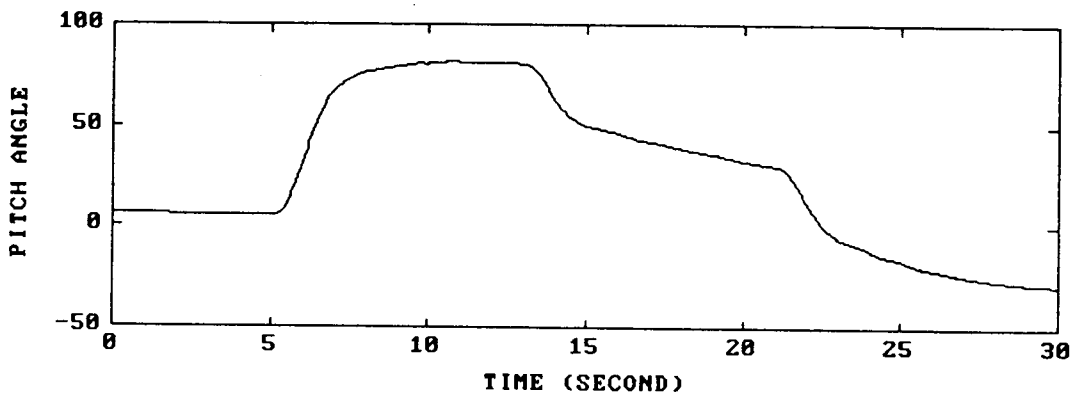

Figure 5.35Pitch Angle in case of Maneuver One, NLPM, and Prediction Controller

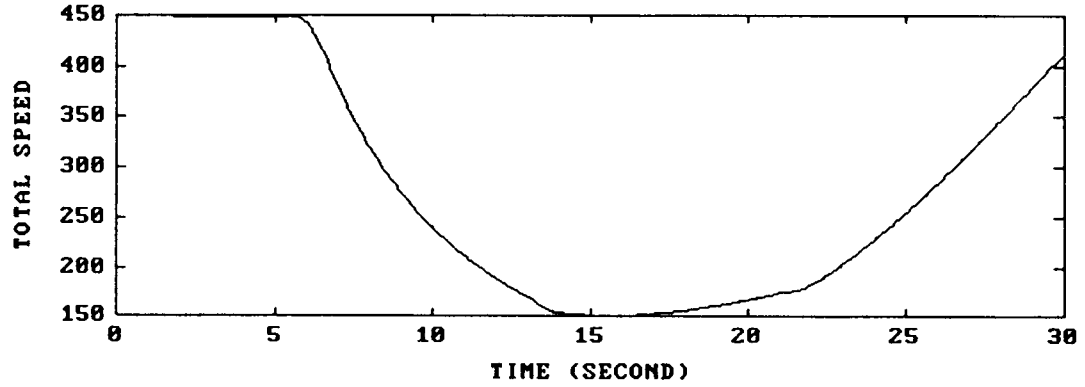

Figure 5.36 Total Speed in case of Maneuver One, NLPM, and Prediction Controller

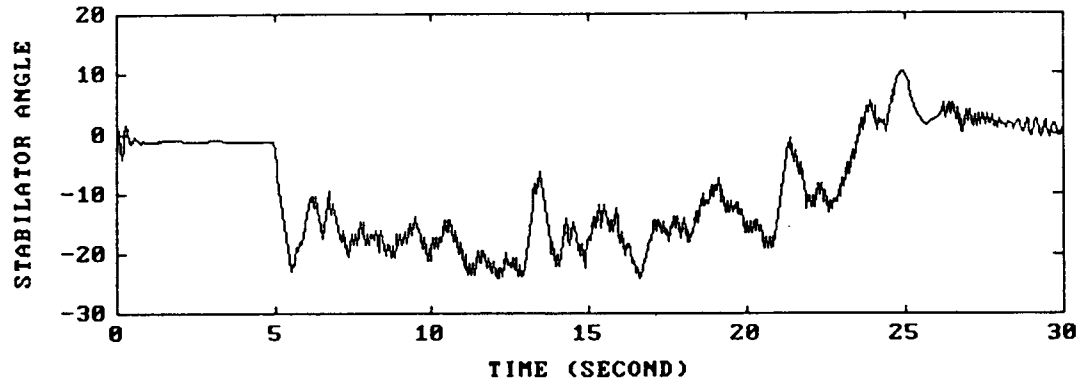

Figure 5.37 Stabilator Angle in case of Maneuver One, NLPM, and Prediction Controller

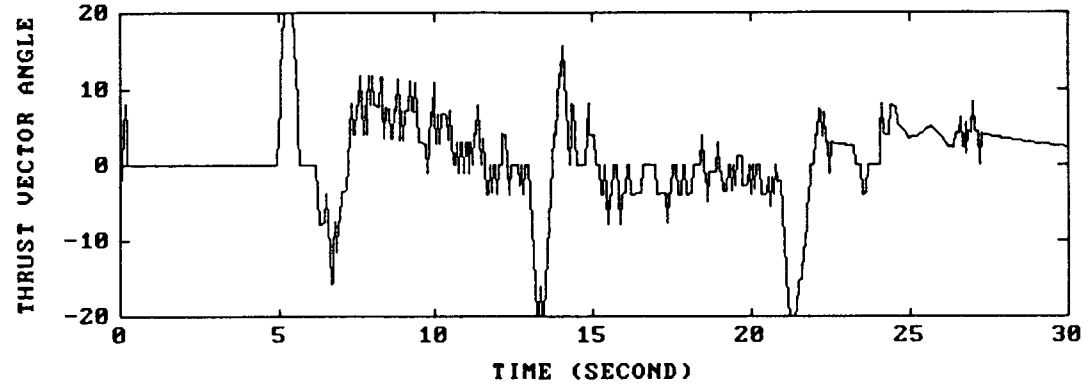

Figure 5.38 Thrust Vector Angle in case of Maneuver One, NLPM, and Prediction Controller.

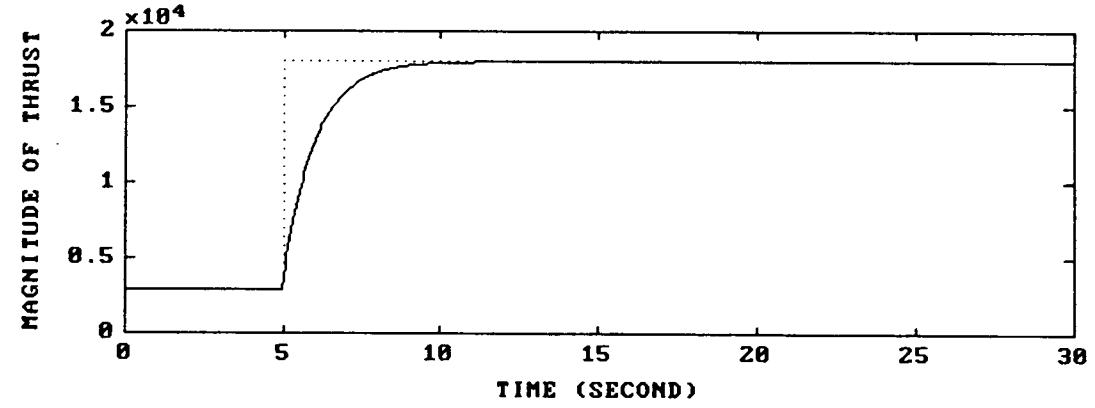

Figure 5.39 Magnitude of Thrust in case of Maneuver One, NLPM, and Prediction Controller

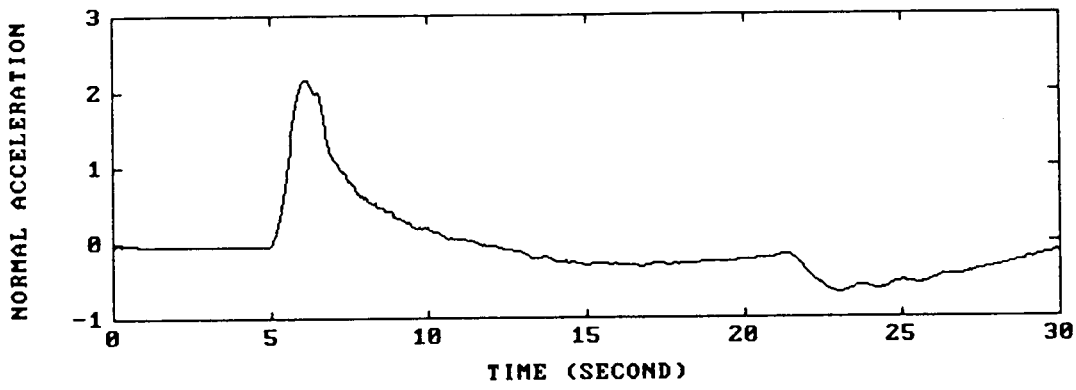

Figure 5.40 Normal Acceleration in case of Maneuver One, NLPM, and Prediction Controller

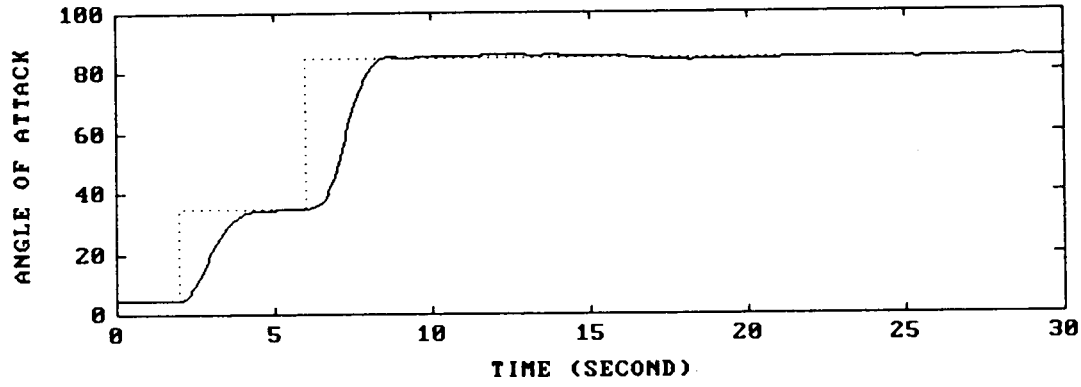

Figure 5.41 Angle of Attack in case of Maneuver Two, NLPM, and Prediction Controller

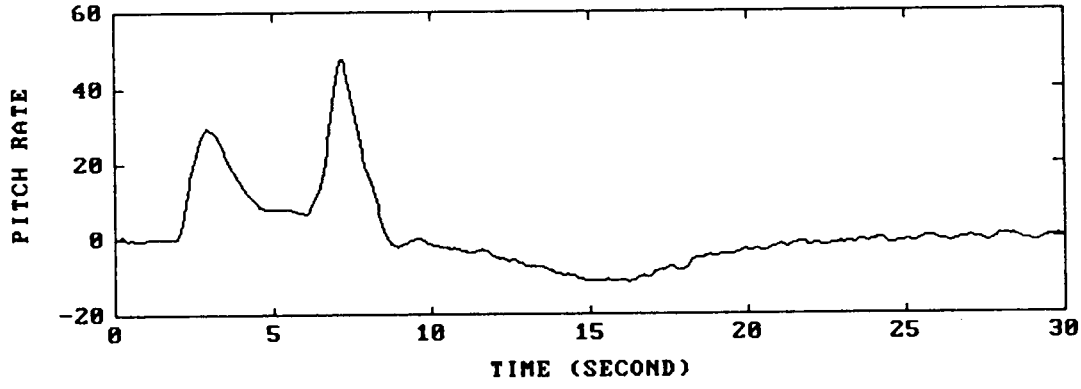

Figure 5.42 Pitch Rate in case of Maneuver Two, NLPM, and Prediction Controller

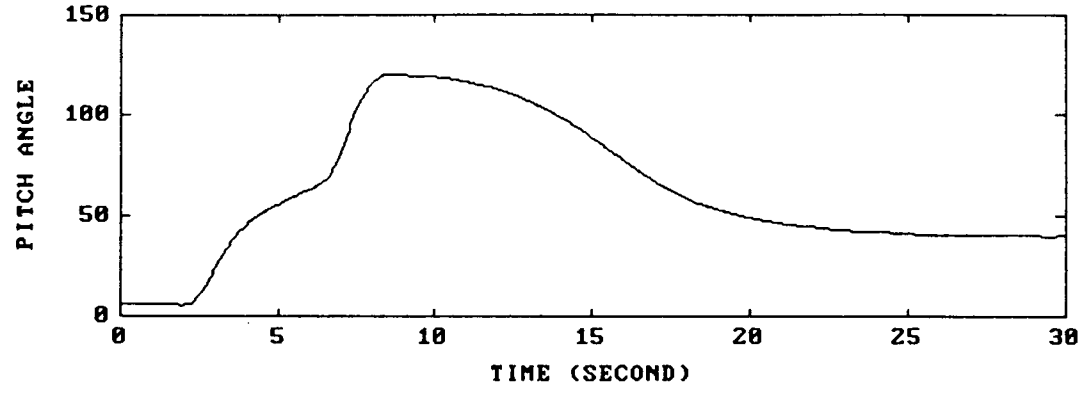

Figure 5.43 Pitch Angle in case of Maneuver Two, NLPM, and Prediction Controller

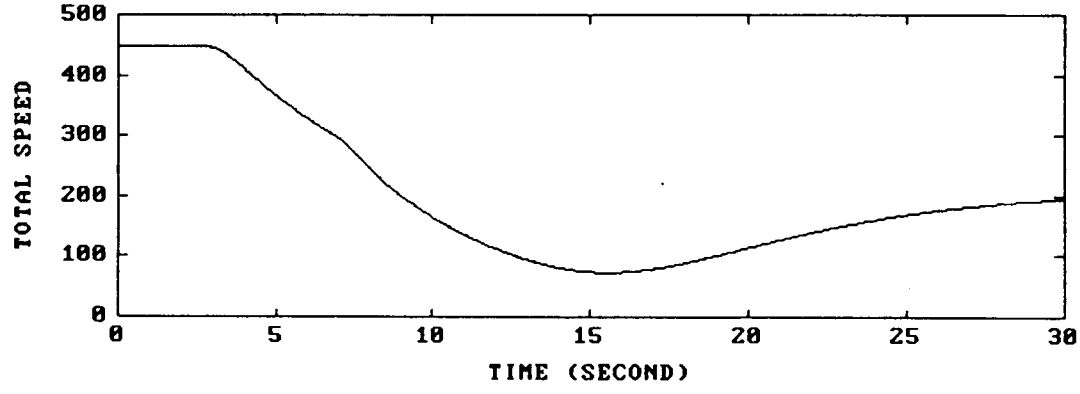

Figure 5.44 Total Speed in case of Maneuver Two, NLPM, and Prediction Controller

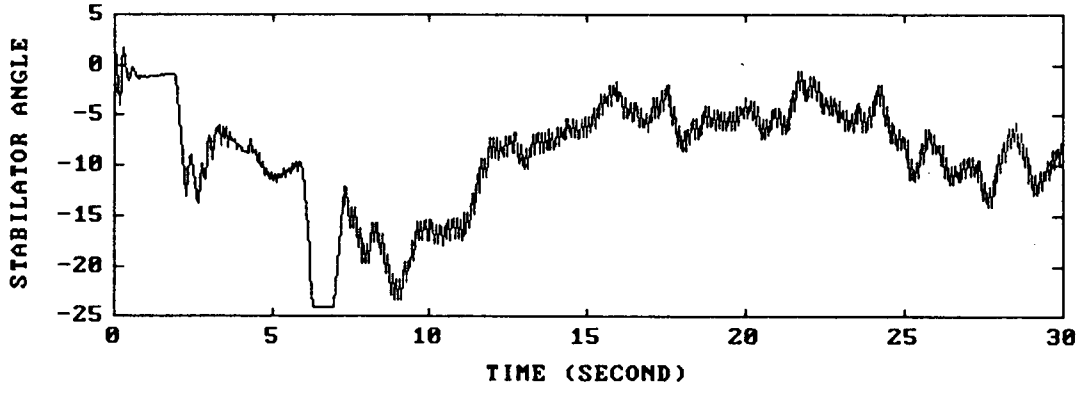

Figure 5.45 Stabilator Angle in case of Maneuver Two, NLPM, and Prediction Controller

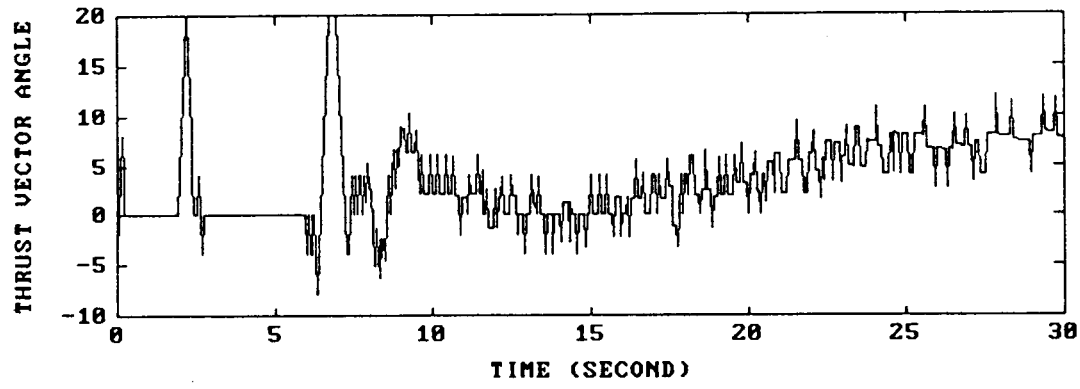

Figure 5.46 Thrust Vector Angle in case of Maneuver Two, NLPM, and Prediction Controller

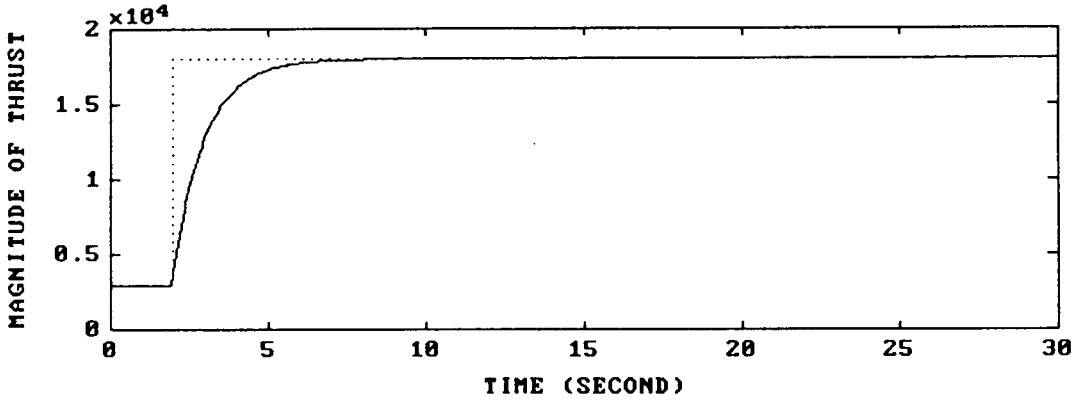

Figure 5.47 Magnitude of Thrust in case of Maneuver Two, NLPM, and Prediction Controller

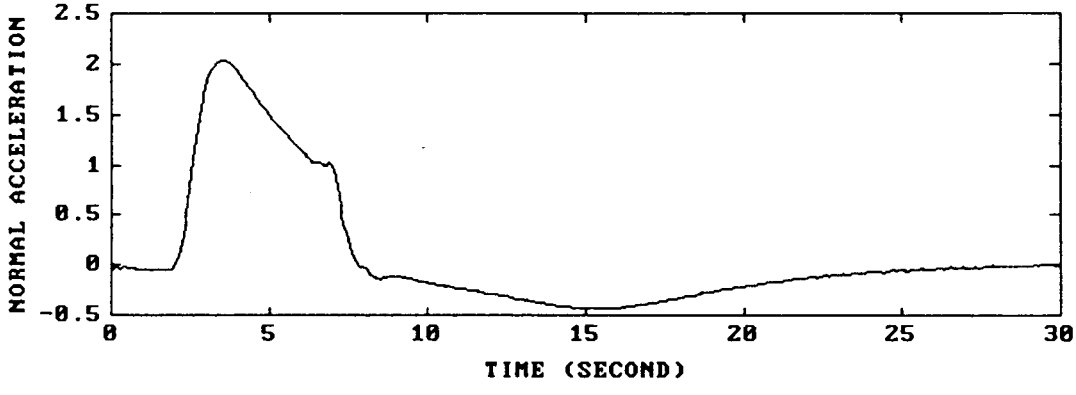

Figure 5.48 Normal Acceleration in case of Maneuver Two, NLPM, and Prediction Controller

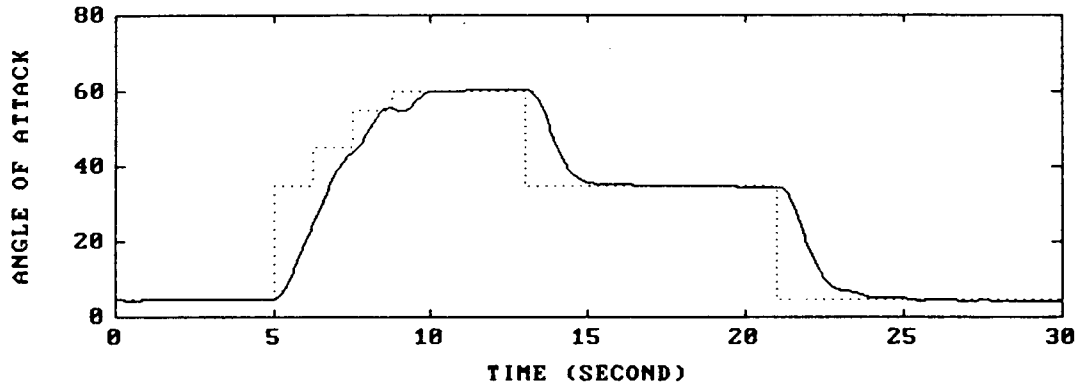

Figure 5.49 Angle of Attack in case of Maneuver One, LPM, and LF Controller

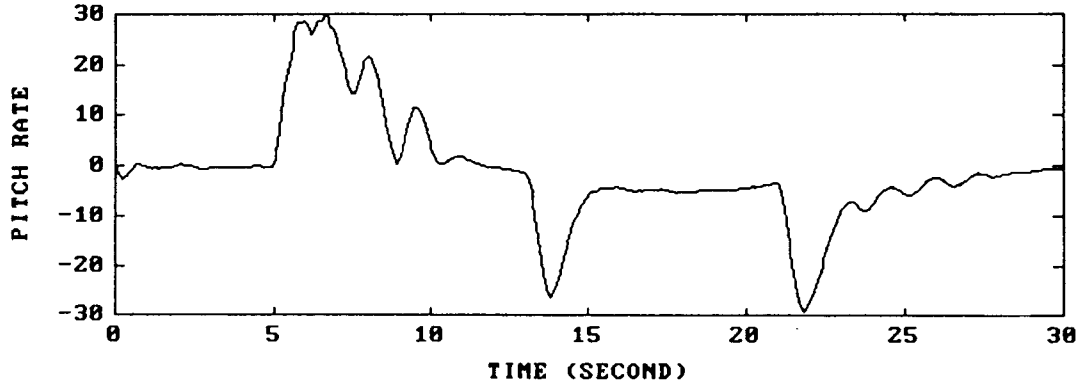

Figure 5.50 Pitch Rate in case of Maneuver One, LPM, and LF Controller

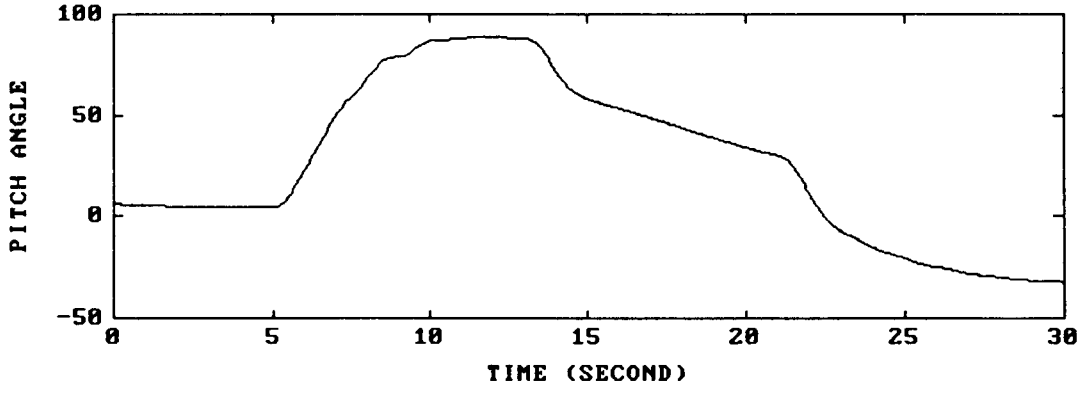

Figure 5.51 Pitch Angle in case of Maneuver One, LPM, and LF Controller

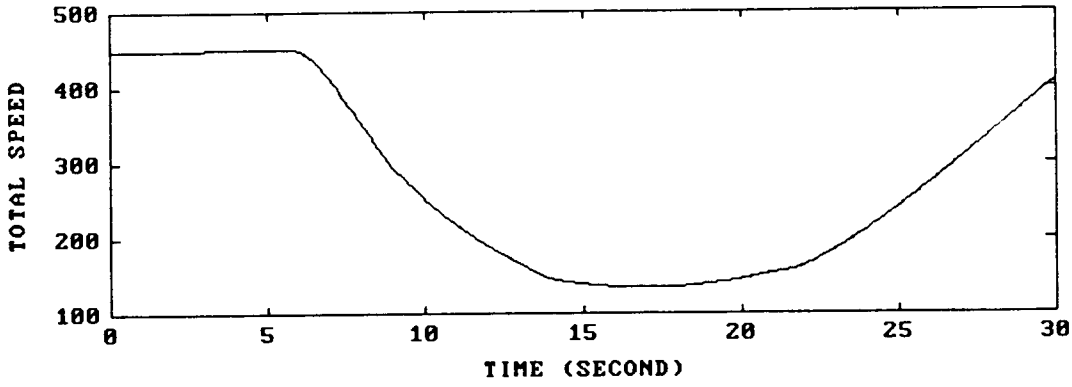

Figure 5.52 Total Speed in case of Maneuver One, LPM, and LF Controller

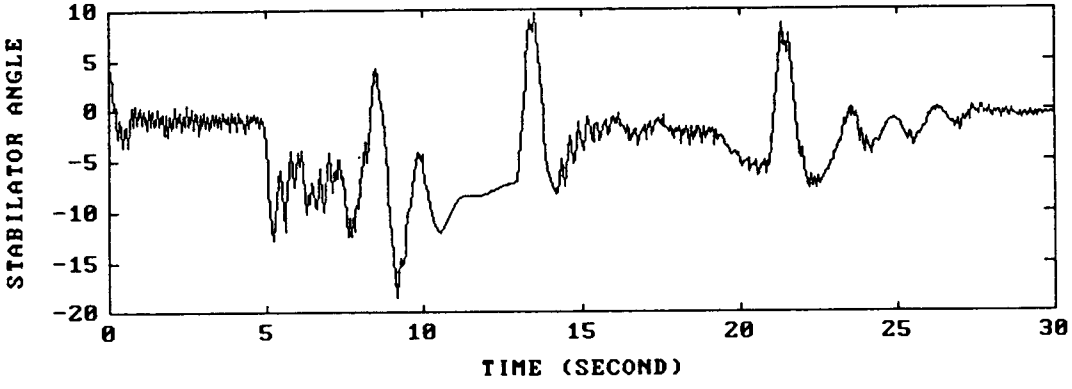

Figure 5.53 Stabilator Angle in case of Maneuver One, LPM, and LF Controller

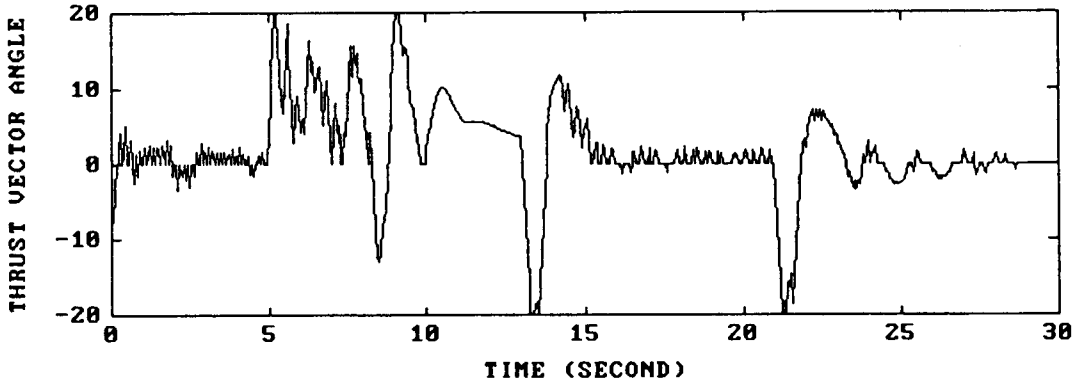

Figure 5.54 Thrust Vector Angle in case of Maneuver One, LPM, and LF Controller.

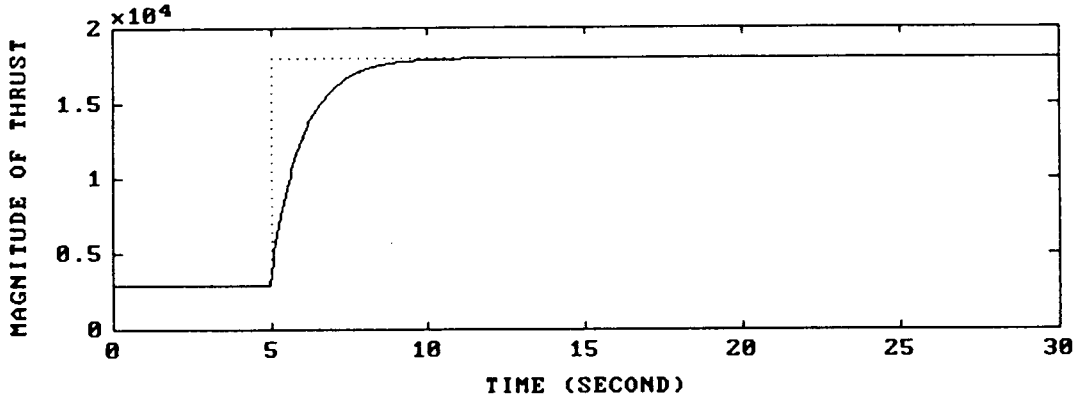

Figure 5.55 Magnitude of Thrust in case of Maneuver One, LPM, and LF Controller

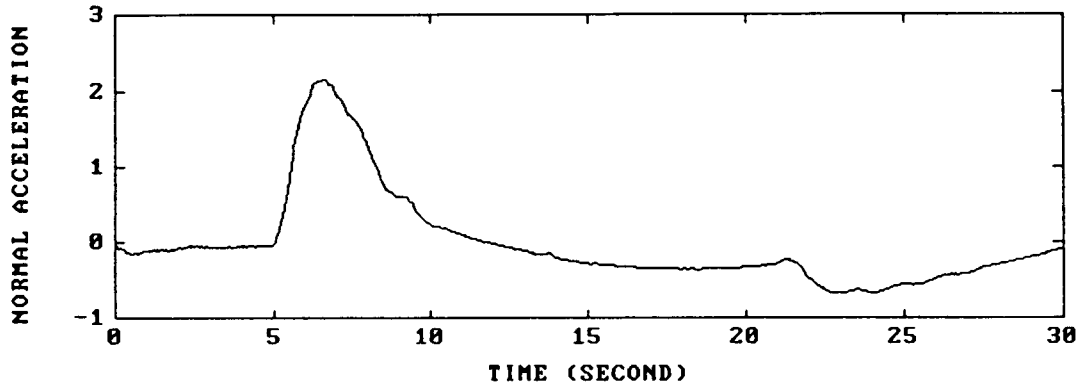

Figure 5.56 Normal Acceleration in case of Maneuver One, LPM, and LF Controller

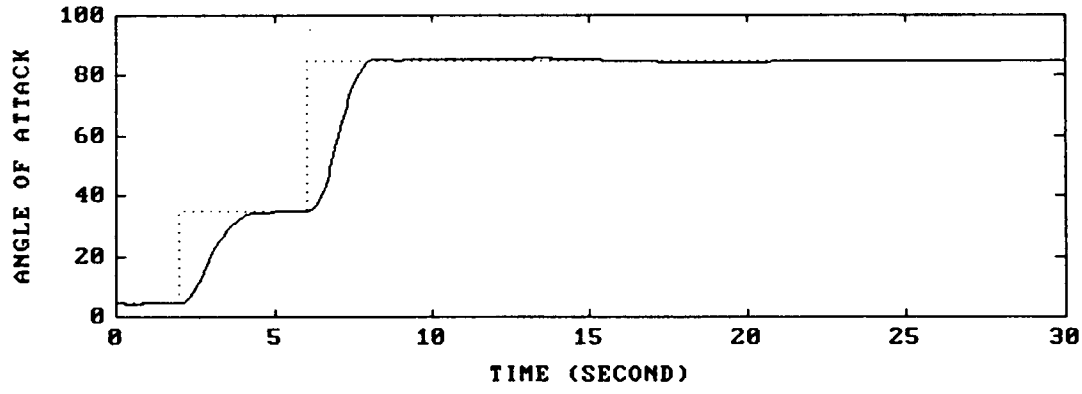

Figure 5.57 Angle of Attack in case of Maneuver Two, LPM, and LF Controller

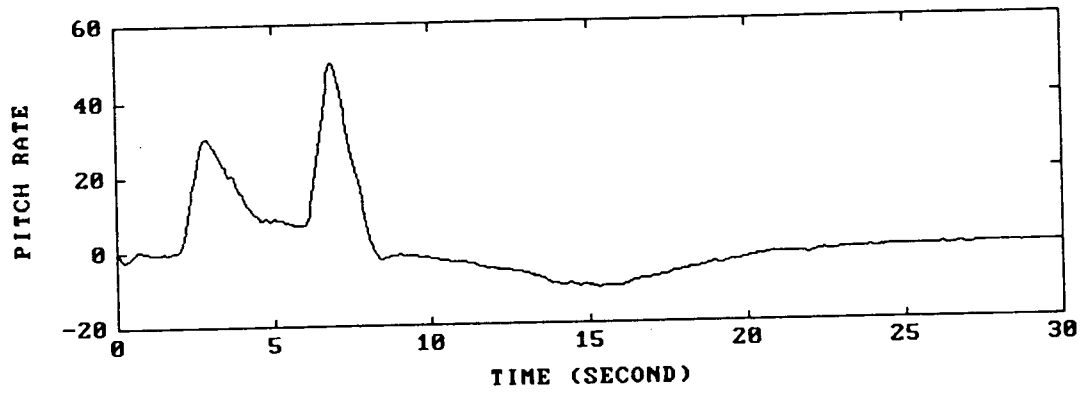

Figure 5.58 Pitch Rate in case of Maneuver Two, LPM, and LF Controller

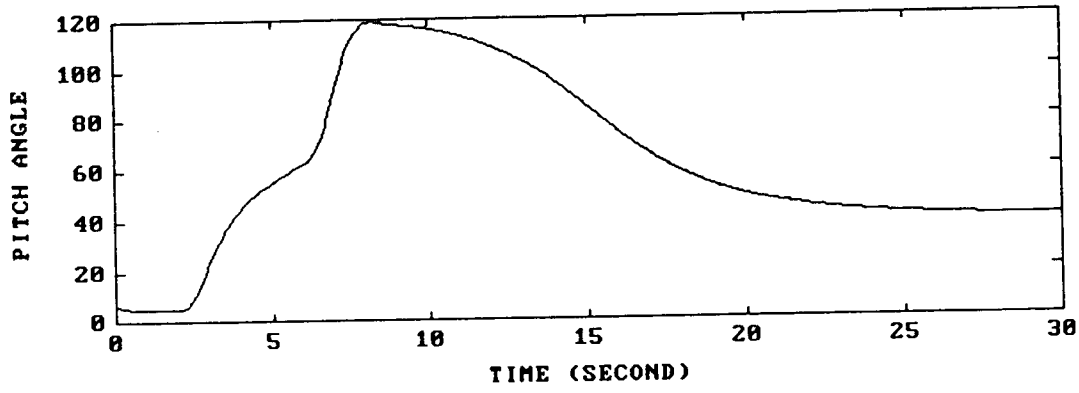

Figure 5.59 Pitch Angle in case of Maneuver Two, LPM, and LF Controller

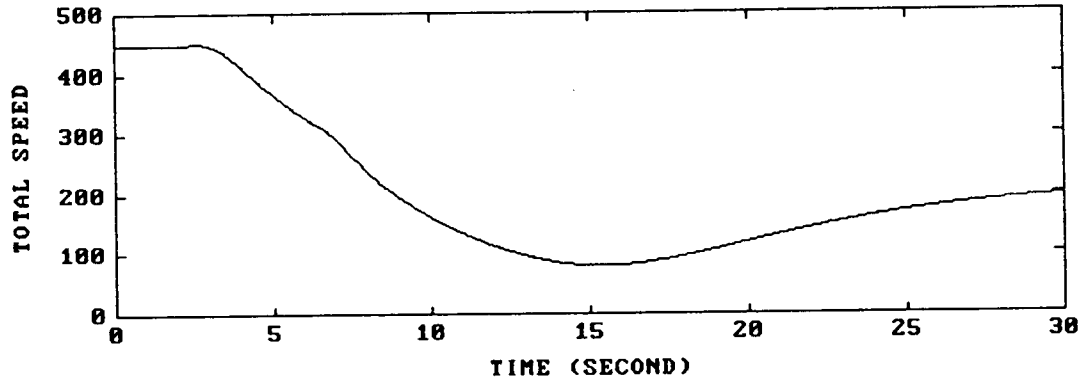

Figure 5.60 Total Speed in case of Maneuver Two, LPM, and LF Controller

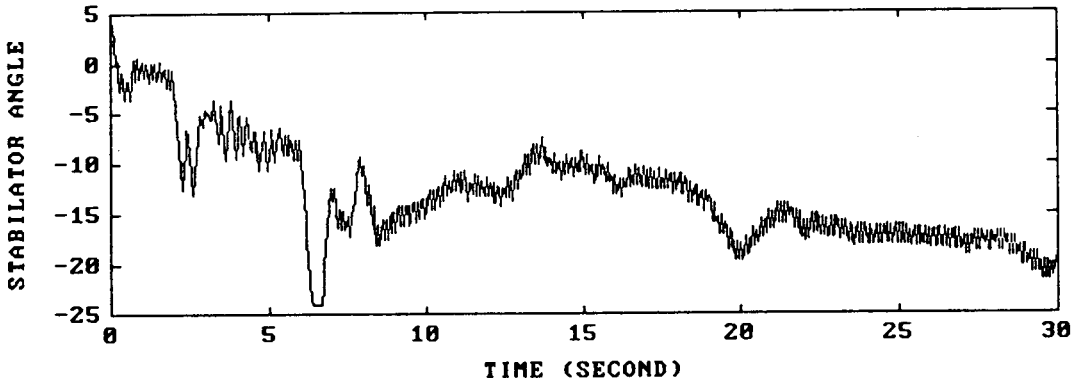

Figure 5.61 Stabilator Angle in case of Maneuver Two, LPM, and LF Controller

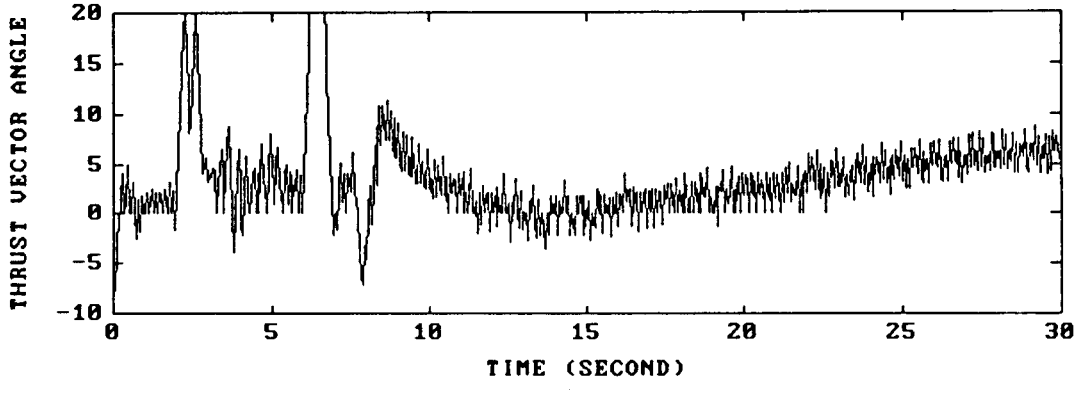

Figure 5.62 Thrust Vector Angle in case of Maneuver Two, LPM, and LF Controller

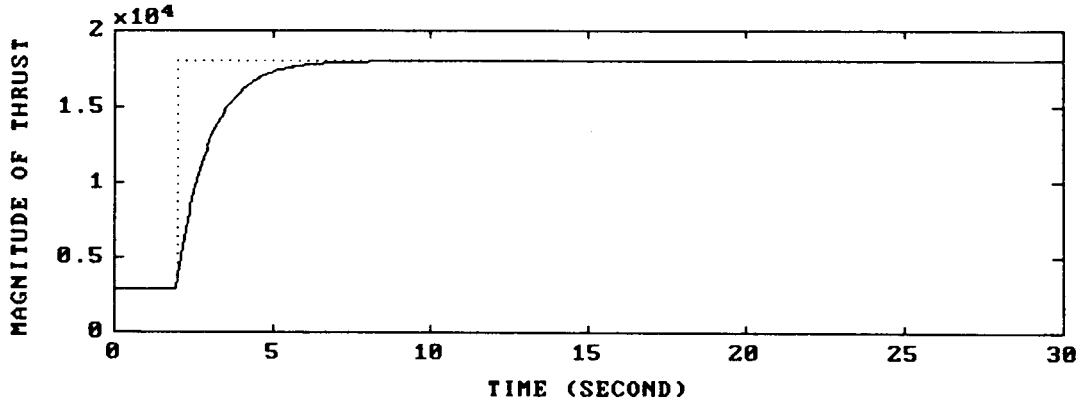

Figure 5.63 Magnitude of Thrust in case of Maneuver Two, LPM, and LF Controller

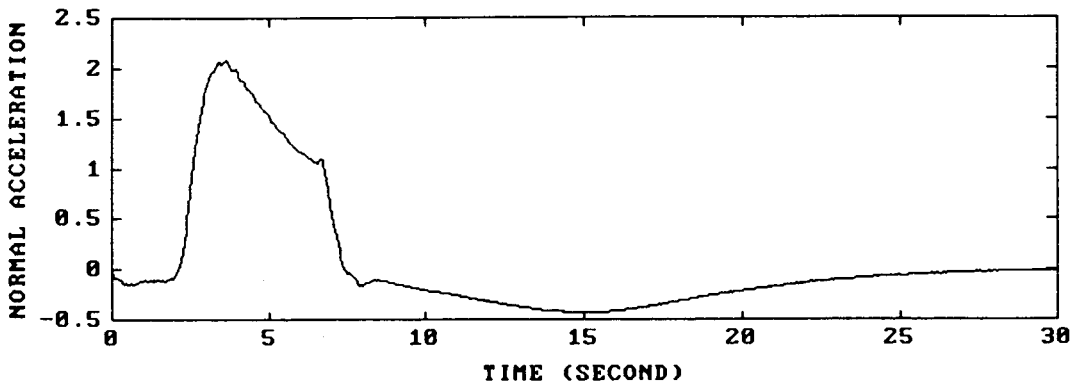

Figure 5.64 Normal Acceleration in case of Maneuver Two, LPM, and LF Controller

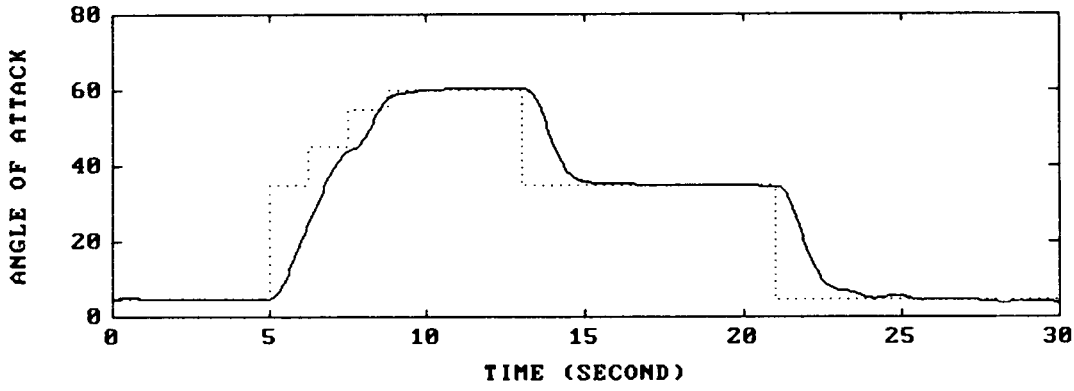

Figure 5.65 Angle of Attack in case of Maneuver One, NLPM, and LF Controller

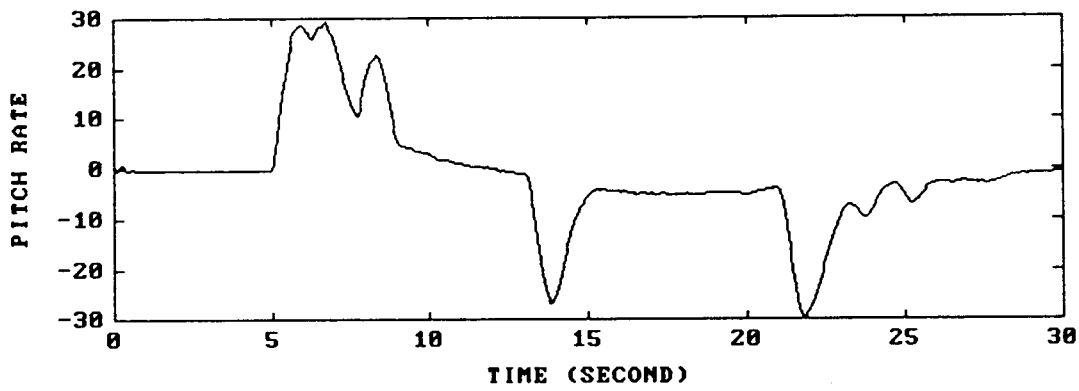

Figure 5.66 Pitch Rate in case of Maneuver One, NLPM, and LF Controller

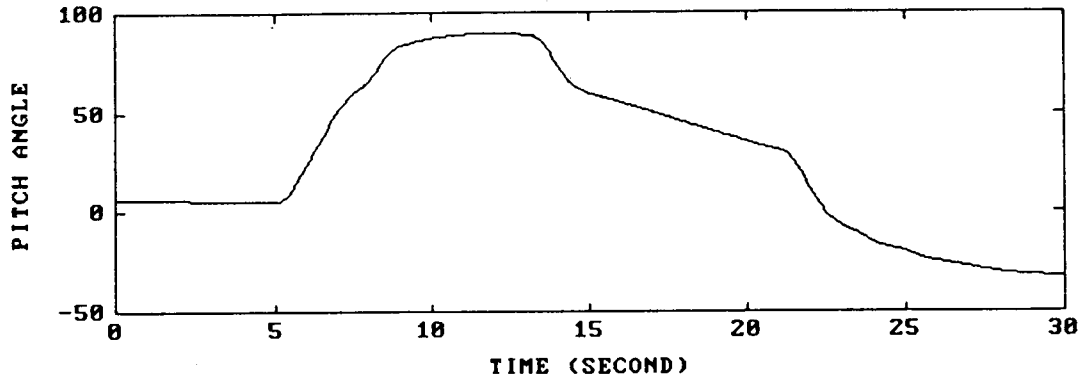

Figure 5.67 Pitch Angle in case of Maneuver One, NLPM, and LF Controller

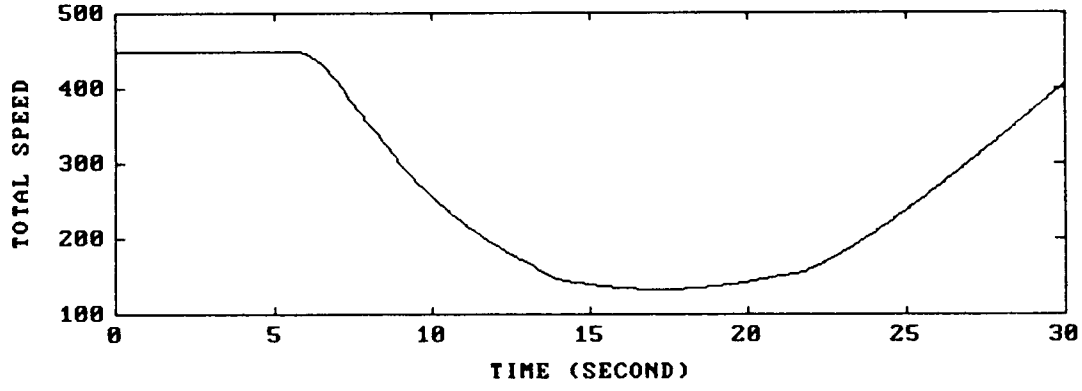

Figure 5.68 Total Speed in case of Maneuver One, NLPM, and LF Controller

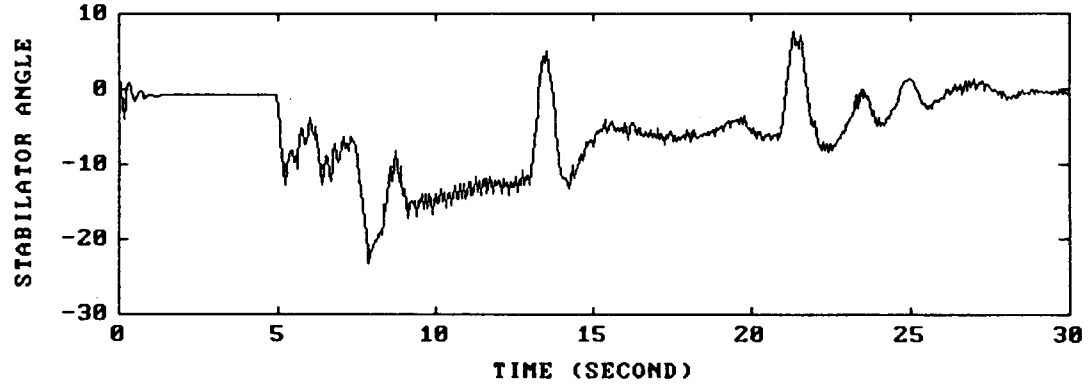

Figure 5.69 Stabilator Angle in case of Maneuver One, NLPM, and LF Controller

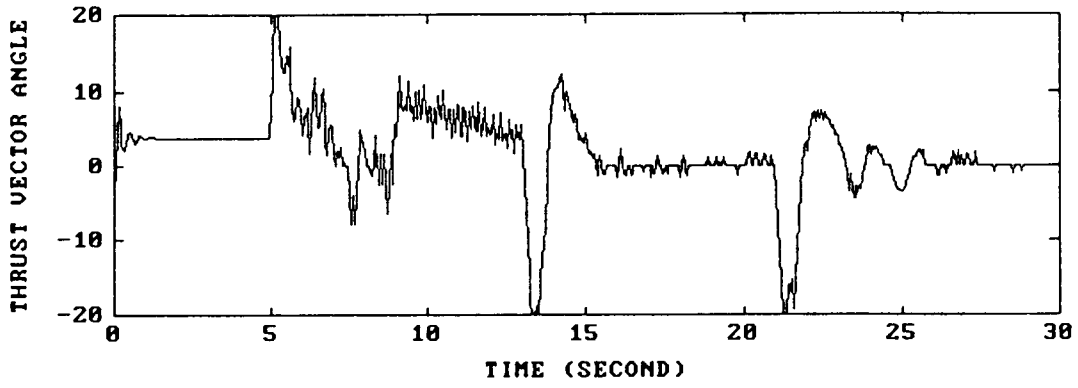

Figure 5.70 Thrust Vector Angle in case of Maneuver One, NLPM, and LF Controller.

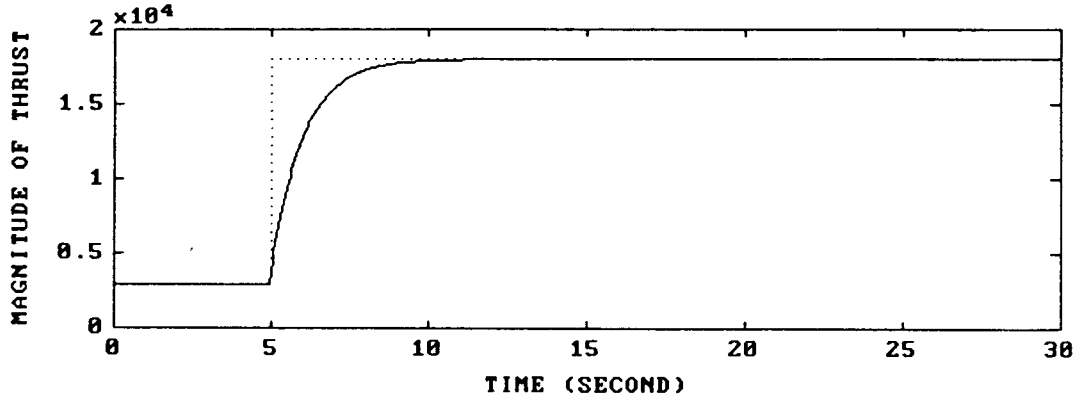

Figure 5.71 Magnitude of Thrust in case of Maneuver One, NLPM, and LF Controller

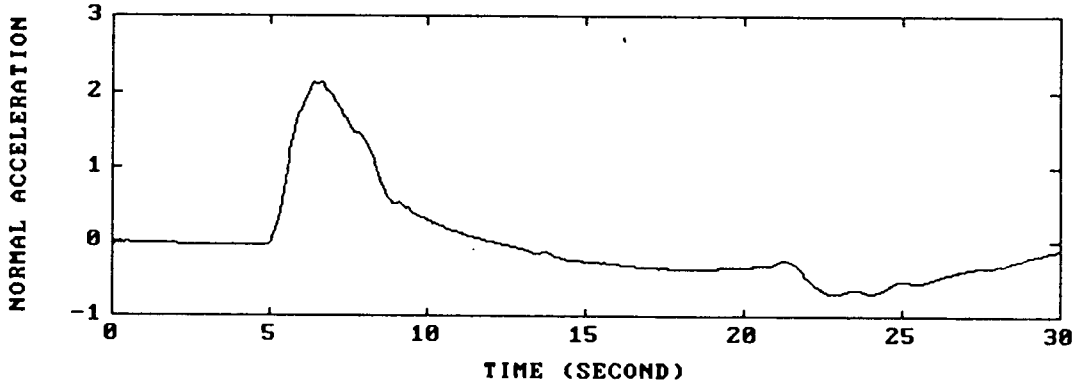

Figure 5.72 Normal Acceleration in case of Maneuver One, NLPM, and LF Controller

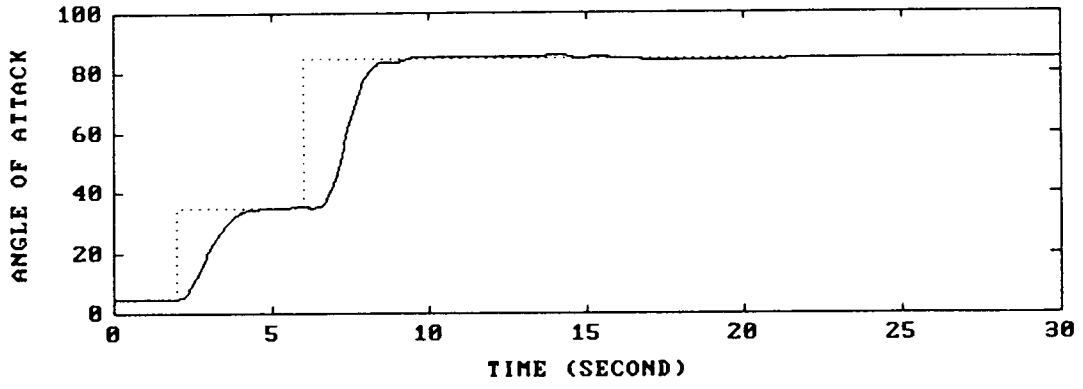

Figure 5.73 Angle of Attack in case of Maneuver Two, NLPM, and LF Controller

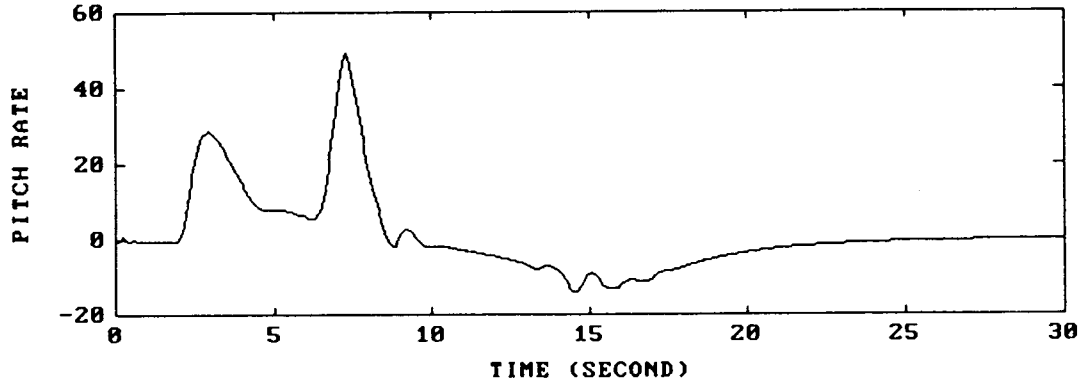

Figure 5.74 Pitch Rate in case of Maneuver Two, NLPM, and LF Controller

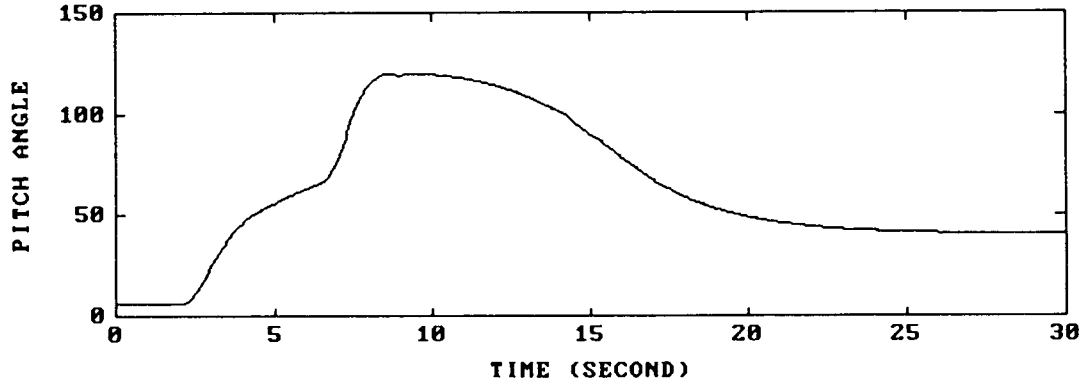

Figure 5.75 Pitch Angle in case of Maneuver Two, NLPM, and LF Controller

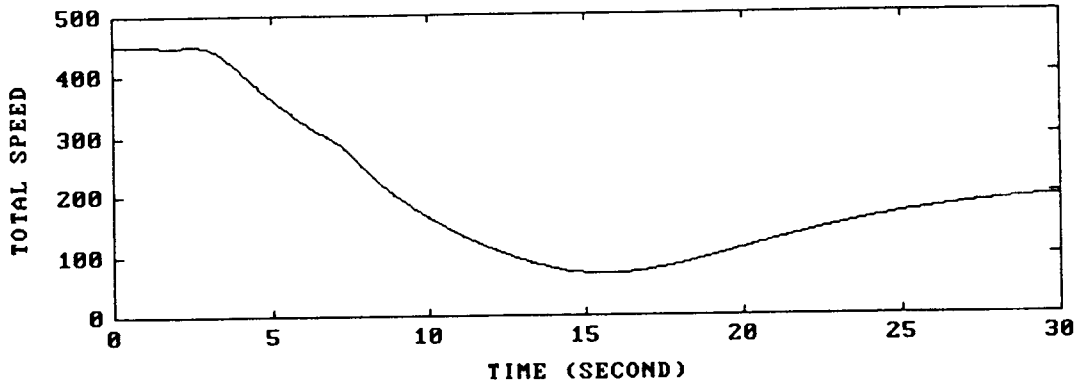

Figure 5.76 Total Speed in case of Maneuver Two, NLPM, and LF Controller

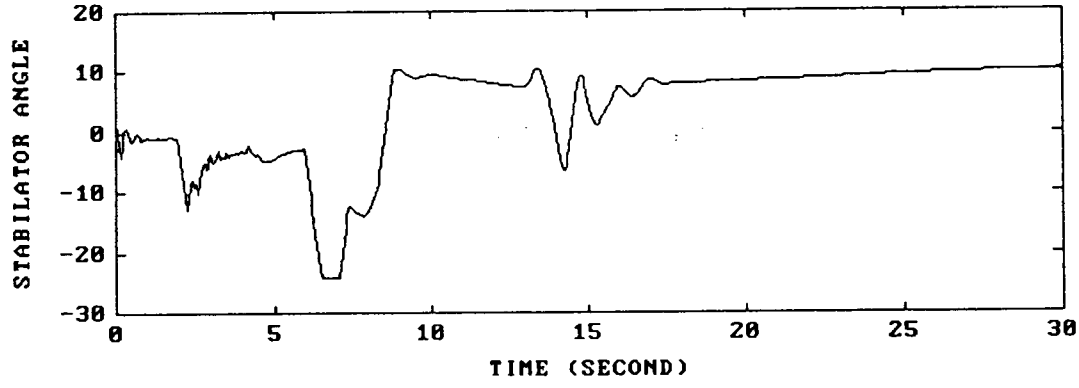

Figure 5.77 Stabilator Angle in case of Maneuver Two, NLPM, and LF Controller

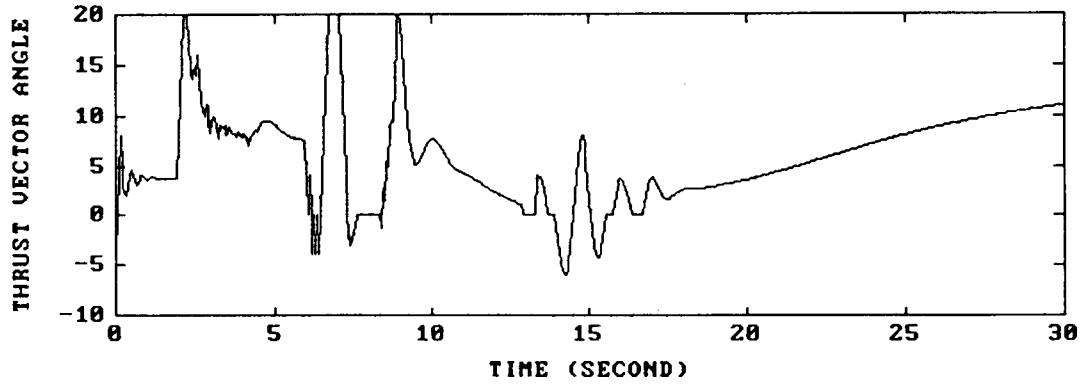

Figure 5.78 Thrust Vector Angle in case of Maneuver Two, NLPM, and LF Controller

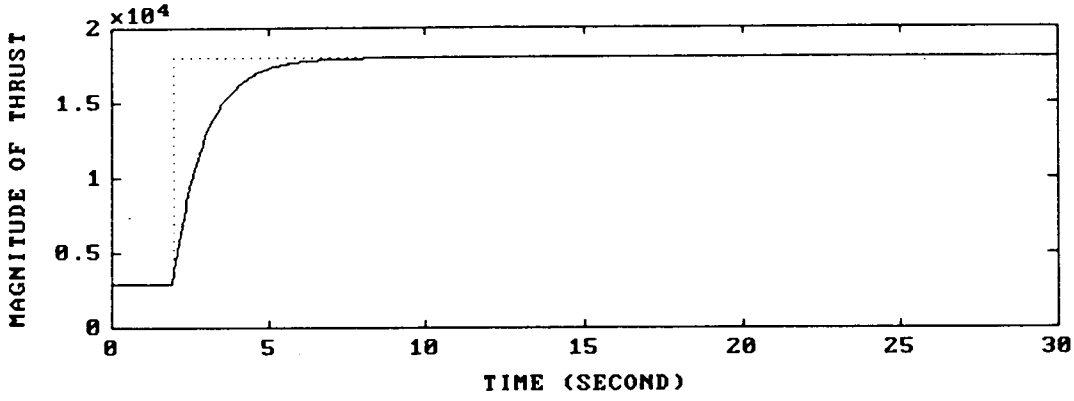

Figure 5.79 Magnitude of Thrust in case of Maneuver Two, NLPM, and LF Controller

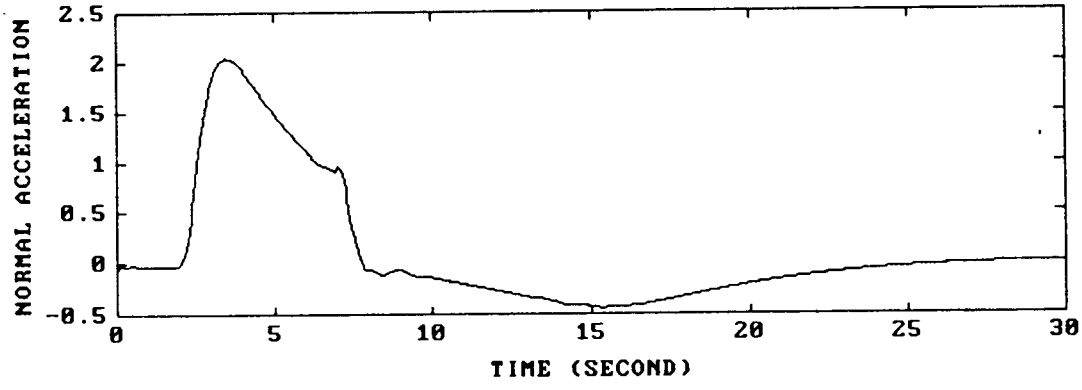

Figure 5.80 Normal Acceleration in case of Maneuver Two, NLPM, and LF Controller

CHAPTER 6

CONCLUSION

In this study, an effective control design methodology using a one-step-ahead prediction adaptive control law and an adaptive control law based on a Lyapunov function has been presented. These control laws were applied to a highly nonlinear maneuverable high performance aircraft. In a modified F/A-18 aircraft, it is difficult to control the angle of attack of around 60 and 85 degrees because the stability derivatives shown Figures 3.1-3.7 are highly nonlinear. For maneuver one the character of the response for maneuver one in the linear prediction model, the bilinear prediction model, and the nonlinear prediction model is similar to the response reported by Ostroff in [51]. The one-step-ahead prediction adaptive controller provided a somewhat faster response. In the case of the one-step-ahead prediction controller, the angle of attack reached 55 degrees in approximately 2.0 seconds and settling time to 60 degrees of angle of attack took about 3 seconds with maximum pitch rate of about 48 degrees per second and normal acceleration of about 2.3g, while the variable gain approach in [49], [50] reached 55 degrees in just under 3.5 seconds and settling time to the same angle of attack took about 6 seconds with maximum pitch rate of about 38 degrees per second. The time optimal control (with a limitation of 40 degrees per second on the thrust vectoring) reached 55 degrees in about 1.8 seconds [39]. In case of H_∞ controller [3], it took for the angle of attack to change from 10 to 20 degrees about 3 seconds with a rise time of

1 second and maximum pitch rate of 14 degrees per second and normal acceleration of about 1.5g. In the case of maneuver one, comparing the bilinear adaptive and nonlinear controller with the linear controller, it is shown that the response obtained by the one-step-ahead prediction bilinear adaptive and nonlinear controller is slightly faster for given command trajectories (60, 35, and 5 degrees of angle of attack) and has a smaller value of oscillation near the command trajectory.

The adaptive controller based on a Lyapunov function provided somewhat slower responses than the one-step-ahead adaptive controller. The command trajectory of the angle of attack is scheduled like the dotted line in Figure 5.49. It took about 3.5 seconds for the angle of attack to achieve 55 degrees. The settling time to 60 degrees is under 5 seconds in case of the linear prediction model, and is approximately 3.5 seconds to 4 seconds for the nonlinear prediction model. The value of the maximum pitch rate is 30 degrees per second with normal acceleration of about 2.2g in case of both. The nonlinear adaptive controller based on a Lyapunov function is smoother than the one-step-ahead prediction nonlinear adaptive controller.

For maneuver two, with a one-step-ahead prediction controller in the case of the linear prediction and the nonlinear prediction model controller, the angle of attack changed from 35 degrees to 80 degrees in approximately 2.5 seconds and the settling time to 85 degrees of angle of attack took about 3.5 seconds with a maximum pitch rate of 50 degrees per second and normal acceleration of about 2.1g. The angle of attack trajectories by the controller based on a Lyapunov function is similar to that of the one-step-ahead prediction controller. In case of maneuver two, the

nonlinear controllers are smoother than the linear controller. Also, the controller based on a Lyapunov function is smoother than the one-step-ahead prediction controller. The nonlinear controller is more effective than the linear controller as angle of attack is increased. This thesis shows that nonlinear control can be utilized effectively to control high performance aircraft such as F-18 aircraft for rapid maneuvers with large changes in angle of attack even if the nonlinear feedback controller operates with a higher-order(more delay terms) linear model reference.

In the future research, a more advanced reference model could be developed for an adaptive reference model. A nonlinear prediction model including measurement noise could be considered and be investigated for effects of noises. It will be extended to control the lateral motions. This will be done gradually, by first constraining the lateral movements to small sideslip angles, as was done by several references - for example, Safanov,et al discuss the Herbst maneuver [11], in which longitudinal and lateral motion are coupled simultaneously, and Ostroff [50].

BIBLIOGRAPHY

[1] K.J. Astrom and B. Wittenmark, *Adaptive Control*, Addison Wesley,1989.

[2] S. Bittanti, P. Bolzern, and M.Campi,"Adaptive Identification via Prediction-Error Directional-Forgetting factor : Convergence Analysis," *Int.J.Control*,Vol.50, 2407-2421 ,1989.

[3] J. Buffington, A.Sparks, and S. Banda, "Full Envelope Robust Longitudinal Axis Design of a Flight Aircraft with Thrust Vectoring," *Proc. IEEE American Control Conf.*, San Francisco, 1993.

[4] W.R. Cluett, J.M. Martin-Sanchez, S.L. Shah, and D.G. Fisher, "Stable Discrete-Time Adaptive Control in the Presence of Unmodeled Dynamics," *IEEE Trans. Automat. Contr.*, Vol. 33, 410-414, 1988.

[5] J. Cao, F.Arret, E. Hoffman, and H. Stalford,"Analytical Aerodynamic Model of A high Alpha Research Vehicle Wind-Tunnel Model," NASA CR-187469, September, 1990.

[6] M.J. Chen and J.P. Norton,"Estimation Technique for Tracking Rapid Parameter Changes," *Int.J.Control*, Vol.45, 1387-1398, 1987.

[7] S. Chen and S.A. Billings, "Representations of Nonlinear Systems : the NARNAX model," *Int.J.Control*, Vol.49, 1013-1032, 1989.

[8] S. Chen and S.A.Billings, "Recursive Prediction Error Parameter Estimator for Nonlinear Models," *Int.J.Control*, Vol.49, 569-594, 1989.

[9] R.Y. Chiang, M.G. Safonov, K.P. Madden, and J.A. Tekway, "A Fixed H Controller for a Supermaneuverable Fight Performing a Herbst Maneuver, " *Proc. IEEE Conf. on Decision and Control*, Honolulu, December 5-7, 1990.

[10] D.A. Collins,"Adaptive Model Reference Control of Highly Maneuverable High Performance Aircraft," M.S. Thesis, Oregon State University, 1993.

[11] G. Daviddov, A. Shavit, and T. Koren, "Estimation of Dynamical Varying Parameters by the Internal Model principle," *IEEE Trans. Automat. Contr.*, Vol.37, 498-503, 1991.

[12] I. Derese and E. Noldus, "Design of Linear Feedback Laws for Bilinear Systems," *Int.J.Control*, Vol.31, 219-237, 1980.

[13] B. Etkin, *Dynamic of Atmospheric Flight*, John Wiley & Sons, 1972.

[14] B. Etkin, *Dynamics of Flight : Stability and Control*, John Wiley & Sons, 1982.

[15] E.B. Feng, J.S. Yu, and W.S. Jiang, "New method for Predictive Controller Design for Bilinear System," *Int. J. Control*, Vol.53, 97-111, 1991.

[16] W. Garrard, D. Enns,and S.A.Snell,"Nonlinear Feedback Control of Highly Manoeuverable Aircraft," *Int.J.Control*, Vol.56, 799-812, 1992.

[17] G.C. Goodwin and E.K. Teoh, "Adaptive Control of a Class of Linear Time Varying Systems," *IFAC Adaptive System in Control and Signal Processing*, San Francisco, USA, 1-6, 1983.

[18] G.C. Goodwin and K.S. Sin, *Adaptive Filtering Prediction and Control*, Prentice Hall,1984.

[19] P.O. Gutman, "Stabilizing Controllers for Bilinear Systems," *IEEE Trans. Automat. Contr.*, Vol.26, 917-922, 1981.

[20] R. Haber and H.Unbehauen, "Structure Identification of Nonlinear Dynamic - A Survey on Input/Output Approaches," *Automatica*, Vol.26, 651-677, 1990.

[21] N. Halyo and D.D Moerder, "A Variable Gain Output Feedback Control Design Methodology," NASA CR-4226, 1989.

[22] H. Kang, G. Vachtsevanos, and F.L. Lewis, "Lyapunov Redesign for Structural Convergence Improvement in Adaptive Control," *IEEE Trans. Automat Contr.*, Vol.35, 250-253, 1990.

[23] P. Ioannou and J. Sun, "Theory and Design of Robust Direct and Indirect Adaptive Control Schemes," *Int.J.Control*, Vol. 47, 775-813, 1988.

[24] I.J. Leontaritis and S. Billings,"Input-Output Parametric Models for Nonlinear System, Part I:Deterministic Nonlinear Systems," *Int.J.Control*, Vol.41, 303-328, 1985.

[25] L. Ljung, *System Identification : Theory for the User*, Prentice Hall, 1987.

[26] R. Longchamp, "Stable Feedback Control of Bilinear Systems," *IEEE Trans. Automat. Contr.*, Vol.25, 302-305, 1980.

[27] McDonnel Aircraft Company, "F/A-18 Flight Control System Design Report," Report # MDC A7813, Vol.I, September, 1988.

[28] McDonnel Aircraft Company, "F/A-18 Flight Control System Design Report, Vol.II : Flight Control System Analysis - Inner Loops," Report # MDC A7813, June,1984.

[29] McDonnel Aircraft Company, "F/A-18 Flight Control System Design Report, Vol.III : Flight Control System Analysis - Automatic Flight Modes," Report # MDC A7813, September, 1984.

[30] McDonnel Aircraft Company, "F/A-18 Flight Control Electronic Set Control Laws," Report # MDC A4107, Vol.I, July, 1988.

[31] McDonnel Aircraft Company, "F/A-18 Flight Control Electronic Set Control Laws," Report # MDC A4107, Vol.II, July, 1988.

[32] McDonnel Aircraft Company, "F/A-18 Stability and Control Data Report, Vol.I : Low Angle of Attack," Report # MDC A7247, November, 1982.

[33] McDonnel Aircraft Company, "F/A-18 Stability and Control Data Report, Vol.II : High Angle of Attack," Report # MDC A7247, August, 1981.

[34] McDonnel Aircraft Company, "F/A-18 Basic Aerodynamic Data," Report # MDC A8575, November, 1982.

[35] R.R. Mohler, S. Cho, C.S. Koo, and R.R. Zakrzewski, Semi-Annual Report on "Nonlinear Stability and Control Study of Highly Maneuverable High Performance Aircraft," OSU-ECE Report NASA 9201, Corvallis, OR, February, 1991.

[36] R.R. Mohler, S. Cho, C.S. Koo, and R.R. Zakrzewski, Semi-Annual Report on "Nonlinear Stability and Control Study of Highly Maneuverable High Performance Aircraft," OSU-ECE Report NASA 9201, Corvallis, OR, August, 1991.

[37] R.R. Mohler, S. Cho, C.S. Koo, and R.R. Zakrzewski, Semi-Annual Report on "Nonlinear Stability and Control Study of Highly Maneuverable High Performance Aircraft," OSU-ECE Report NASA 9201, Corvallis, OR, August, 1992.

[38] R.R. Mohler, S. Cho, C.S. Koo, and R.R. Zakrzewski, Semi-Annual Report on "Nonlinear Stability and Control Study of Highly Maneuverable High Performance Aircraft," OSU-ECE Report NASA 9201, Corvallis, OR, February, 1993.

[39] R.R. Mohler, S. Cho, C.S. Koo, and R.R. Zakrzewski, Semi-Annual Report on "Nonlinear Stability and Control Study of Highly Maneuverable High Performance Aircraft," OSU-ECE Report NASA 9201, Corvallis, OR, July, 1993.

[40] R.R. Mohler, V. Rajkumar, and R.R. Zakrzewski, "Nonlinear Time-Series Based Adaptive Control Applications," *Proceedings of the 30th Conference of Decision and Control,* Brighton, England, 2917-2919, 1991.

[41] R.R. Mohler, R.R. Zakrzewski, S. Cho, and C.S. Koo, "New Results on Nonlinear Adaptive High Alpha Control," Comcon 3, Victoria, 1991.

[42] R.R. Mohler, *Bilinear Control Process*, Academic Press,1973.

[43] R.R. Mohler, *Nonlinear Systems : Dynamic and Control*, prentice Hall, 1991.

[44] R.R. Mohler, *Nonlinear Systems : Applications To Bilinear*, Prentice Hall, 1991.

[45] NASA Langley Reaserch Center, "Simulation Model Description of a Twin-trail High Performance Airplane,"

[46] R.C. Nelson, *Flight Stability and Automatic Control*, McGraw Hill, 1989.

[47] K.G. Nam and A.Arapostathis, "A Model Reference Adaptive Control Scheme for Pure-Feedback Nonlinear System," *IEEE Trans. Automat. Contr.*, Vol.33, 803-811, 1988.

[48] R. Ortega, L. Praly, and I.D. Landau, "Robustness of Discrete Time Direct Adaptive Controllers," IEEE Trans. Automat. Contr., Vol. 30, 1179-1187, 1985.

[49] A.J. Ostroff," Superagility Application of Variable Gain Output Feedback Control Design Methodology," NASA High Angle of Attack Technology Conference, Hampton, Virgina, 1990.

[50] A.J. Ostroff,"Application of Variable-Gain Output Feedback for High Alpha Control," ASAA Paper No. 89-3576, *Guidance, Navigation and Control,Con.*, Boston, 1989.

[51] A.J. Ostroff, "High-Alpha Application of Variable-Gain Output Feedback Control," *Journal of Guidance,Control,and Dynamics*, Vol.15,491-491,1992.

[52] A.J. Ostroff,"Longitudinal-Control Design Approach for High-Angle-of - Attack Aircraft,"NASA Technical Paper 3302,1993.

[53] Padalo and Arbib, *System Theory*, Saunders,1974.

[54] M.D.L. Sen, A. Martinez-Esnaola and I. Obieta,"Stable Adaptive Control for Not-Necessarily Stable Discrete Linear Plant with Bounded Non-linear Inputs," *Int.J.Control*, Vol.53, 335-368, 1991.

[55] S.L. Shar and W.R. Cluett,"Recursive Least Squares Estimation Schemes for self-Tuning Control," *The Cadadian Journal of chemical Engineering*, Vol.69,89-96,1991.

[56] J.J.E. Slotine and W. Li," *Applied Nonlinear Control*," Prentice Hall, 1991.

[57] N.R. Sripada and D. Grant Fisher, "Improved Least Squares identification," *Int.J.Control*, Vol.46, 1889-1913, 1987.

[58] C. Wen and D.J. Hill, "Adaptive Linear Control of Nonlinear System," *IEEE Trans. Automat. Contr.*, Vol.35, 1253-1257, 1990.

[59] B.E. Ydstie and R.W.H. Sargent,"Convergence and Stability Properties of an Adaptive Regulator with Variable Forgetting Factor," *Automatica*, Vol.22, 749-751, 1986.